UNIVERSITY OF SALAMANCA

Statistics Department
Doctoral in Applied Multivariate Statistics
Doctoral Thesis

A sustainability approach using fuzzy logic and data mining

Candidate: José Fernando Romero Cañizares

Chairs: María Purificación Vicente Galindo and Yannis Phillis

2021

UNIVERSIDAD DE SALAMANCA

Departamento de Estadística
Doctorado en Estadística Multivariante Aplicada
Tesis Doctoral

Un enfoque de sustentabilidad utilizando lógica difusa y minería de datos

Autor: José Fernando Romero Cañizares

Directors: María Purificación Vicente Galindo, Yannis Phillis

2021

Dr. María Purificación Vicente Galindo
Professor at the University of Salamanca

and

Dr. Yannis Phillis

Prof. Emeritus at Technical University of Crete-Greece

Certify that **José Fernando Romero Cañizares** has, under their supervision in the Department of Statistics of the University of Salamanca, completed the requirements towards the degree Doctor in of Philosophy in Applied Multivariate Statistics, and authorize the defense of his dissertation entitled **A SUSTAINABILITY APPROACH USING FUZZY LOGIC AND DATA MINING**.

And for the record, they sign this certificate in Salamanca on May 26, 2021

María Purificación Vicente Galindo Yannis A Phillis

Dra. María Purificación Vicente Galindo
Profesora Titular de la Universidad de Salamanca

y

Dr. Yannis Phillis

Profesor Emérito de la Universidad Técnica de Creta

Certifican que **Don. José Fernando Romero Cañizares** ha realizado en el Departamento de Estadística de la Universidad de Salamanca, bajo su dirección, el trabajo para optar al Grado de Doctor en Estadîstica Multivariante Aplicada, que presenta con el título **UN ENFOQUE DE SUSTENTABILIDAD UTILIZANDO LÓGICA DIFUSA Y MINERÍA DE DATOS,** autorizando expresamente su lectura y defensa.

Y para que conste, firman el presente certificado en Salamanca el 26 de mayo de 2021.

María Purificación Vicente Galindo   Yannis Phillis

Statistics Department

University of Salamanca

María Purificación Vicente Galindo **Yannis Phillis**

A SUSTAINABILITY APPROACH USING FUZZY LOGIC AND DATA MINING

A dissertation submitted in partial satisfaction of the requirements for the degree Doctor of Philosophy in applied science

Candidate:

José Fernando Romero Cañizares

Salamanca

2021

Departamento de Estadística
Universidad de Salamanca

María Purificación Vicente Galindo **Yannis A Phillis**

UN ENFOQUE DE SUSTENTABILIDAD UTILIZANDO LÓGICA DIFUSA Y MINERÍA DE DATOS

Trabajo para optar por el título de Doctor en Estadística Multivariante Aplicada por la Universidad de Salamanca

Presenta:

José Fernando Romero Cañizares

Salamanca

2021

ACKNOWLEDGEMENTS

First of all, I would like to thank God for allowing me to reach this important moment in my life.

My tutors, Dra. María Purificación Vicente Galindo, Professor of Statistics at the University of Salamanca, and especially Dr. Yannis A Phillis, Professor Emeritus at the Technical University of Crete have provided invaluable help and support during my years of study. Without their advice and unique knowledge, I would have been unable to finish my research work. I thank my alma mater, ESPOCH, that has seen me grow throughout my career. Dr. Purificación Galindo Villardón encouraged me to continue deepening my statistical knowledge. Her professionalism and wisdom are unmatched.

I would like to thank my relatives, my brothers, and my nephew Pablo for all their time and advice. I would be remiss if I did not mention my late grandmother Carmen, to whom I owe an incalculable debt. She was a true architect of my life.

Finally, I want to thank my two sons David and Andrés for encouraging me to achieve this goal and my wife Inés for being my constant support in showing me that time is never wasted if you want to pursue something important.

" Only by revaluing what is ours is it possible to build a promising future"

José Fernando Romero Cañizares

TABLE OF CONTENTS

TABLE DE CONTENIDO

LIST OF TABLES

LISTA DE TABLAS

LIST OF FIGURES

LISTA DE FIGURAS

INTRODUCTION

What is sustainability? How can sustainability be measured? Questions such as these are still fertile ground for debate and will likely remain at this stage for a long time. “How can we make sustainable development a reality?” is perhaps the main question that humanity must answer. The COVID-19 pandemic has demonstrated beyond any doubt that inequalities between and within countries, due to globalization and global trade, are a major factor preventing us from preserving our planet. Sustainable development goals are now the agreed criteria to monitor states, and this work will demonstrate that numerical and graphical methods are valuable tools in assessing progress. Fuzzy Logic is a reliable procedure for transforming human qualitative knowledge into quantitative variables that can be used in the reasoning of the type “if, then” to obtain answers pertaining to sustainability assessment. Applications of machine learning techniques and artificial intelligence procedures span almost all fields of science. Here, for the first-time, unsupervised machine learning is applied to sustainability assessment, combining numerical approaches with graphical procedures to analyze global sustainability.

INTRODUCCIÓN

¿Qué es sostenibilidad? ¿Cómo se puede medir la sostenibilidad? Preguntas como éstas son objeto de debate y es probable que lo sigan siendo por mucho tiempo. "¿Cómo podemos hacer del desarrollo sostenible una realidad? Quizás sea la pregunta principal que la humanidad debe responder. La pandemia del COVID-19 ha demostrado sin lugar a dudas que las inequidades existentes entre y dentro de los paises, debido a la globalización e intercambio comercial, son los factores más importantes que nos ponen en alerta sobre la necesidad de preservar nuestro planeta. Los objetivos de desarrollo sostenible son actualmente criterios consensuados para monitorear los paises, y este trabajo demostrará que los métodos numéricos y gráficos son herramientas adecuadas para medir su progreso. La teoría de la lógica difusa es un procedimiento altamente confiable que transforma las variables cualitativas del pensamiento humano en variables cuantitativas bajo las reglas de "si, entonces" para obtener respuestas relacionadas a la evaluación de la sostenibilidad. Aplicaciones del aprendizaje de máquina y los procedimientos de inteligencia artificial abarcan casi todos los campos de la ciencia. En esta oportunidad, por primera vez un aprendizaje de máquina no supervisado es aplicado para evaluar la sostenibilidad, combinando procedimientos numéricos y gráficos para análizar la sustentabilidad de los países, convirtiéndose de esta manera en un complemento a la Lógica difusa.

CHAPTER 1. STATE OF THE ART.

1.1. Principal considerations in sustainability and sustainable development

Sustainability and sustainable development are not synonymous. For neoclassical economists, sustainable development means economic growth, whereas sustainability, in other disciplines, gives priority to environmental and social concerns. Additionally, the classic division between developed (rich) and developing (poor) countries focused only on economic indicators is not justified without further examination, because a more global vision of sustainable development should include environmental and cultural aspects of society. Sustainable development defined as "... meeting the needs of the present without compromising the ability of future generations to meet their own needs" (Brundtland, 1987) is considered the cornerstone of humanity's concern to care for our own home.

For the development and formalization of the concept of sustainability several authors, e,g., (Giddings et al., 2002) and (Waas et al., 2011), underline four major stages or key periods. An initial period of discussion of the term lasted until the end of the 1970s, followed by a period of stagnation from 1980 to 1986. The period from 1987 to 1995 noted the greatest gains, concluding with a fourth period of modest progress.

Several events in each period marked milestones in the achievement of sustainability. The 1992 Rio Earth Summit declared that sustainability is central to the viability of nations and that we require immediate and concerted action on the concept and also scientific research. Agenda 21, the main outcome of the Summit, stressed the need for developing indicators of sustainability “to provide solid bases for decision-making at all levels and to contribute to a self-regulating sustainability of integrated environmental and development systems” (United Nations, 1992). Developing an integrated and widely accepted framework for the measurement of sustainability was a challenging task. The summit of 1992 was followed by the Rio Summit of 2012, which marked some additional progress towards sustainability (Waas et al., 2011)Several important factors were addressed at that meeting, such as climate change and the replacement of fossil fuels with more carbon-neutral forms of energy, transportation, water resources, biodiversity, and desertification.

The 2000 Millennium Summit set the Millennium Development Goals (MDGs) to be achieved by the year 2015. On September 25th of that year, 193 member states of the United Nations adopted a set of 17 Sustainable Development Goals (SDGs), which will guide the social, economic, and environmental actions that all countries will take to achieve a sustainable future by the year 2030 (Sachs et al., 2016).

These 17 SDGs do not distinguish between "developed" and "developing" nations. Instead, the goals apply to all countries. These goals are interconnected and based on the principle of “leaving no one behind.” Thus, an awareness of the urgency of conserving our planet is growing among most countries that have made pledges to follow a sustainable path.

The 2016 edition of the SDG Index and Dashboards Report provides a report card for every country regarding performance towards the 2030 Agenda. The annual report shows how leaders can deliver on their promises, and it urges countries not to lose their momentum for important reforms. The Spanish Network for Sustainable Development (REDS) presented the Sustainable Development Objectives Index (SDG Index & Dashboards 2017) in Madrid on July 12, 2017, a global report prepared by the Sustainable Development Solutions Network (SDSN) and the Bertelsmann Stiftung Institute. The latest available report is The Sustainable Development Goals Report 2018, which found that conflict and climate change were major contributing factors leading to growing numbers of people facing hunger and forced displacement, as well as curtailing progress towards universal access to basic water and sanitation services.

It is well known that revenues are needed for protecting society; active labor market policies in economies facing deep structural change; just transitions for environmental sustainability; quality education and healthcare; research and development outlays in an era when innovation is vital for competitiveness and social security (Sachs, 2020).

1.1.1 How can sustainability be measured?

This is a difficult question. However, today everybody agrees that sustainability is a non-negotiable goal because otherwise, humanity runs the risk of extinction. There are several approaches that measure sustainability at the national level and rank countries accordingly. The comparison of countries could be done with numerical or graphical approaches. A graphical ranking makes the sustainability position of the countries very transparent, placing them on a global performance ranking, which also allows for regional comparison.

Furthermore, we now understand, that the current technologies can help us achieve decarbonization through carbon-free electricity, end-use electrification, synthetic green fuels, a smart grid; and energy and material efficiency with a little more Research and Development at a very low cost. According to (Sachs, 2019), “decarbonization to save the planet is actually the best deal of our time".

In summary, regarding world sustainability assessment, we have identified at least 4 methods to assess sustainability performance. The first, and perhaps most widely used, is Sustainability Assessment by Fuzzy Evaluation (SAFE), first proposed in Phillis & Andriantiatsaholiniaina, (2001) and Phillis et al., (2004). SAFE model was then refined and expanded in Phillis et al., (2011); Grigoroudis et al., (2014) and Grigoroudis et al., (2021). The second is the United Nations Sustainable Development Goals. The third is an adaptive neuro-fuzzy inference system (ANFIS) proposed byTan, Y et al., (2017) , and the fourth is a graphical sustainability analysis using disjoint biplots, proposed by Cañizares et al., (2020). For the first time, we are aiming at analyzing the sustainability of the world’s countries using the Variational Autoencoders Approach and Graphical Analysis (VAE&GA).

1.1.2 How can statistics help decision-makers?

It is clear that sustainability is a problem of global dimensions. It is equally clear that scientific tools must be developed alongside existing ones that assess progress towards sustainability. Implicit and explicit methods have been proposed to assess sustainability to deal with qualitative and quantitative variables.

Sometimes decision-makers are only interested in immediate risks and not in long-term decisions, so using numerical or graphical tools can show where a particular country is located as well as pinpoint the indicators necessary to improve sustainability.

Reliable, impartial, and timely data are needed to forecast and monitor the actions taken. For that reason, statistics are tools that can help support good decision-making even more in this era of big data, artificial intelligence, and the Internet.

1.2. Numerical Sustainability Assessment

1.2.1 Sustainability Assessment by Fuzzy Evaluation (SAFE)

Sustainability is in general a function of precise data, such as concentrations of pollutants or GNI per capita, as well as vague variables, such as human rights or corruption. To handle vagueness and its concomitant uncertainty, fuzzy logic might be used as a way to emulate human thinking in a straightforward manner. Fuzzy logic is well suited to treat qualitative, imprecise, or uncertain information (Zadeh, 1971). Sustainability Assessment by Fuzzy Evaluation (SAFE) is a model that assesses sustainability using fuzzy logic. Quantitative and qualitative input variables are converted into linguistic variables through membership functions. A system of fuzzy reasoning evaluates the various composite components of sustainability and sustainability as a whole via “if-then” rules. Finally, the output of the system is converted into a crisp value of sustainability by means of a defuzzification process (Grigoroudis et al., 2014). The model, which will be outlined below, provides country rankings and performs sensitivity analyses that reveal key indices that each country should focus on to improve sustainability (Grigoroudis et al., 2021)

SAFE uses basic indicators of environmental integrity, economic efficiency, and social welfare. Via statistical analysis and fuzzy reasoning, SAFE determines measures of human, ecological and overall sustainability. Data about basic indicators such as emissions are passed through an exponential smoothing filter to account for the memory of past performance and then are normalized on [0, 1] according to their sustainability standing, where 0 corresponds to totally unsustainable and 1 to totally sustainable values. Missing data are generated via an imputation procedure. Next, a multistage fuzzy inference engine is used together with pertinent rule bases to obtain fuzzy values for composite sustainability variables. A height defuzzification procedure yields crisp sustainability numbers at each stage. The final number of overall sustainability is used to rank countries. Finally, a sensitivity analysis reveals those indicators that have the greatest potential of improving sustainability. It should be stressed that the model is flexible in that its indicators can change in number and importance according to reality.

Several basic indicators are used to compute the four components of the ecosystem dimension, air, land, water, and biodiversity, and the four components of the human system dimension, policies, wealth, health, and knowledge. Finally, an index OSUS of overall sustainability in [0, 1] is derived for each country. The hierarchical structure of indicators in the SAFE model is outlined in Figure 1.

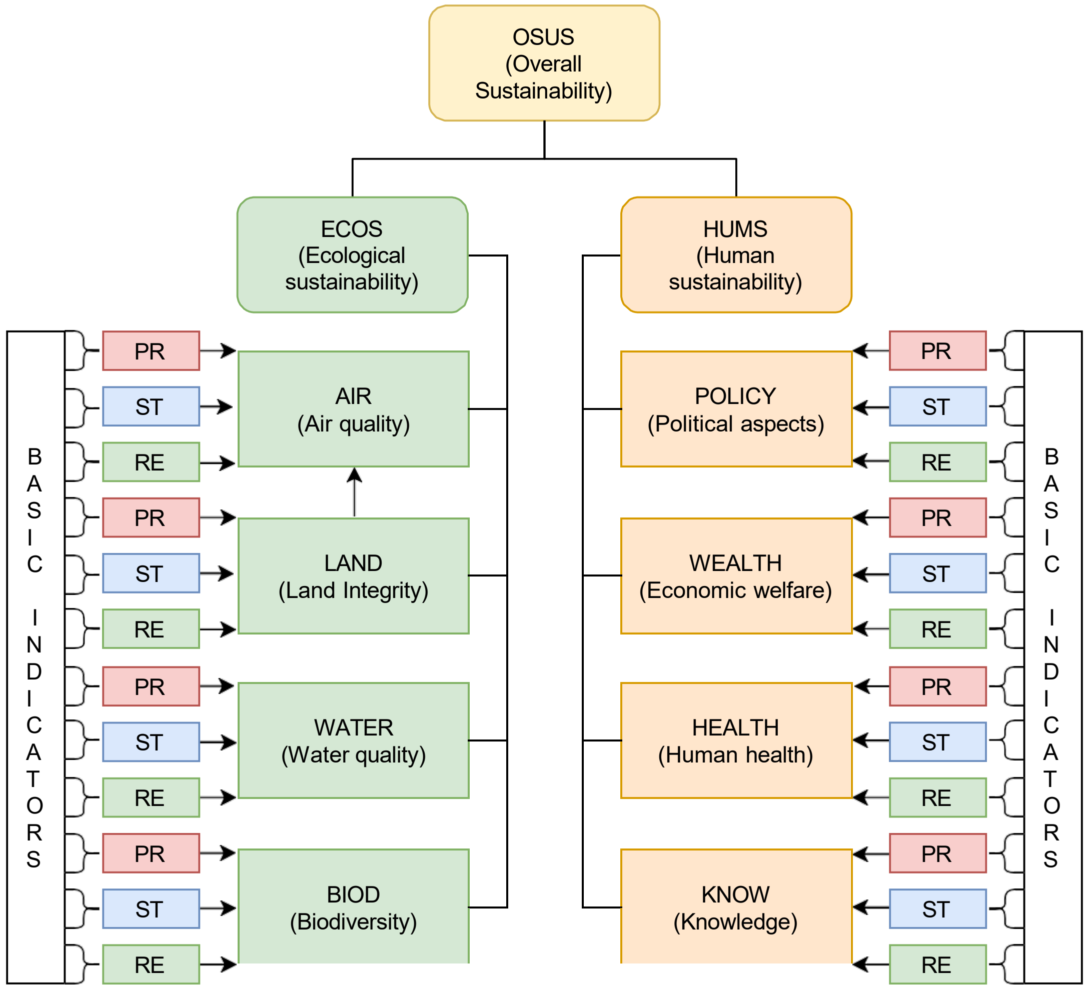

Figure 1. The SAFE model

The SAFE model methodology is described using specific information, with the authorization and permission of Dr. Yannis A. Phillis.

Each secondary component is assessed using the Pressure-State-Response approach of the Organization for Economic Cooperation and Development (OECD, 1991), which assumes that humans exert pressures on the environment which alter its conditions (state) and call for certain responses by the society.

In the SAFE model, tertiary indicators

a. Pressure (PR),
b. State (ST), and
c. Response (RE)

are obtained by combining certain basic indicators. For example, the indicator PR(BIOD) measures the pressure on biodiversity using six basic indicators which give the percentage of all threatened (endangered, vulnerable) species: mammals, birds, plants, fishes, reptiles and amphibians.

The sequence of data processing is the following:

1. Collection of available data and Exponential smoothing.
2. Normalization in [0,1].
3. Imputation of missing data imputation.
4. Fuzzy assessment of sustainability:
    - fuzzification of basic indicators
    - assessment of tertiary indicators (PR(LAND, ST(LAND), RE(LAND), …)
    - assessment of secondary indicators (LAND, ..., POLICY, ...)
    - assessment of ecological and human components (HUMS, ECOS)
    - overall sustainability (OSUS)
5. Defuzzification of OSUS
6. Sensitivity analysis-decision making

Basic indicators of sustainable development (Appendix 1).

Definitions of indicators are taken from Esty et al. (2005), Food and Agricultural Organization(FAO), International Union for the Conservation of Nature (IUCN, 1994), Organization of Economic Cooperation and Development (OECD, 2000; 2004; and website), Ordoubadi (2005), United Nations Environmental Program (UNEP), United Nations Statistics Division (2006), United Nations Development Program (UNDP, 2003), United Nations Educational, Scientific, and Cultural Organization (UNESCO), United Nations Framework Convention on Climate Change (UNFCCC), World Health Organization (WHO), World Bank (1995; 2008), and the Freedom House Annual Survey (2007). Many of these references also provide annual data about basic indicators for most countries of the world.

Normalization

To make indicators comparable and to facilitate analysis, the data are normalized by assigning the value 0 to the least desirable indicator values and the value 1 to the most desirable indicator values or targets, which are determined by experts, standards, laws, etc.

For example, HIV/AIDS prevalence rate per cent of population had a maximum value of 23.4% over all countries in 2011 (most recent data). Given its significant potential for rapid spread, even a value of 2% for this indicator is considered to be very bad. The Joint United Nations Programme on HIV/AIDS provides an upper bound of 0.9% on the average HIV prevalence rate (UNAIDS 2007). The least desirable value is chosen as twice the upper bound. All HIV/AIDS prevalence rates greater than or equal to 1.8% are assigned the value 0. The rate 0%, which is the target for this indicator, corresponds to 1.

Let c be an indicator and z_c its value for the country whose sustainability we want to assess. The target of c can be a single value T_c or an interval on the real line of the form $[\tau_c, T_c]$ representing a range of equally desirable values for the indicator. Least desirable values can be sole points or sets of values below or above some critical threshold. Critical values are denoted υ_c and U_c, so that all values $z_c \leq \upsilon_c$ or $z_c \geq U_c$ are assigned a normalized value 0.

In practice υ_c is the minimum value of z_c over all countries under examination and U_c its maximum. In some cases though we choose these numbers differently. For example, we have $U_{\text{AIDS}} = 1.8\%$ whereas the maximum HIV/AIDS prevalence rate worldwide is 23.4%. Thus, if an indicator must be *at most* equal to T_c to be sustainable, then we have the case of Fig. 2. Here we do not need υ_c and τ_c. An HIV/AIDS prevalence rate of 0.9% is assigned the normalized value 0.5 because it is halfway between the target 0% and the critical threshold 1.8% of least desirable values.

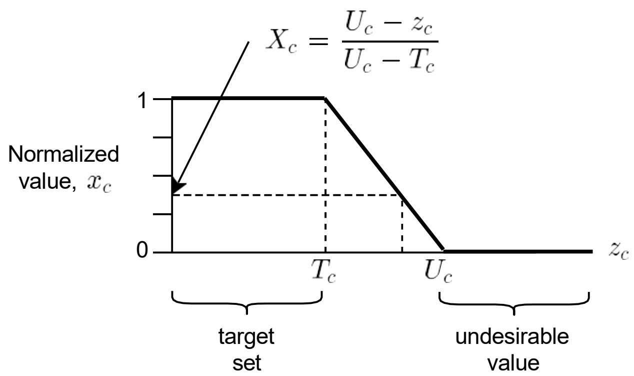

Figure 2. Normalization by linear interpolation: smaller is better (SB).

Similarly, if an indicator must be *at least equal* to τ_c to be sustainable, we have the case of Fig. 3 and we do not need T_c and U_c.

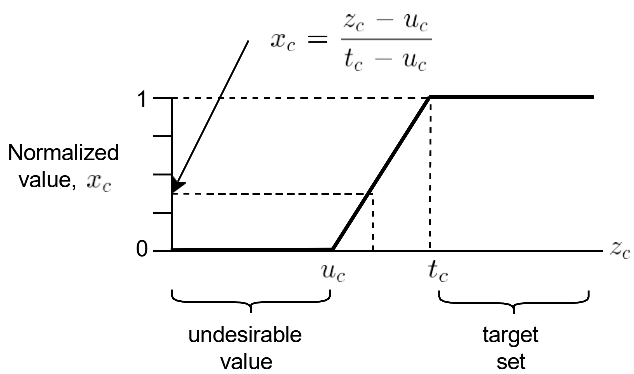

Figure 3. Normalization by linear interpolation: larger is better (LB).

Finally, if an indicator must lie in $[\tau_c, T_c]$ to be sustainable, then we have the full diagram of Fig. 4.

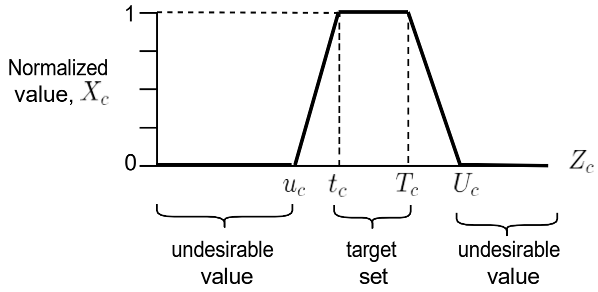

Figure 4. Normalization by linear interpolation: nominal is best (NB).

A normalized value x_c for z_c is calculated as follows:

$$x_c = \begin{cases} 0 & z_c \leq u_c \\ \dfrac{z_c - u_c}{t_c - u_c} & u_c \leq z_c \leq t_c \\ 1 & t_c \leq z_c \leq T_c \\ \dfrac{U_c - z_c}{U_c - T_c} & T_c \leq z_c \leq U_c \\ 0 & U_c \leq z_c \end{cases}$$

Exponential smoothing

Annual indicator data are often unavailable or imprecise. Moreover, past environmental pressures have significant cumulative effects. To deal with these issues, present and past indicator data are combined into a single value using exponentially weighted sums. Suppose that K measurements of indicator c are available for some country. Let $x_c(t_1)$, $x_c(t_2)$, ..., $x_c(t_K)$ be the normalized values in years t_1, t_2, ..., t_K. These years need not be consecutive due to missing data. An aggregate value x_c for indicator c is computed by exponential smoothing, using the weighted average

$$x_{!} = \frac{x_{!}(t_{"}) + x_{!}(t_{"} - 1)\beta^{\#!\$\#!"\#} + \cdots + x_{!}(t_{\%})\beta^{\#!\$\#\#}}{1 + \beta^{\#!\$\#!"\#} + \cdots + \beta^{\#!\$\#\#}}$$

in which older observations are assigned geometrically decreasing weights with parameter $\beta \in [0, 1]$. The smoothing parameter β is chosen so as to minimize the mean squared error

$$[x_{!(\#_{\#})} - x_{!}(t_{\%})]^{(} + \cdots + [[x_{!(\#_{!})} - x_{!}(t_{)})]^{(}$$

The quantity $x_{!}(t_{)})$ is the weighted average of indicator data *prior to* year t_k, and is given by

$x_{!}(t_{\%}) = 0$

$x_{!}(t_{)*\%}) = \frac{+\$(\#\%)*+\$(\#\%\$\%)\_{}^{\&}!"^{\&}!"\#*\ldots*+\$(\#\#)\_{}^{\&}!"^{\&\#}}{\%*\_{}^{\&}!"^{\&}!"\#*\ldots*\_{}^{\&}!"^{\&\#}}$, k= 1,…, K-1

It should be noted that the weights β differ among countries as well as among indicators. If no indicator data are available for some country, a value x_c is imputed using an approach to describe in the next section.

Imputation of missing data

As a first step of the imputation procedure, countries are grouped by similarity according to geographic, economic, and cultural criteria. This is done as follows:

1. Country groups are formed according to geography as given by the United Nations Statistics Division (2010)
2. These groups are refined, taking into account economic criteria. Such country groupings are also given by the United Nations Statistics Division (2010) and the World Bank (2010). For example:
    a. The group of Baltic countries is separated from the group of Scandinavian countries, since the latter forms a group of high-income OECD countries, although they all belong to the geographic area of North Europe.

   b. UK and Ireland are grouped together with other Western European countries, although they are located in North Europe in order to form a homogenous group of OECD countries and high-income developed economies.

3. Pairs of groups with moderate similarity are found using geographical and economic criteria. For example:
   a. Western European countries are moderately similar to other OECD members which belong to the groups of North America, Scandinavia, South Europe, and Japan.
   b. The group of South America consists of middle-income countries which are moderately similar to Central American countries, but not to the high-income OECD countries in North America.

In the second step, a distance matrix is set up that measures how different are the available data of a country from those of another similar country. The basic indicators fall within 8 groups:

1. LAND,
2. WATER,
3. BIOD,
4. AIR,
5. POLICY,
6. WEALTH,
7. HEALTH, and
8. KNOW.

Suppose that some basic input from indicator group g is not available for country i. Let j be an index of countries similar to i, i.e., s_{ij} = 1 or 2. For each pair (i, j), the Euclidean distance d_{ijg} is computed using those normalized indicators of group g for which data are available for both i and j. The Euclidean distance is given by the square root of the average of squared indicator differences:

$$d_{ijg} = \sqrt{\frac{\sum_{c \in \text{group g indicators available for both i and j}} (x_{ic} - x_{jc})^2}{\text{number of groups g indicators available for both i and j}}}$$

where x_{ic} is the normalized value of indicator c for country i, which is obtained by exponential smoothing. When no group g indicator is available for both countries i and j the corresponding Euclidean distance is assumed to be infinite, i.e., dijg=∞.

In the third and last step of the imputation procedure the missing value of an indicator is filled in using the average value of this indicator over all countries with maximum similarity and minimum Euclidean distance. Suppose that an indicator of group g is not available for country i. The following algorithm is used to find countries that meet the similarity and distance criteria. Index j runs exclusively over those countries for which the indicator to be imputed is available.

1. Compute d_{ijg} for each country j in the same group as i (s_{ij} = 2). Find those countries for which $d_{ijg} \leq 0.1$ (10% of the maximum value of a normalized indicator). If no countries are found, then go to step 2.
2. Compute d_{ijg} for all moderately similar countries (s_{ij} = 1). Choose those countries for which $d_{ijg} \leq 0.1$. If no country satisfies this, then go to step 3.

3. Find countries in the same group as i ($s_{ij} = 2$) for which $d_{ijg} \leq 0.2$ (20% of the maximum value of a normalized indicator). If no countries are found, then go to step 4.
4. Find moderately similar countries ($s_{ij} = 1$) for which $d_{ijg} \leq 0.2$. If no countries are found, then go to step 5.
5. Compute d_{ijg} for each unrelated country j ($s_{ij} = 0$) and select those with the minimum distance.

Using the above algorithm, a complete data base is formed for countries and indicators per country. On average, 1.86 or about two countries are chosen to impute each of the missing inputs. The average value of distances d_{ijg} is 0.105, with an average range of 0.012.

Fuzzy assessment

Sustainable decision-making involves complex, often ill-defined parameters with a high degree of uncertainty due to incomplete understanding of the underlying issues. The dynamics of any socio-environmental system cannot be described by traditional mathematics because of its inherent complexity and ambiguity. In addition, the concept of sustainability is polymorphous and fraught with subjectivity. It is therefore more appropriate to use fuzzy logic for its assessment.

The SAFE model uses fuzzy logic to compute composite indicators (outputs) from basic ones (inputs). The computations are done with words using knowledge that is represented by linguistic rules of the form

if

(inputs)

then

(outputs).

Below we give two examples of such "if-then" rules, which are used in the first and last stages of the SAFE inference process.

Assessing a tertiary variable from basic indicators:

if

'Threatened Mammals' is Medium

'Threatened Birds' is Strong

and 'Threatened Plants' is Medium

and 'Threatened Fishes' is Weak

and 'Threatened Reptiles' is Strong

and 'Threatened Amphibians' is Strong

then

PR(BIOD) is Bad.

Assessing OSUS from its primary components:

if

ECOS is Bad

and HUMS is Good

then

OSUS is Intermediate.

The terms Medium, Bad, Intermediate, etc. in the rules given above represent fuzzy sets. Each rule has a given degree of truth or *firing strength*, which is an aggregate measure of the degree to which its inputs belong to the corresponding fuzzy sets. The method we describe next, called *fuzzification*, is used to compute the degree to which a basic indicator belongs to a specific fuzzy set.

Fuzzification

The normalized basic indicators are fuzzified using three fuzzy sets with linguistic values:

- *Weak* (W),
- *Medium* (M), and
- *Strong* (S).

For composite indicators (primary, secondary, and tertiary components) five linguistic values are used:

- *Very Bad* (VB),
- *Bad* (B),
- *Average* (A),
- *Good* (G), and
- *Very Good* (VG).

The overall sustainability is measured using nine fuzzy sets:

- *Extremely Low* (EL),
- *Very Low* (VL),
- *Low* (L),
- *Fairly Low* (FL),
- *Intermediate* (I),
- *Fairly High* (FH),
- *High* (H),
- *Very High* (VH), and
- *Extremely High* (EH).

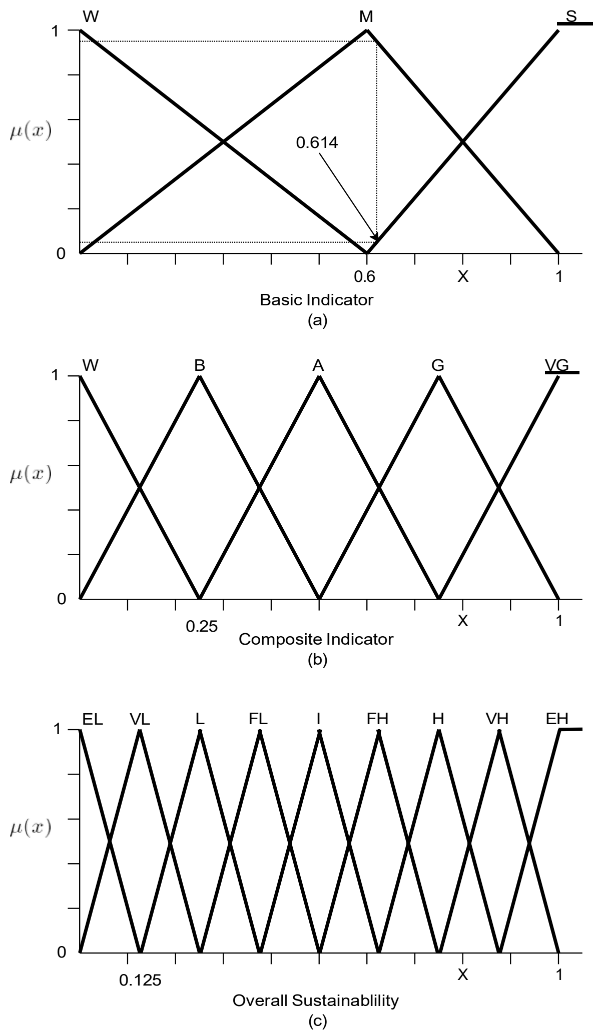

Figure 5. Fuzzy sets and corresponding membership functions μ(x).

Each indicator value x belongs to one or more fuzzy sets with certain membership grades. For simplicity, triangular membership functions $\mu(x)$ are used, as shown in Fig.5. For example, in 2002, 13.7% of the mammal species in Greece were endangered. The target value for this indicator is $T = \tau = 0\%$ and the upper threshold of unsustainable values is $U = 35.5\%$. The normalized value for this indicator is $x = (13.7 - 35.5)/(0 - 35.5) = 0.614$. As shown in Fig. 5a, this value belongs to the fuzzy set Medium with *membership grade* $\mu_M(0.614) = 0.965$ and to the fuzzy set Strong with grade $\mu_S(0.614) = 0.035$.

Rule bases

The rules used in each inference step express linguistically the dependence of a composite indicator on other, more elementary indicators. This section describes a compact representation of the rule bases, which avoids storing all rules in the computer memory. This is done in three steps outlined below.

1. The fuzzy sets of Fig. 6 are assigned integer values 0, 1, 2, …, where 0 corresponds to the fuzzy sets with the lowest sustainability. The fuzzy set Weak in Fig. 5a is assigned the value 0, Medium is assigned the value 1, and Strong is assigned the value 2. The corresponding weights for the composite indicators of Fig. 5b are Very Bad→0, Bad→1, Average→2, Good→3, and Very Good→4, and for OSUS (Fig. 5c) Extremely Low→0, Very Low→1, …, Extremely High→8. Moreover, each indicator used as input to an inference engine is also assigned a positive weight, which measures its relative importance against the other inputs. Currently, all inputs of the SAFE inference engines are assigned the weight 1.
2. For each rule, a weighted sum of inputs is computed and assigned to the output variable.
3. if

   'Threatened Mammals' is Medium

   'Threatened Birds' is Strong

   and 'Threatened Plants' is Medium

   and 'Threatened Fishes' is Weak

   and 'Threatened Reptiles' is Strong

   and 'Threatened Amphibians' is Strong

then

PR(BIOD) is Bad.

The weighted sum of its inputs is:

weight of PR(BIOD) = 1 + 2 + 1 + 0 + 2 + 2 = 8.

The resulting weight is assigned to some fuzzy set. The larger the weight the larger or better the fuzzy set of the output. For example, the rule base for the composite indicator PR(BIOD) comprises 729 rules (3^6 six-tuples of the fuzzy sets W, M, and S). It is represented compactly as follows

$$\text{fuzzy set of PR (BIOD)} = \begin{cases} \text{VB} & \text{if weight} & \leq & 7 \\ \text{B} & \text{weight} & = & 8 \\ \text{A} & \text{weight} & = & 9 \\ \text{G} & \text{weight} & = & 10 \\ \text{VG} & \text{weight} & = & 11,12 \end{cases}$$

The same rule base is used for PR(LAND), which has also six inputs. The rule bases used to assess other composite indicators are given below.

Tertiary components with only one input have the same fuzzy sets and membership grades as their inputs. RE(WATER) depends solely on the basic indicator “Public wastewater treatment plants (percent of population connected)” and RE(AIR) depends on “Renewable energy production (percent of total primary energy supply).” Contrary to the other basic indicators which are mapped on three fuzzy sets, these two indicators are fuzzified using the five fuzzy sets VB, B, A, G, and

VG and the resulting membership grades are passed on to RE(WATER) and RE(AIR).

Tertiary components with two inputs:

$$\left\{\begin{array}{c}\text{ST(LAND)}\\ \text{PR(BIOD)}\\ \text{ST(BIOD)}\\ \text{PR(AIR)}\\ \text{RE(POLICY)}\\ \text{RE(WEALTH)}\end{array}\right\} = \left\{\begin{array}{llll}\text{VB} & \text{if weight} & = & 0\\ \text{B} & \text{weight} & = & 1\\ \text{A} & \text{weight} & = & 2\\ \text{G} & \text{weight} & = & 3\\ \text{VG} & \text{weight} & = & 4\end{array}\right.$$

Tertiary components with three inputs:

$$\text{PR (WATER)} = \left\{\begin{array}{llll}\text{VB} & \text{f we ght} & = & 0, 1, 2\\ \text{B} & \text{we ght} & = & 3\\ \text{A} & \text{we ght} & = & 4\\ \text{G} & \text{we ght} & = & 5\\ \text{VG} & \text{we ght} & = & 6\end{array}\right.$$

$$\left\{\begin{array}{c}\text{ST(WATER)}\\ \text{PR(POLICY)}\\ \text{ST(WEALTH)}\\ \text{PR(KNOW)}\end{array}\right\} = \left\{\begin{array}{llll}\text{VB} & \text{f we ght} & = & \text{0 or 1}\\ \text{B} & \text{we ght} & = & 2\\ \text{A} & \text{we ght} & = & 3\\ \text{G} & \text{we ght} & = & 4\\ \text{VG} & \text{we ght} & = & \text{5 or 6}\end{array}\right.$$

Freshwater availability and quality have become an increasingly crucial concern for many countries. The rule base of PR(WATER) is more pessimistic than those of the other tertiary components. Indeed, out of the seven possible weights (0–6) of PR(WATER), the four smallest ones or 60% correspond to the fuzzy sets VB and B. This is in agreement with widely accepted practices for the assessment of environmental pressures. For example, OECD (2004) considers water stress to be high when the annual water withdrawals are at least 40% of the total renewable water resources. Equivalently, 60% of values are VB or B. The same reasoning is followed in the rule bases of pressure indicators PR(LAND) and PR(BIOD) which have six inputs.

Tertiary components with four inputs:

$$\left\{\begin{array}{c} \text{RE(LAND)} \\ \text{ST(AIR)} \\ \text{PR(HEALTH)} \\ \text{ST(HEALTH)} \end{array}\right\} = \left\{\begin{array}{llcl} \text{VB} & \text{f we ght} & = & 0, 1, 2 \\ \text{B} & \text{we ght} & = & 3 \\ \text{A} & \text{we ght} & = & 4 \\ \text{G} & \text{we ght} & = & 5 \\ \text{VG} & \text{we ght} & = & 6, 7, 8 \end{array}\right.$$

$$\text{ST(POLICY)} = \left\{\begin{array}{llcl} \text{VB} & \text{f we ght} & \leq & 3 \\ \text{B} & \text{we ght} & = & 4 \text{ or } 5 \\ \text{A} & \text{we ght} & = & 6 \\ \text{G} & \text{we ght} & = & 7 \\ \text{VG} & \text{we ght} & = & 8 \end{array}\right.$$

ST(POLICY) gives the state of human rights and is assessed using more strict criteria than the other components.

Tertiary components with five inputs:

$$\left\{\begin{array}{c} \text{RE(HEALTH)} \\ \text{RE(KNOW)} \end{array}\right\} = \left\{\begin{array}{llll} \text{VB} & \text{f we ght} & \leq & 3 \\ \text{B} & \text{we ght} & = & 4 \\ \text{A} & \text{we ght} & = & 5 \\ \text{G} & \text{we ght} & = & 6 \\ \text{VG} & \text{we ght} & > & 7 \end{array}\right.$$

Tertiary components with six inputs:

$$\left\{\begin{array}{c} \text{PR(LAND)} \\ \text{PR(BIOD)} \end{array}\right\} = \left\{\begin{array}{llll} \text{VB} & \text{f we ght} & \leq & 7 \\ \text{B} & \text{we ght} & = & 8 \\ \text{A} & \text{we ght} & = & 9 \\ \text{G} & \text{we ght} & = & 10 \\ \text{VG} & \text{we ght} & > & \text{11 or 12} \end{array}\right.$$

$$\left\{\begin{array}{c} \text{PR(HEALTH)} \\ \text{ST(KNOW)} \end{array}\right\} = \left\{\begin{array}{llll} \text{VB} & \text{f we ght} & \leq & 4 \\ \text{B} & \text{we ght} & = & 5 \\ \text{A} & \text{we ght} & = & 6 \\ \text{G} & \text{we ght} & = & 7 \\ \text{VG} & \text{we ght} & \geq & 8 \end{array}\right.$$

Environmental pressures are judged using stricter rules, as discussed previously.

Secondary components with three inputs (PR, ST, RE):

$$\left\{\begin{matrix} \text{LAND, WATER} \\ \text{BIOD,AIR} \\ \text{POLICY, WEALTH} \\ \text{HEALTH,KNOW} \end{matrix}\right\} = \begin{cases} \text{VB} & \text{f we ght} & = & 0 \text{ or } 1 \\ \text{B} & \text{we ght} & = & 2,\ 3,\ 4 \\ \text{A} & \text{we ght} & = & 5,\ 6,\ 7 \\ \text{G} & \text{we ght} & = & 8,\ 9,\ 10 \\ \text{VG} & \text{we ght} & = & 11 \text{ or } 12 \end{cases}$$

Finally, the rule bases of the primary components of sustainability and the overall sustainability index are:

$$\left\{\begin{matrix} \text{ECOS} \\ \text{HUMUS} \end{matrix}\right\} = \begin{cases} \text{VB} & \text{if weight} = & 0,1,2 \\ \text{B} & \text{weight} = & 3,4,5,6 \\ \text{A} & \text{weight} = & 7,8,9,10 \\ \text{G} & \text{weight} = & 11,12,13 \\ \text{VG} & \text{weight} = & 15 \text{ or } 16 \end{cases}$$

$$\text{OSUS} = \begin{cases} \text{EL} & \text{if weight} = & 0 \\ \text{VL} & \text{weight} = & 1 \\ \text{L} & \text{weight} = & 2 \\ \text{I} & \text{weight} = & 4 \\ \text{FH} & \text{weight} = & 5 \\ \text{H} & \text{weight} = & 6 \\ \text{VH} & \text{weight} = & 7 \\ \text{EH} & \text{weight} = & 8 \end{cases}$$

Fuzzy inference

Each inference stage, or inference engine, of the SAFE model has its own set of rules, or rule base, and combines certain input indicators into a composite output indicator.

The inference engines of SAFE uses product-sum algebra to compute the membership grades of the output indicator to the corresponding fuzzy sets. Products and sums correspond to the logical operations of conjunction ("and") and disjunction ("or"). The operation "and" is involved in the rules and the operation "or" corresponds to an operation that aggregates all rules. Product-sum inference is described below by means of an example.

Each rule is assigned a *firing strength* which measures the degree to which the rule matches the inputs. Suppose, for example, that ECOS is A (Average) with membership grade 0.4 and G (Good) with grade 0.6, and HUMS is A with membership grade 0.9 and G with grade 0.1. Consider four rules of the rule base for OSUS:

a. *R* 1

if

ECOS is A

and HUMS is A

then

OSUS is I (Intermediate).

b. *R* 2

if

ECOS is A

and HUMS is G

then

OSUS is FH (Fairly High).

c. *R* 3

if

ECOS is G

and HUMS is A

then

OSUS is FH (Fairly High).

d. R 4

if

ECOS is G

and HUMS is G

then

OSUS is H (High)

The firing strength of a rule is given by the product of the input membership grades, and this value is passed to the membership grade of the output to the corresponding fuzzy set. Thus,

- firing strength of $R_1 = 0.4 \times 0.9 = 0.36$ = membership grade of OSUS to the fuzzy set I
- firing strength of $R_2 = 0.4 \times 0.1 = 0.04$ = membership grade of OSUS to the fuzzy set FH
- firing strength of $R_3 = 0.6 \times 0.9 = 0.54$ = membership grade of OSUS to the fuzzy set FH
- firing strength of $R_4 = 0.6 \times 0.1 = 0.06$ = membership grade of OSUS to the fuzzy set H.

If several rules assign the same fuzzy set to the output variable (here we have a disjunction or union of rules), then the overall membership grade of the output is the sum of the individual firing strengths. In the above example, both rules R_2 and R_3 assign the fuzzy FH to OSUS. Thus, the output of the inference engine is:

$\mu_{\mathrm{I}}(\mathrm{OSUS}) = 0.36$, $\mu_{\mathrm{FH}}(\mathrm{OSUS}) = 0.04 + 0.54 = 0.58$, $\mu_{\mathrm{H}}(\mathrm{OSUS}) = 0.06$.

Defuzzification

Finally, a crisp value for OSUS is computed via the height method of defuzzification,

$$OSUS = \frac{\sum_{all\ fuzzy\ sets\ L\ of\ OSUS}(y_L \mu_L(OSUS))}{\sum_{all\ fuzzy\ sets\ L\ of\ OSUS}(\mu_L(OSUS))}$$

where y_L is the *peak value* of the fuzzy set L—a value of OSUS for which the membership function of L is maximized.

For the example given in the previous section, only I, FH, and H are involved in the defuzzification. It is seen in Fig. 6c that $y_{\mathrm{I}} = 0.5$, $y_{\mathrm{FH}} = 0.625$, and $y_{\mathrm{H}} = 0.75$. Therefore, the overall sustainability is given by

$$\mathrm{OSUS} = \frac{0.5 \text{ x } 0.36 + 0.625 \text{ x } 0.58 + 0.75 \text{ x } 0.06}{0.36 + 0.58 + 0.06} = 0.5875$$

Sensitivity analysis

Sensitivity analysis plays a fundamental role in decision making because it determines the effects of a change in a decision parameter on system performance. In this section, we attempt to provide an answer to the question of how to design policies for sustainable development. The SAFE model could aid decision makers to formulate sustainable policies by assessing sustainability for different scenarios of development. A scenario is defined by the available sustainability indicators, which largely reflect the results of policies and actions taken in a particular period. When these values are changed and the resulting changes on sustainability observed, we could identify the most important indicators contributing to sustainable development. This procedure is known as sensitivity analysis.

Sensitivity analysis entails the computation of the gradients of ECOS, HUMS, and OSUS with respect to each basic indicator. A gradient gives the increase of sustainability per unit increase of some basic indicator. To perform sensitivity analysis, we follow the steps:

1. ***Calculation of OSUS:***

a. For a given country, normalize and smooth all indicator data using the methods descr ibed in previous sections.

b. Fuzzify the basic inputs.

c. Compute the membership grades of composite indicators to the fuzzy sets VB, B, A, G, and VG. Start from the inference engines

that use only basic indicators as inputs and proceed successively to the ones that use c omposite indicators. Finally, compute

the membership grades of OSUS to the nine fuzzy sets EL, VL, …, EH and compute a crisp value for OSUS by height defuzzification.

2.***Introduction of perturbation:***

For some basic indicator, say, c increases its normalized value $x_c \in [0, 1]$ by some fixed a mount δ, for example, 0.1 or 10%.

If the result is greater than one, then truncate it to one to avoid overshooting permissible regions of indicators.

3.***Sensitivity analysis:***

Assess the overall sustainability using the same set of data as in step 1 except for indicator c whose value is now $x_c + \delta$.

Denote the new assessment by OSUS ($x_c + \delta$). The gradient of OSUS with respect to x_c is defined by the forward difference:

$$\Delta_c = \text{OSUS}\,(x_c + \delta) - \text{OSUS}.$$

Reset the basic indicator c to its original value x_c.

4.***Loop:***

Repeat steps 2 and 3 for all basic indicators.

5.***Ranking:***

Identify the gradients with the largest values, which correspond to the basic indicators th at affect OSUS the most.

An important feature of the SAFE model is monotonicity. Whenever a basic indicator of sustainability is improved, the components of sustainability that depend on this indicator as well as OSUS increase or at least do not decrease, that is, if $\delta \geq 0$, then $\Delta_c \geq 0$. The use of product-sum algebra in all inference engines ensures that the hierarchical fuzzy system is monotonic (Kouikoglou and Phillis, 2009).

By changing several indicators simultaneously in step 3 we can compute gradients of higher orders and formulate more comprehensive environmental policies. For example, the second-order gradient of OSUS with respect to indicators c and c' is

$$\Delta_{c,c'} = \text{OSUS}(x_c + \delta, x_{c'} + \delta) - \text{OSUS}.$$

Sensitivity analysis is biased towards indicators which belong to small groups. For example, RE(AIR) depends only on renewable resources production. Therefore, an increase in the latter directly affects the former. ST(AIR), on the other hand, depends on four basic indicators, labeled 26–29. An improvement of one of these indicators will result in a small improvement of ST(AIR). To avoid this bias, a basic indicator c is ranked according to the product

$$D_c = (1 - x_c)\Delta_c$$

where $1 - x_c$ is the distance of indicator c from the sustainable value, and Δ_c is the gradient of OSUS with respect to x_c. Thus, those indicators that affect OSUS the most and are farther in the unsustainable region are pinpointed and ranked accordingly.

1.2.2 Sustainability Assessment by United Nations Sustainable Development Goals (UN-SDGs)

As with SAFE, indicator data are normalized over [0, 1] and then aggregated using arithmetic or geometric mean, due to that the geometric mean ranking has small differences from that of the arithmetic mean, the arithmetic average was used.

The Sustainable Development Goals covering the following sustainability goals:

1. End poverty
2. Food Security
3. Ensure healthy and promote wellbeing
4. Inclusive and equitable quality education
5. Gender equality
6. Clean water and sanitation
7. Affordable and clean energy
8. Decent work and economic growth

9. Industry, innovation, and infrastructure
10. Reduced inequalities
11. Sustainable cities and communities
12. Responsible consumption and production
13. Climate action
14. Life below water
15. Life on land
16. Peace, justice, and strong institution
17. Partnership to achieve goals

1.3. Graphical approaches

1.3.1 CD HJ-Biplot methods

Models that measure sustainability rely on large databases leading to various indicators. It is desirable to reduce dimensionality and summarize the information captured by a large number of variables in a simple way that can enable a straightforward depiction of the overall sustainability state of the world. Biplot methods are tools widely used to obtain a joint representation of objects or individuals. An HJ-Biplot is a multivariate graphical representation of a matrix $\mathbf{X}$, using markers (vectors) $j_1, j_2, \ldots j_n$ for its rows, and $h_1, h_2, \ldots h_p$ for its columns, chosen so that both markers can overlap in the same reference system with maximum representation quality (Galindo Villardón, 1986) . Using biplots to depict data associated with many countries and many corresponding sustainability indicators proves to be quite useful in this regard (De Soete & Carroll, 1994; Rocci, R., Gattone, S. A., & Vichi, M., 2011).

The clusters disjoint HJ-Biplot (Nieto-Librero et al., 2017) is based on ideas from Macedo & Freitas (2015), disjoint biplots (Vichi & Saporta, 2009; Vigneau & Qannari, 2003;

Vines, 2000), clustering biplots (De Soete & Heiser, 1993; Kiers, H. A. L., Vicari, D., & Vichi, M.l., 2005; Rocci, R., Gattone, S. A., & Vichi, M., 2011; Vichi & Kiers, 2001), HJ-Biplots (Galindo Villardón, 1986), and biplot methods in Gabriel, (1971).

The clustering disjoint HJ-Biplot (CD Biplot) algorithm combines the k-means procedure used to form clusters with the HJ-Biplot, which improves graphical data representation. The goal is to find the directions that maximize separation between centroids, which represent mean values of a set of point coordinates of P clusters of individuals (e.g., names of countries) found in the data, and to obtain a representation in an HJ-Biplot. In a CD HJ-Biplot, the extracted factorial axes are disjoint; that is, each variable (here the sustainability indicators by country) of the starting matrix only contributes to the solution of one axis with zero contributions to the other axes. This disjoint nature is achieved by dividing the total space into disjoint subspaces and extracting from each the direction of maximum variability across all variables.

The goal of the CD HJ-Biplot algorithm is to specify appropriate matrices for the coordinates of countries, indicators, and centroids in the graph. To ensure an appropriate representation of the data, an alternating least squares (ALS) algorithm is used to solve a non-convex optimization problem by reducing it to linear regression. This is done by fixing one matrix at a time while optimizing the other. The clustering disjoint biplot model results from the application of an HJ-Biplot on the transformed data matrix, where each object is replaced by its centroid. The centroids are obtained by applying a k-means algorithm on the original data matrix. Each iteration of the algorithm has two steps: allocation of the objects by using the k-means algorithm followed by a search for a reduced space by using an HJ-Biplot on the resulting centroids to obtain the J sustainability indicators that contribute to one of the Q components, or equivalently the axes in the CD HJ-Biplot (Nieto-Librero et al., 2017)

The HJ-BIPLOT multivariate procedure allows simultaneous visualization of variables and cases, the graphical display obtained has maximum quality of representation for rows and columns (Alvarez & Villardon, 2015), explore relationships between centrality measures and classify them according to their centrality(Bernal et al., 2020), the results are similar to other scientific results on linear relationship (Suarez et al., 2016). Combinations of various techniques were implemented, such as Hj-Biplot, cluster analysis, dasymetric mapping and cross-entropy, with good results (Xavier et al., 2018). To improve the interpretation of the results the elastic net HJ biplot, was proposed, which applies the penalty of elastic net (Cubilla-Montilla et al., 2021) .

This technique has already been used in contexts such as Medicine, Psychology and social science: to analyze the corporate social responsibility practices carried out by Brazilian companies (Gallego-Alvarez et al., 2014). To analyze the effect of coercive isomorphism (legal system) on Corporate Social Responsibility (CSR) at the country level by using the multivariate statistical techniques X-STATIS and HJ-biplot, which allow us to capture the role played by these institutional forces in the evolution and patterns around the commitment to sustainability (Amor-Esteban, Galindo-Villardon, et al., 2018) . Biplot technology (HJ and Logistic mode), allows a multivariate comparison of sustainability indicators (continuous variables) and economics variables(Urruticoechea & Vernazza, 2019). Demonstrate the usefulness of the HJ-Biplot in bibliometric studies. Using HJ-Biplot it is possible to interpret simultaneously the position of the centers, represented by dots; indicators, represented by vectors; and the relationships between them (Diaz-Faes et al., 2013).

Based on both neo-institutional theory and comparative institutional analysis, the role that mimetic forces play in the patterns and evolution of behavior concerning company sustainability. Through employing the multivariate statistical methods HJ-biplot and X-STATIS, which provide a useful visualization of a complex data structure in a low-dimensional space (Amor-Esteban, Galindo-Villardon, et al., 2018). To analyze whether there are differences in the scores obtained by a broad sample of countries in the Sustainable Society Index according to the geographical area in which the country is located (Gallego-Álvarez et al., 2015). Also, for analyze the media coverage of the Catalan Parliament's ban on bullfights (Litago et al., 2017). Based on institutional and stakeholder theory, the influence that the cultural system has on the degree of responsibility of business behavior and how normative isomorphism influences the Corporate Social Responsibility practices at the country level were examined, given the multidimensional character of the data, the exploratory statistical techniques X-STATIS and HJ-biplot was used (Amor-Esteban, Garcia-Sanchez, et al., 2018). Multi-Scale Integrated Analysis of Societal and Ecosystem Metabolism (MuSIASEM) with the HJ-Biplot allows us to easily know the detailed behavior of the labor productivity and energy consumption of a particular country (Tejedor-Flores et al., 2017).

In Geology and environmental issues: the chemical analyzes of the principal and trace elements of all the samples were statistically analyzed using the inertia method based on an HJ-biplot (Garcia-Talegon et al., 1999). Quantification and reporting greenhouse gas emissions, being one of the most important monitoring and auditing proposed to mitigate climate change, which in turn affects business (Martinez-Ferrero & Gallego-Alvarez, 2013). Relationships between different pollutants and temporal evolution of pollution in

Salamanca (Cabrera et al., 2006), and identification of pollution patterns in geochemical studies (Nieto-Librero et al., 2017)

In the amazing field of agriculture, the following are conspicuous examples of its versatility: Identification of the link between bioactive compounds of tomatoes (Valchev et al., 2020). Examine the effects of cultivar, agricultural practices, climatic factors, and their interactions (Hernandez et al., 2014). Represent the variation of soil erodibility properties grouped in land uses, native grassland were the ones that least correlated with other land uses (Ferreira et al., 2015).

1.3.2 Machine learning techniques

The development of artificial intelligence in 1956 has increasingly spread into various disciplines such as medicine (Dorado-Diaz et al., 2019), disease analysis (Zhang et al., 2020), ECG arrhythmias classification (Hou et al., 2020), breast mass segmentation in high-resolution mammograms (Yan et al., 2019), predicting In-Stente Restenosis (Avram et al., 2020), agriculture (Bolandnazar et al., 2020), biology (Neftci & Averbeck, 2019), video captioning (Sun et al., 2019), bioinformatics (Inza et al., 2010), bioinformatics (Pambabay-Calero et al., 2021)and engineering optimization problems (Anita, Yadav, A., & Kumar, N., 2020), among others.

Modern computational approaches and machine learning techniques speed up calculation processes. Scenarios of machine learning vary according to the categories of training data available, the sequence and algorithm of processing training data, and the test data utilized to assess the learning algorithm.

Machine learning uses artificial neural networks. An artificial neural network (ANN) is a computer system that is made up of a collection of connected units called neurons that are organized into layers. Neurons are commonly called nodes. Each connection between two nodes has an associated weight, which is just a number that represents the strength of the connection between the two nodes. Layers positioned between the input and output layers are known as hidden layers (Deeplizard, 2017).

The number of nodes contained in each type of layer is:

- Input layer - One node for each component of the input data.
- Hidden layers - Arbitrarily chosen number of nodes for each hidden layer.
- Output layer - One node for each of the possible desired outputs.

Data flows through the network starting at the input layer and moving through the hidden layers until the output layer is reached. We pass the weighted sum from each node from the previous layer plus a bias term to an activation function, which transforms the sum into a number that is often between a lower bound and some upper bound (ibid).

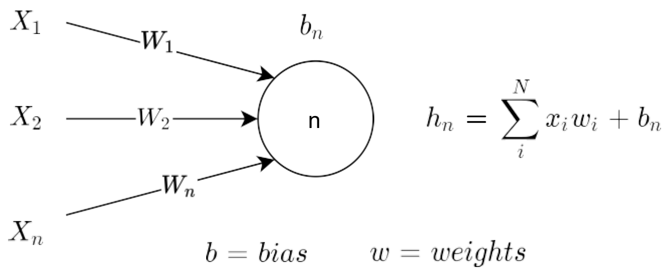

A commonly used activation function is the rectified linear unit (ReLU), that transforms the input to the maximum of either 0 or the input itself. The idea here is, the more positive the neuron is, the more activated it is.

$$\mathrm{ReLU}\ (\mathrm{x}) = \max\ (0, \mathrm{x})$$

The loss function measures how similar the reconstructed version is to the original version. The more similar the reconstructed output is to the original input, the lower the loss. One common loss function is mean squared error (MSE). After passing all of our data through our model, we will continue to pass the same data over and over again. This process of repeatedly sending the same data over the network is considered training. It is during this training process that the model will learn (ibid).

The weights are optimized using an optimization algorithm. The optimization process depends on the chosen optimization algorithm (optimizer). The best-known optimizer is called stochastic gradient descent (SGD).

The objective of SGD is to minimize some given function that we call a loss function. Therefore, SGD updates the model weights in such a way that this loss function works as close as possible to its minimum value. We start the training process with arbitrarily set weights, and then we gradually update these weights as we get closer and closer to the minimized loss (ibid).

During training after the loss is calculated for our inputs, the gradient of that loss is calculated concerning each of the weights in our model. Once we have the value of these gradients, this is where the idea of our learning rate comes in. The gradients will then get multiplied by the learning rate.

$$\text{old weight} - (\text{learning rate} * \text{gradient})$$

This learning rate is a small number that typically ranges from 0.01 to 0.0001, but the actual value can vary, and whatever value we get for the gradient will become quite small once we multiply it by the learning rate (ibid).

To calculate the weight's new value, we use this formula:

$$\text{new weight } = \text{old weight } - (\text{learning rate } * \text{ gradient})$$

The principal machine learning scenarios are supervised, semi-supervised, and unsupervised learning.

Supervised learning uses a series of labeled samples as training data in order to predict all unseen instances, which occur in problems of classification, regression, and ranking. This type of learning is applied in several areas such as anomaly detection, face recognition, signal and image classification, weather forecasting (Qiuyu Zhu, 2020; Yang, Y., Zheng, K., Wu, B., Yang, Y., & Wang, X., 2020).

In the case of Semi-supervised learning, the learner receives a training sample composed of both labeled and unlabeled instances and predicts all unseen instances. This is preferred when it is easy to access unlabeled data, due to labels that are costly to obtain. Classification, regression, and ranking processes are some typical applications (Fu, H., Lei, P., Tao, H., Zhao, L., & Yang, J., 2019; Fu, X., Wei, Y., Xu, F., Wang, T., Lu, Y., Li, J., & Huang, J., 2019; Zhu & Li, 2020). Across a variety of experiments performed on various image and audio datasets, the source separation performance of our method is as good as the method that performs source separation under source class supervision. Furthermore, the proposed method does not require the class labels and can predict the labels (Hizli et al., 2020).

In Unsupervised learning, the learner solely receives unlabeled training data and predicts all unseen instances. Clustering and reduction of dimensionality (Chorowski, J., Weiss, R. J., Bengio, S., & Van Den Oord, A., 2019; Yusiong & Naval, 2019), as well as anomaly detection, and association rule-mining (Sarkar, D., Bali, R., & Sharma, T., 2018) are some applications. Deep learning and especially Variational Auto-Encoders (VAEs) have shown great potential in unsupervised learning of data distribution (Zimmerer et al., 2019).

With unsupervised learning, each piece of data that is passed into our model during training is just an unlabeled input object. Since the training data labels are unknown to the model, there is no way to measure accuracy. Accuracy is not typically a metric that we use to analyze an unsupervised learning process. Essentially, with unsupervised learning, the model will be given an unlabeled dataset and will attempt to learn some kind of *structure* from the data and extract the useful information or features from this data.

There are different forms of clustering techniques, as follows: Centroid-based approaches: K-medoids and K-means; Hierarchical clustering approaches: divisive and agglomerative; Distribution based clustering approaches: Gaussian mixture models; and density-based techniques: optics dbscan.

One of the most popular applications of unsupervised learning is the use of clustering algorithms. A clustering algorithm analyzes data and learns their structure even though they are not labeled. By learning the structure, you can start to cluster your data into groups.

Complex data distribution can be analyzed using an autoencoder, which leads to dimensionality reduction with nonlinear feature extraction techniques. Based on the basic structure of the universal autoencoder, it is possible to understand the optimal comprehensive results of encoding, decoding, classification, and good generalization performance of the model at the same time.

Dimensionality reduction is an important technique in machine learning and data mining, accelerating the processing of high-dimensional data. An effective method for dimensionality reduction can find a subset of low-dimension features that extracts the most relevant information (Xie et al., 2019)

Dimensionality reduction plays an important role in data mining and machine learning data processing, making high-dimensional data processing more efficient. Dimensionality reduction can extract the representation of low-dimensional features from high-dimensional data, and an effective dimensionality reduction method can not only extract most of the useful information of the original data, but also perform the function of removing useless noise (Liu et al., 2020).

Variational autoencoder is an autoencoder, used principally in unsupervised deep learning scenarios, whose encoding distribution is regularized during the training to achieve organized latent space representations (continuity and completeness), and use these representations to generate some additional data. Variational autoencoder learns a latent vector model for its input data. So instead of letting your neural network learn an arbitrary function, you are learning the parameters of a probability distribution that models your data (Deeplizard, 2017).

One of the main challenges facing the industry when it comes to big data for fault diagnosis is the high dimensionality of such data. This can be addressed using a dimensionality reduction method, such as principal components analysis. More recently, variational auto-encoders are one of the most promising techniques for unsupervised learning with successful applications in image processing and speech recognition. The results show that variational auto-encoders are a competent and promising tool for dimensionality reduction (San Martin et al., 2019).

First, an encoder network turns the input samples x into two parameters using a latent vector, called z_mean and z_log_sigma. Then, we randomly sample similar points z from the latent normal distribution that is supposed to generate the data, via z = z_mean + exp(z_log_sigma) * epsilon, where epsilon is a random normal tensor (Zhu et al., 2020) . Finally, a decoder network maps these latent vector points back to the original input data (ibid).

The parameters of the model are trained via two loss functions:

a ***reconstruction loss*** that forces the decoded samples to match the initial inputs, and the Kullback-Leibler (KL) divergence between the learned latent distribution and the prior distribution, acting as a ***regularization term***. This helps to learn well-formed latent vectors and to reduce overfitting to training data (ibid).

The KL divergence regularization is deduced based on the principle of variational Bayes inference (Ping et al., 2019).

The goal in unsupervised learning is to discover uniformities in the input data because particular patterns appear more frequently than others in the input space configuration. In statistics, this is known as density estimation, and with the clustering approach, it is possible to find clusters or input clusters. Such grouping also allows the identification of outliers (Bengio, 2009).

Clustering techniques are machine learning approaches used to find similar patterns and relationships between data samples, and then cluster these samples into different groups. Each cluster has some attributes or correlation characteristics. Because, they are fully unsupervised, they seek to cluster data without prior training, guidance, or knowledge of characteristics, relationships, and associations of the data (Sarkar, D., Bali, R., & Sharma, T., 2018).

K-means stands for learning predictive clustering, and we can learn a clustering model from training data. Therefore, taking into account that our database is numerical, we decided to use the Euclidean distance to minimize some distance-related quantity over all instances of the set. In addition, it is important to mention that in a K-means problem there is no effective solution to identify the global minimum. Generally speaking, while K-means converge in finite time to a stationary point, there can be no certainty whether the convergence point is the global minimum or not, no matter how far we are from it (Flach, 2012).

We propose using the variational autoencoder plus graphical analysis (VAE&GA) grounded on Gaussian-distributed class centroids of latent variables to training the network to ensure the maximization of inter-class distance and the minimization of inner-class distance in assessing world sustainability.

1.4. Problem identification and definition

The research problem lies in understanding how graphical approaches a complement to numerical classification methods can be and how the unsupervised machine learning procedure can help overcome criticism of fuzzy logic that is fundamental in the opinion of experts in the field. The emphasis of this work is on the use of the CD-HJ-Biplot procedure to complement the presentation of research results in the form of classification tables, such as: SAFE and UN-SDG, adopting a more integrative approach framed in numerical and pictorial tools.

1.5. Research aim

Evaluating sustainability is urgent and necessary today. The question: How can sustainability be measured? remains unanswered because it is difficult to understand and reconcile between people, government entities, and others. There are too many dimensions involved in analysis, and people's perception varies from considering sustainability as a word that is being overstated, a fashionable word, or to a complex task given its holistic nature, which requires an integral approach. For this reason, we propose the application of Clustering Disjoint-HJ-Biplot and variational autoencoders to graphically visualize the performance of a country's sustainability helping decision-makers propose better alternatives to achieve the so longed for sustainability.

1.6. Research objectives

The specific objectives of this work were:

i. To evaluate the CD-HJ Biplot approach assessing sustainability as a complement of a Fuzzy Logic procedure using SAFE and United Nation Sustainable Development Goals databases.

ii. To evaluate the Variational autoencoder as a data training procedure.

CHAPTER 2. MATERIALS AND METHODS

2.1. Database acquirement and Software

The database of SAFE 2019 covers 69 basic indicators for a period of twenty-six years (1990–2016) (Grigoroudis, E., Kouikoglou, V., and Phillis, 2019), and was generously provided by my advisor Dr. Phillis. Y. A. The data were originally collected from such sources as Eurostat, World Health Organization, Organization for Economic Co-operation and Development, United Nations, World Bank, and similar authoritative entities.

The Sustainable Development Goals database contains 77 indices for 149 countries for the year 2016 SDG and was taken from the Index and Dashboards - Global Report.. https://www.sdgindex.org/reports/sdg-index-and-dashboards-2016. This report (including the SDG Index & Dashboards) is a complement to the official indicators and voluntary-led review processes. The report is not an official monitoring tool. It uses publicly available data published by official data providers (World Bank, WHO, ILO, others) and other organizations including research centers and non-governmental organizations (Sachs, J., Schmidt-Traub, G., Kroll, C., Durand-Declare, D., &Teksoz, K., 2016).

2.2. Data analysis

To analyze SAFE and UNDGs databases we used the CD-HJ-Biplot algorithm provided by Ana Belen Nieto (Nieto-Librero, A. B., Sierra, C., Vicente-Galindo, M. P., Ruíz-Barzola, O., & Galindo-Villardón, M. P., 2017), and for the Variational autoencoders model design, training, testing and plotting, we used Google colaboratory with Python 3.7, and the following libraries for the numerical computation and machine learning: Pandas 1.1.4, Tensorflow 2.1, and Keras 2.3.1 (Appendix 2).

2.2.1. CD-HJ-Biplot algorithm

The main considerations of this algorithm are reported as follows:

To start the iterations set $k=0$. Then consider countries first. A matrix $\mathbf{U}$ contains the names of I countries in its rows and the P clusters in its columns and allocates these countries into clusters. Then a matrix $\bar{\mathbf{X}}$ of the centroids in the original space is calculated together with a matrix $\mathbf{Z}$ that identifies the countries by cluster centroid.

Next, the J indicators are allocated into Q subsets via a stochastic binary matrix $\mathbf{V}_0$ of order $J \xi Q$ where J is the number of sustainability indices and Q the number of components. $\mathbf{V}_0 = |u_{jq}|$, where $u_{jq}=1$ if indicator j contributes to the component q, and $u_{jq}=0$ otherwise. Then, the coordinates of the indicators in the new space of disjoint components are computed by matrix $\mathbf{B}_0$ and the coordinates of the objects in the same space of the Q disjoint components by matrix $\mathbf{A}$, and the coordinates of the corresponding centroids by matrix $\bar{\mathbf{A}}$.

Step 1: Cluster of countries

The process starts from an original data matrix $\mathbf{X}$ of order $I \xi J$ that contains the information of I names of countries over which J normalized sustainability indicators have been measured.

Define the binary matrix $\mathbf{U}_0$ of order $I \xi P$ that contains names of countries in its rows, and cluster numbers u_{ip} in its columns, such that $u_{ip}=1$ if the country i belongs to cluster p and $u_{i}\ =0$ otherwise. This matrix is stochastic.

The object centroid matrix $\bar{\mathbf{X}}_0$ of order $P \xi J$ is generated so that the following squared error is minimized concerning to $\bar{\mathbf{X}}_0$ (for details see (Nieto-Librero, A. B., Sierra, C., Vicente-Galindo, M. P., Ruíz-Barzola, O., & Galindo-Villardón, M. P., 2017):

$$\left\|\mathbf{X}-\mathbf{U}_0\bar{\mathbf{X}}_0\right\|^2 \tag{1}$$

Differentiation yields:

$$\mathbf{X}_0 = \left(\mathbf{U}_0^T\mathbf{U}_0\right)^{-1}\mathbf{U}^T\mathbf{X} \tag{2}$$

Next compute the matrix $\mathbf{Z}_0 = \mathbf{U}_0\bar{\mathbf{X}}_0$, which contains the centroid values of the clusters to which each object belongs rather than the original $\mathbf{X}$ values.

Step 2: Indicators

Define $\mathbf{V}_0$, the matrix with only one nonzero element per row, equal to 1. The nonzero elements of the q-th column of $\mathbf{V}_0$ identify the indicators that contribute to the component q. Using $\mathbf{Z}_0$ and $\mathbf{V}_0$, the matrix $\mathbf{B}_0$ of the coordinates of the indicators is constructed column by column.

We form a submatrix $\mathbf{W}_{0q}$ with the nonzero columns q of $\mathbf{V}_0$. These columns signify the indicators that contribute to component q. We then decompose $\mathbf{W}_{0q}$ as follows

$$\mathbf{W}_{0q} = \mathbf{R}\bar{\mathbf{\Lambda}}\mathbf{T}^T \tag{3}$$

where $\mathbf{R}$ and $\mathbf{T}^T$ are orthonormal matrices (their columns are orthogonal and their norm equals 1), and $\bar{\mathbf{\Lambda}}$ the diagonal matrix of eigenvalues of the q-th decomposition. The coordinates of the indicators in the HJ-Biplot are $\mathbf{B}_{0_q} = \mathbf{T}\bar{\mathbf{\Lambda}}$.

The coordinates of countries and corresponding centroids are:

$$\mathbf{A}_0 = \mathbf{X}\mathbf{B}_0\bar{\mathbf{\Lambda}}^{-1} \tag{4}$$

$$\bar{\mathbf{A}}_0 = \bar{\mathbf{X}}\mathbf{B}_0\bar{\mathbf{\Lambda}}^{-1} \tag{5}$$

where $\bar{\mathbf{\Lambda}}_0$ is the usual diagonal of eigenvalues for the q-th decomposition.

Finally, the value of the objective function $F_0 = \left\|\mathbf{U}_0\bar{\mathbf{A}}_0\right\|^2$ is computed.

k-th iteration

Given $\mathbf{U}_{k-1}$, $\bar{\mathbf{X}}_{k-1}$, $\mathbf{Z}_{k-1}$, $\mathbf{A}_{k-1}$, $\bar{\mathbf{A}}_{k-1}$, $\mathbf{V}_{k-1}$, $\mathbf{\Lambda}_{k-1}$, $\mathbf{B}_{k-1}$, and the objective function F_{k-1} at step $k-1$, we proceed as follows:

Cluster of countries

$\mathbf{U}_k$ is updated via the coordinate matrix of countries $\mathbf{A}_{k-1}$ and the matrix of centroid coordinates $\bar{\mathbf{A}}_{k-1}$ through a *k*-means algorithm in the reduced space. Each country is thus assigned to the closest centroid. Then the following matrices are updated $\bar{\mathbf{X}}_k = \left(\mathbf{U}_k^T\mathbf{U}_k\right)^{-1}\mathbf{U}^T\mathbf{X}$ and $\mathbf{Z}_k = \mathbf{U}_k\bar{\mathbf{X}}$. If a cluster is empty, the procedure in the initial iteration is repeated.

Sustainability indicators

Now we update $\mathbf{V}_k$. Consider row j. Rows $1,\ldots,j-1,j+1,\ldots,J$ are fixed, while all elements of the row j are set equal to zero. The nonzero element of the row j is positioned in all Q positions, thus constructing Q different matrices $\bar{\mathbf{V}}_{kq}$. The matrices $\mathbf{A}_k$, $\bar{\mathbf{A}}_k$, and $\mathbf{B}_k$, as well as F_k are computed using each of the constructed $\bar{\mathbf{V}}_{kq}$. We choose the nonzero element that yields the maximum of the objective function and fix its position in the row j. This procedure is repeated for the remaining rows of $\mathbf{V}_k$. Having the updated $\mathbf{V}_k$, we go back to step 2 to update $\mathbf{A}_k$, $\bar{\mathbf{A}}_k$, $\mathbf{\Lambda}_k$, and $\mathbf{B}_k$.

Stopping

The stopping criterion is set at a difference between F_k and F_{k-1} less than or equal to 10^{-6}. To avoid entrapment, the algorithm is run several times at a minimum of 1,000 to find a stable solution (Nieto-Librero, A. B., Sierra, C., Vicente-Galindo, M. P., Ruíz-Barzola, O.,

& Galindo-Villardón, M. P., 2017). In Figure 2 the CD HJ-Biplot algorithm is shown pictorially.

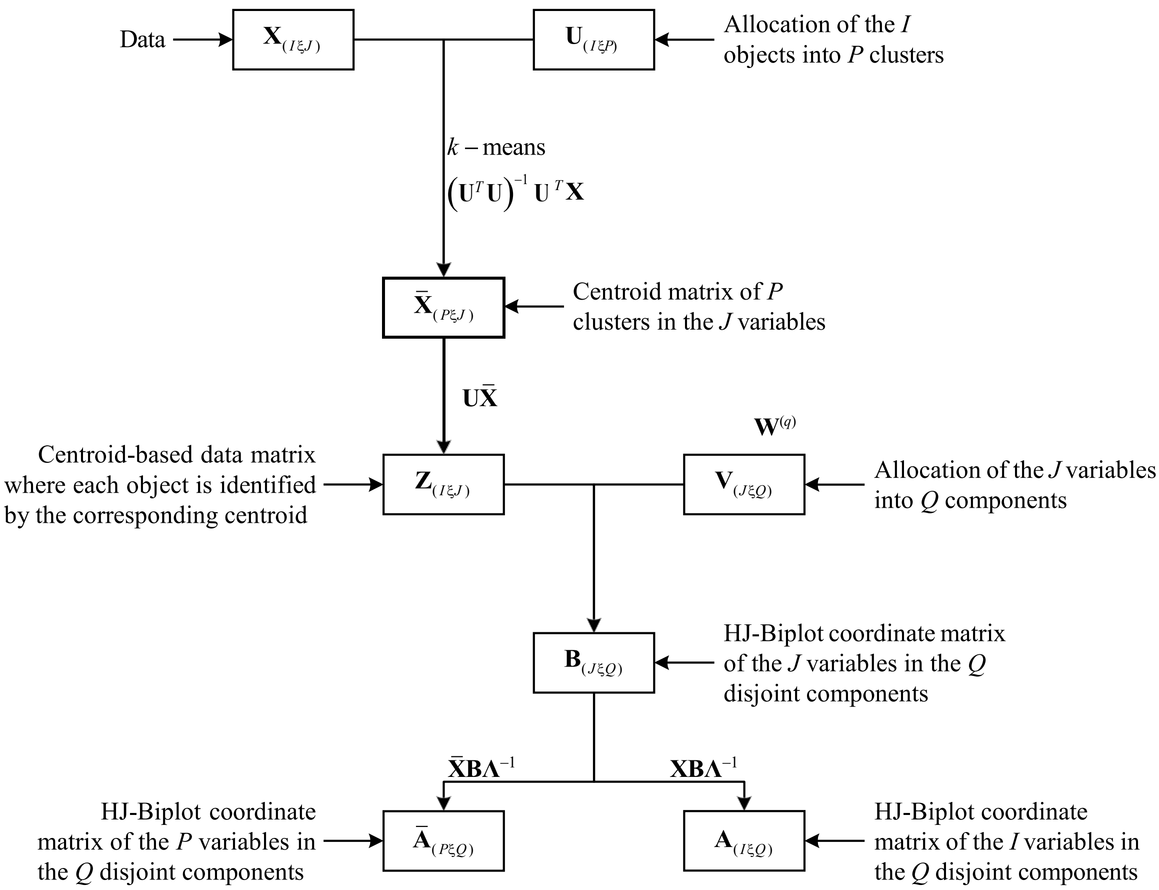

Figure 6. The CD HJ-Biplot algorithm

Source: *(Nieto-Librero, A. B., Sierra, C., Vicente-Galindo, M. P., Ruíz-Barzola, O., & Galindo-Villardón, M. P., 2017)*

2.2.2. Mathematical remarks of variational autoencoders

We decided to use the variational autoencoder technique (VAE) to generate another graphic representation of the SAFE data set. To achieve this, we start from the initial SAFE data set. Each country in the dataset has 69 sustainability indices. Therefore, the input layer has 69 nodes corresponding to each index. Then we encoded them in a latent space called z, generally of few dimensions (2 in our case), and from this latent space, we reconstruct the initial data set with the greatest possible precision (Figure 3).

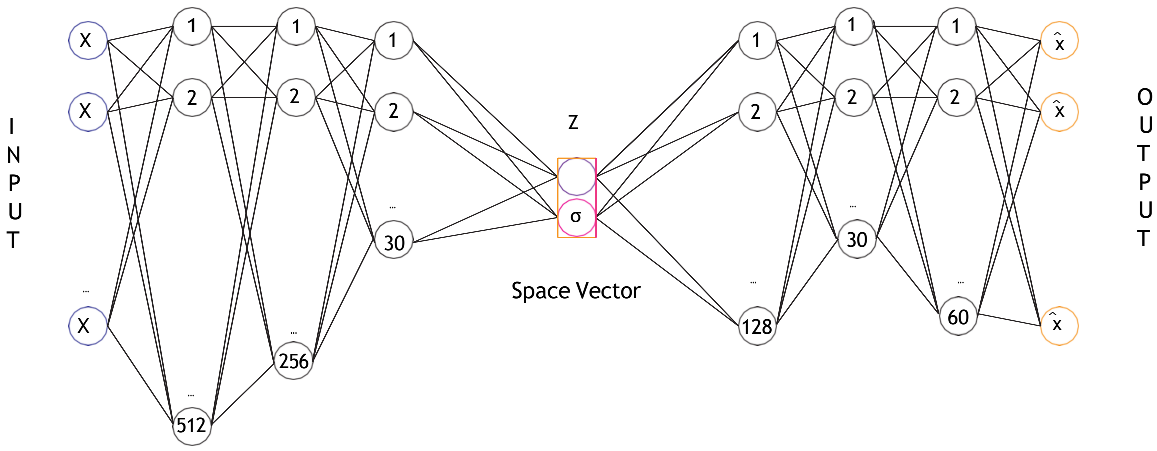

Figure 7. Variational autoencoder graphical model

The SAFE data is represented by x, and it is assumed that it is generated from a latent variable z (the encoded representation) that is not directly observed. Thus, for each data point, a latent representation z is sampled from the prior distribution p(z), and the data x is sampled from the conditional likelihood distribution p(x|z) Rocca (2019).

The "probabilistic decoder" defined by p(x|z) describes the distribution of the decoded variable given the encoded one, whereas the "probabilistic encoder" defined by p(z|x), describes the distribution of the encoded variable given the decoded one (ibid).

The link between the prior p(z), the likelihood p(x|z), and the posterior p(z|x) follow Bayes theorem:

$$p\ (z|x) = \frac{A\ (\chi|Z)A(C)}{A(+)} = \frac{A\ (\chi|Z)A(C)}{\oint ADXE\mu FA(\mu)G\mu}$$

It is assumed that p(z) is a standard Gaussian distribution, and that p(x|z) is a Gaussian distribution whose mean is defined by a deterministic function f of the variable z and whose covariance matrix has the form of a positive constant c that multiplies the identity matrix I. The function f is assumed to belong to a family of functions denoted F.

$$p(z) = N(0, I)$$

$$p(x|z) = N(f(z), cI) \qquad f \in F \qquad c > 0$$

2.2.2.1. Variational inference formulation

The training of all neural networks is an iterative process where the error of the output data with some expected value is calculated, and this error is minimized in the following iterations. In this case, the output value x (data generated) is used and the error is calculated taking into account the original input data. In addition, the Kullback-Leibler (KL) divergence between z and x. is introduced to calculate how similar these two are.

We approximate p(z|x) with a Gaussian distribution q_x(z) whose mean and covariance are defined by two functions, g, and h, of the parameter x. These two functions belong to the families of the functions G and H respectively (ibid).

$$q_x(z) \equiv N(g(x), h(x)) \qquad g \in G \qquad h \in H$$

In order to find the best approximation among these families, it is necessary to minimize the Kullback-Leibler (KL) divergence between the approximation and the target p(z|x) to optimize the functions g and h. Thus, we are looking for the optimal g * and h* such that

(g *, h*) = arg min KL(qx(z), p(z|x))

(g,h) EGxH

Replacing Bayes theorem such that

= arg min ($\mathbb{E}$ z~qx (log qx(z) - $\mathbb{E}$ z~qx (log $\frac{\mathrm{H}(x|z)\mathrm{H(C)}}{\mathrm{A}(+)}$))

(g,h) EGxH

Applying the properties of logarithms such that

= arg min ($\mathbb{E}$ z~qx (log qx(z)) - $\mathbb{E}$ z~qx (log p(z))- $\mathbb{E}$ z~qx (log p(x|z)) + $\mathbb{E}$ z~qx (log p(x))) (g,h) EGxH

Maximizing with negative KL (-KLD)

= arg max (𝔼 z~qx (log p(x|z)) – KL(qx (z), p(z)))

(g,h) EGxH

= arg max (𝔼 z~qx (-$\frac{|+\$I(C)||'}{(!}$) – KL (qx(z), p(z)))

(g,h) EGxH

In the penultimate equation, we can observe the tradeoff that exists approximating the posterior p(z|x), between maximizing the likelihood of the "observations" (maximization of the expected log-likelihood, for the first term) and staying close to the prior distribution (minimization of the KL divergence between q_x(z) and p(z), for the second term) (ibid).

In practice, the function f, which defines the decoder, is unknown and must also be chosen. Therefore, let us remember that our initial objective is to find an efficient encoding-decoding scheme whose latent space is regular enough to be used for generative purposes. If the regularity is governed mainly by the assumed prior distribution over the latent space, the performance of the overall encoding-decoding scheme is highly dependent on the choice of the function f. In fact, since p(z|x) can be approximated (by variational inference) from p (z) and p(z|x) and since p (z) is a simple standard Gaussian, the only two levers we have at our disposal in our model to make optimizations are the parameter c (which defines the variance of the probability) and the function f (which defines the mean of the probability) (ibid).

Consider that we can obtain for any function f in F (each defining a different probabilistic decoder p(x|z)) the best approximation of p(x|z)), denoted q* _x (z). Despite its probabilistic nature, we look for the most efficient encoding-decoding scheme possible, and then we choose the function f that maximizes the expected logarithmic probability of x given z when z is sampled from q*_x (z).

It is equivalent to saying that, for a given input x, we want to maximize the probability of having $x.$ = x when we sample z from the distribution q * _x (z) and then we sample $x.$ from the distribution p(x|z). Therefore, we look for the optimal f * such that:

$$f^* = \underset{f\ \ F}{\arg\max}\ \mathbb{E}\ z\sim q_x^* (\log p(x|z))$$

$$= \underset{f\ \ F}{\arg\max}\ \mathbb{E}\ z\sim q_x^* \left(- \frac{||+\$I(C)||'}{(!} \right)$$

where q*_x(z) depends on the function f. Then, the optimal f*, g*, and h* is:

$$(f^*,g^*,h^*) = \underset{(f,g,h)\ \ FxGxH}{\arg\max}\ \left(\mathbb{E}\ z\sim q_x \left(- \frac{||+\$I(C)||'}{(!} \right) - KL\left(q_x(z), p(z)\right)\right)$$

It identifies the reconstruction error between x and f(z), the regularization term given by the KL divergence between q_x (z) and p(z) (which is a standard), and the constant c that governs the balance between the two previous terms. The larger the c, the more we assume a high variance around f(z) for the probabilistic decoder in our model and, therefore, the more we favor the regularization term over the reconstruction term (the opposite occurs when c is low) (ibid).

2.2.2.2. Neural networks into the model

F, G, and H correspond to the families of functions defined by the network architecture and the optimization is carried out on the parameters of these networks.

In practice, g and h are not defined by two completely independent networks, but rather share a part of their architecture and their weights so that:

$g(x) = g_2(g_1(x))$ $\quad\quad$ $h(x) = h_2(h_1(x))$ $\quad\quad$ $g_1(x) = h_1(x)$

The covariance matrix of q_x (z), h(x) is a square matrix. To simplify the calculation and reduce the number of parameters, an additional assumption is made such that the approximation of p(z|x), q_x(z), is a multidimensional Gaussian distribution with diagonal covariance matrix (assumption of independence of variables). With this assumption, h(x) is simply the vector of the diagonal elements of the covariance matrix and therefore has the same size as g(x). However, this reduces the family of distributions considered for the variational inference and as a result, the approximation of p(z|x) obtained may be less precise (Figure 8) (ibid).

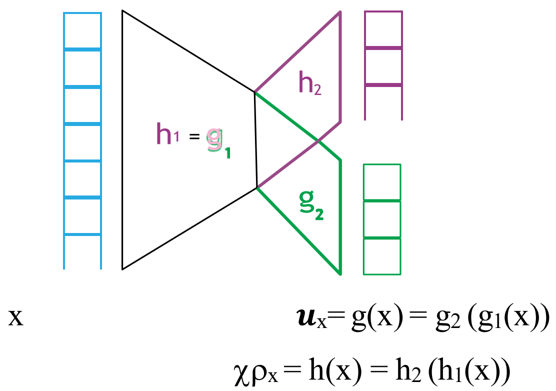

Figure 8. Encoder part of the VAE.

Source: (Rocca, 2019)

Contrary to the part of the encoder that models p(z|x) and for which a Gaussian was considered with mean and covariance that are functions of x (g and h), the model assumes for p(z|x) a Gaussian with fixed covariance. The function f of the variable z that defines the mean of that Gaussian is modeled by a neural network and can be represented as follows (Figure 9) (ibid):

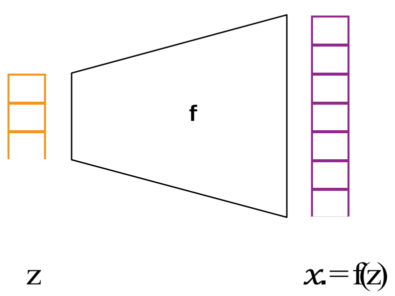

Figure 9. Decoder part of the VAE.

Source: (Rocca, 2019)

The general architecture is then obtained by concatenating the encoder and decoder parts. However, we must be very careful about how we sample the distribution returned by the encoder during training. The sampling process must be expressed in a way that allows the error to be backpropagated through the network. So, using the fact that if z is a random variable that follows a Gaussian distribution with mean g (x) and with covariance H(x)=h(x).h ^A^ t(x), then it can be expressed as (ibid):

$$z=h(x)\,\zeta + g(x) \qquad\qquad \zeta \sim N(0, I)$$

Finally, the objective function of the variational autoencoder architecture (Figure 10) is given by the last equation in which the theoretical expectation is replaced by a more or less precise Monte-Carlo approximation. Then, considering this approximation and denoting C = 1 / (2c), the loss function is recovered and is composed of a reconstruction term, a regularization term, and a constant to define the relative weights of these two terms (ibid).

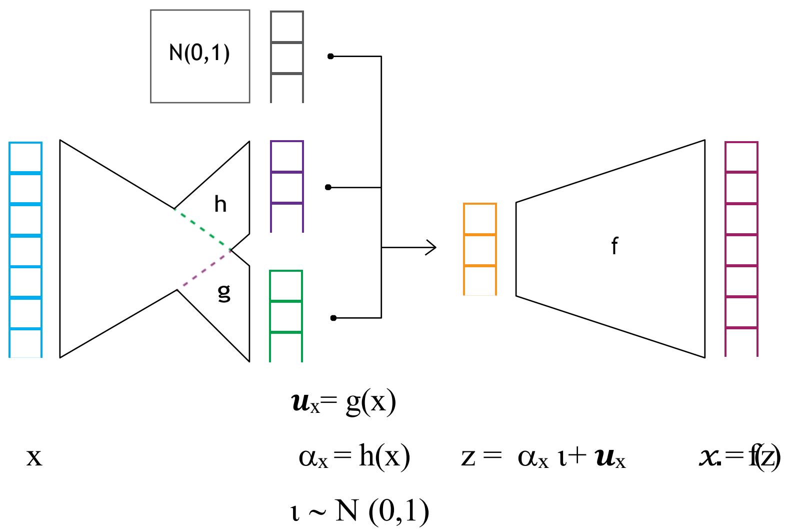

$$\text{Loss} = C\|x - \hat{x}\|^2 + KL[N(u_x, \alpha_x), N(0,1)] = C\|x - f(z)\|^2 + KL[N(g(x), h(x)), N(0,1)]$$

Figure 10. Variational autoencoders representation

Source: (Rocca, 2019)

CHAPTER 3. RESULTS AND DISCUSSION

3.1. Graphical sustainability analysis

Graphical sustainability analysis is proposed as a complement to numerical approaches. Therefore, Clustering Disjoint HJ-Biplot and Variational Autoencoders & graphical analysis are analyzed as a complement of SAFE and UN-SDGs.

3.1.1 Clustering Disjoint HJ-Biplot Analysis for SAFE

The sustainability rankings of SAFE 2018 are shown in Appendix 3. Its database generated the CD HJ-Biplot in Figure 11. The biplot placed the top 35 countries of SAFE in the lower left quadrant of Figure 7, forming group 1 (Table 1).

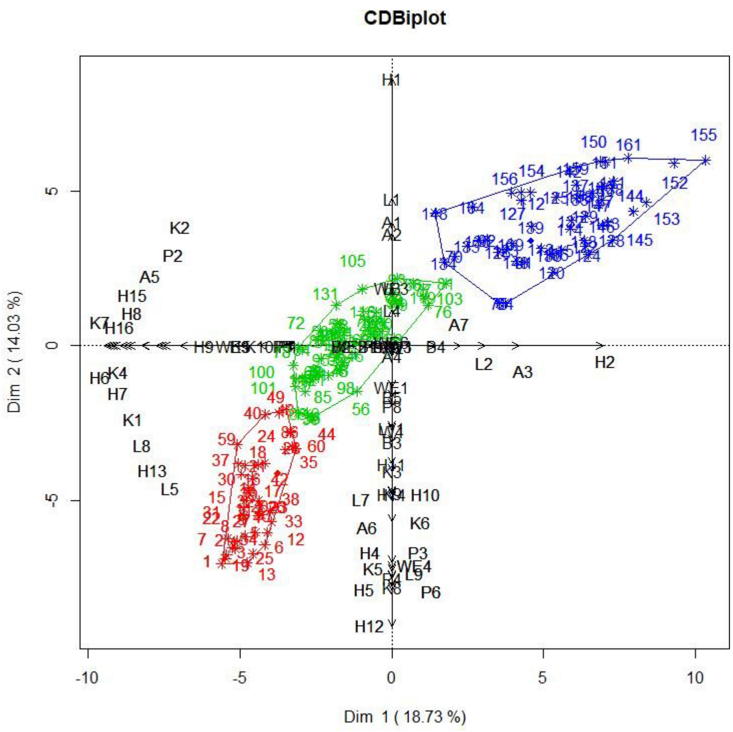

Figure 11. CD HJ-Biplot representation of sustainability indicators and countries 2018

The most influential indicators in the negative X and positive Y axes all belong to the human dimension, except for population growth and forest area (Table 2). The bottom 30 countries were placed in the upper right quadrant of Figure 11 and form group 3 (Table 1).

Again, Table 2 shows the most influential indicators along the positive X and negative Y axes, which now belong to both human and ecosystem dimensions.

Table 1. Clustering membership for 161 countries worldwide (SAFE indicators)

	Country	Cl		Country	Cl		Country	Cl		Country	Cl
1	Denmark	1	42	Israel	1	83	Sri Lanka	2	124	Zambia	3
2	Norway	1	43	Brunei	1	84	Armenia	2	125	Cameroon	3
3	Sweden	1	44	Russia	1	85	Trinidad and Tobago	2	126	Cambodia	3
4	Switzerland	1	45	Moldova	2	86	Kuwait	1	127	Djibouti	3
5	United Kingdom	1	46	Brazil	2	87	Bosnia and Herz.	2	128	Sierra Leone	3
6	Austria	1	47	Thailand	2	88	Honduras	2	129	Togo	3
7	Netherlands	1	48	Venezuela	2	89	Colombia	2	130	India	3
8	Finland	1	49	Cuba	1	90	Tajikistan	2	131	Libya	2
9	Slovenia	1	50	Turkey	2	91	Zimbabwe	3	132	Papua N.G.	3
10	Iceland	1	51	Peru	2	92	Lao PDR	3	133	Burkina Faso	3
11	France	1	52	Fiji	2	93	Indonesia	2	134	Guatemala	2
12	Ireland	1	53	Tunisia	2	94	El Salvador	2	135	Bangladesh	3
13	Germany	1	54	Azerbaijan	2	95	China	2	136	Tanzania	3
14	Poland	1	55	Mexico	2	96	Turkmenistan	2	137	Mali	3
15	Czech Rep.	1	56	Mongolia	2	97	Jordan	2	138	Liberia	3
16	Slovakia	1	57	Argentina	2	98	Seychelles	2	139	Gambia	3
17	Lithuania	1	58	Morocco	2	99	Belize	2	140	Myanmar	3
18	Hungary	1	59	South Korea	1	100	Saudi Arabia	2	141	Ethiopia	3
19	Luxembourg	1	60	Singapore	1	101	Qatar	2	142	Nigeria	3
20	Portugal	1	61	Malaysia	2	102	Uzbekistan	2	143	Madagascar	3
21	Latvia	1	62	North Macedonia	2	103	Botswana	2	144	Guinea	3
22	Australia	1	63	Kyrgyzstan	2	104	Nepal	3	145	Mozambique	3
23	Spain	1	64	Ghana	3	105	Algeria	2	146	Burundi	3
24	Croatia	1	65	Paraguay	2	106	Congo Rep.	3	147	Uganda	3
25	Estonia	1	66	Serbia	1	107	Lebanon	2	148	Iraq	3
26	Belgium	1	67	Ecuador	2	108	Iran	2	149	Angola	3
27	Italy	1	68	Cape Verde	2	109	Senegal	3	150	Niger	3
28	Uruguay	1	69	Dominican Rep.	2	110	Un. Arab Emirates	1	151	Congo D.R.	3
29	New Zealand	1	70	Gabon	3	111	Jamaica	2	152	Chad	3
30	Cyprus	1	71	Guyana	2	112	Eq. Guinea	3	153	Guinea-Bissau	3
31	Japan	1	72	Ukraine	2	113	Kenya	3	154	Pakistan	3
32	Malta	1	73	Georgia	2	114	Lesotho	3	155	Central African Rep.	3
33	Canada	1	74	Suriname	2	115	Benin	3	156	Yemen	3
34	United States	1	75	Namibia	2	116	Egypt	2	157	Eritrea	3
35	Chile	1	76	Nicaragua	2	117	Bahrain	2	158	Haiti	3
36	Costa Rica	2	77	Bolivia	2	118	Côte d'Ivoire	3	159	Mauritania	3
37	Greece	1	78	Mauritius	2	119	South Africa	2	160	Sudan	3
38	Bulgaria	1	79	Kazakhstan	2	120	Rwanda	3	161	Afghanistan	3
39	Romania	2	80	Panama	2	121	Oman	2			
40	Belarus	1	81	Philippines	2	122	Malawi	3			
41	Albania	2	82	Vietnam	2	123	Swaziland	3			

Table 2. Contribution of variables to each axis (SAFE indicators)

	Positive	Negative
Factorial Axis 1	H2 (+8.4) [Neoplastic incidence], A3 (+5.063) [NOx emissions], L2 (+3.711) [Pesticides], A7 (+2.732) [Renewables], B4 (+1.768) [Mountain protection KBA].	K7 (-11.418) [Secondary school enrollment], H6 (-11.308) [Infant mortality], H16 (-11.288) [Access sanitation], K4 (-11.163) [Mean years schooling], H8 (-11.069) [Life expectancy], H7 (-10.782) [Maternal mortality], H15 (-10.616) [Access safe water], K1 (-10.477) [Primary student-teacher], A5 (-9.934) [Mortality household], L8 (-9.906) [Municipal waste collected], P2 (-9.356) [Undernourishment], H13 (-9.212) [Hospital beds], K2 (-9.077) [Secondary student-teacher], L5 (-8.4) [Pop growth], H9 (-7.438) [Immunization DPT].
Factorial Axis 2	H1 (+10.412) [Cardiovascular incidence], L1 (+5.728) [Hazardous w], A1 (+4.815) [CO2_emissions], A2 (+4.361) [SO2_emissions], L3 (+2.27) [Fertilizers], E3 (+2.269) [Government debt], L4 (+1.417) [SLR land impact].	H12 (-10.916) [Physicians], P6 (-9.525) [Corruption], K8 (-9.387) [Literacy rate], H5 (-9.346) [Malaria incidence], L9 (-9.056) [Municipal waste recycled], P4 (-9.042) [Civil liberties], K5 (-9.005) [Schooling years gender gap], E4(-8.788) [GNI], P3 (-8.674) [Political rights], H4 (-8.425) [Tuberculosis incidence], K6 (-6.834) [Primary school enrollment], A6 (-6.822) [PM2.5], L7 (-5.939) [Forest area], H10 (-5.789) [Immunization measles], H14 (-5.764) [Health expenditure], K9 (-5.7.16) [RD expenditure].

The first axis of the CD HJ-Biplot is characterized by both human and ecological sustainability indicators (Table 2). More specifically, the positive side of factorial axis 1 is mainly related to environmental sustainability variables (NOx emissions, pesticide consumption, renewables, protected areas, etc.), while the negative side is mainly associated with human sustainability indicators, mostly health and knowledge indicators, such as school enrolment, mean years of schooling, student-teacher ratio, infant or maternal mortality, life expectancy, access to improved water sources and improved sanitation, etc. Similarly, the positive side of factorial axis 2 is related to human sustainability indicators of health and economy, such as cardiovascular incidences and government debt, as well as environmental indicators, such as CO_2 and SO_2 emissions, hazardous wastes, fertilizer consumption, and SLR land impact. The negative side of axis 2 is linked to human sustainability indicators, mainly health, policy, and knowledge. These findings, in addition to characterizing the axes of the CD HJ-Biplot reveal correlations between the aforementioned sustainability indicators.

The CD HJ-Biplot revealed three country groups (Figure 11). Group 1 is located in the lower-left quadrant and consists of the most sustainable countries. These countries have high performance (low values) in major human sustainability indicators, e.g., student-teacher ratio, infant or maternal mortality, malaria or tuberculosis incidences, corruption, civil liberties, political rights, and schooling years gender gap. On the other hand, group 3 is located in the upper right quadrant and contains the least sustainable countries, which are characterized by low performance (high values) in specific environmental sustainability indicators, e.g., CO_2, SO_2, and NOx emissions, pesticide consumption, hazardous wastes, fertilizer consumption, and SLR land impact together with the human sustainability indicators cardiovascular incidences and government debt. Group 2 consists of countries having a moderate performance in the previous sustainability indicators.

According to Table 1, the clusters of the CD HJ-Biplot agree with the overall ranking of the SAFE model. More specifically, the SAFE ranking and the CD HJ-Biplot clusters are consistent for 85.7% of the countries. Additionally, the average SAFE scores of groups 1, 2, and 3 are 74.60, 59.94, and 46.65, respectively. Some inconsistencies may be justified by the overall variance explained by the generated CD HJ-Biplot which is approximately 33%.

3.1.2 Clustering Disjoint HJ-Biplot analysis for UN-SDGs index database

The sustainability rankings of UN-SDGs are shown in Appendix 4 (see also Sachs, J., Schmidt-Traub, G., Kroll, C., Durand-Declare, D., Teksoz, K., 2016). The corresponding database generated the CD HJ-biplot in Figure 5. The biplot placed in the lower left quadrant of the top 18 countries comprising group 1 in Table 3. Similarly, the bottom 41 countries located in the upper right quadrant were placed into group 3. Table 4 extracts the most influential indicators in the negative X and Y axes.

As in the previous biplot (Figure 11), the positive side of the first axis in Figure 12 is characterized mainly by high values of sustainability indicators related to zero hunger, such as the prevalence of stunting or wasting in children under 5 years of age, as well as good health and well-being: neonatal mortality rate, tuberculosis incidences, rate of traffic-related deaths, etc. The negative side of axis 2 is mainly related to economic growth indicators, such as employment, quality education (PISA score, expected years of schooling), and well-being (healthy life expectancy at birth, daily smokers). The positive side of factorial axis 2 is related to well-being indicators, such as adolescent fertility rate, maternal mortality rate, and prevalence of undernourishment, while the negative side is mainly associated with the industry, innovation, and infrastructure indicators, for example, quality of overall infrastructure, the proportion of the population using the internet, mobile broadband subscriptions, number of R&D researchers, and R&D expenditure.

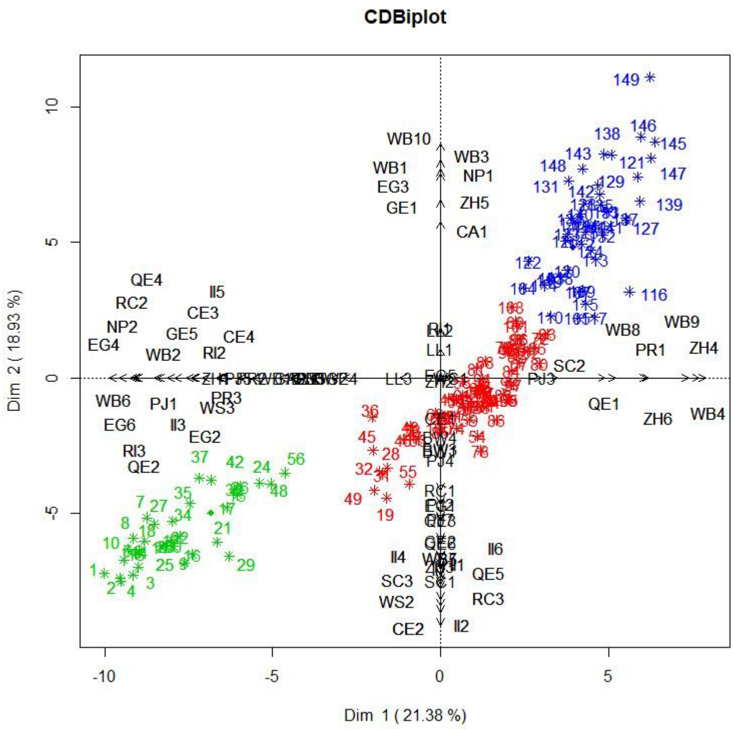

Figure 12. CD HJ-Biplot representation of UN-SDGs index

The country grouping in Figure 8 is quite similar to that in Figure 4: 90% of the countries that are categorized into a specific group according to SAFE are categorized into the same group based on UN-SDGs variables. More specifically, group 1 (in the lower left quadrant) consists of the most sustainable countries, group 3 (in the upper right quadrant) the least sustainable countries, and group 2 (close to the origin of axes) consists of countries with a moderate sustainability performance.

The UN-SDGs ranking and the CD HJ-Biplot clustering are consistent for 91.3% of the countries. The average UN-SDGs scores of groups 1, 2, and 3 are 75.14, 61.27, and 41.31, respectively, showing that the CD HJ-Biplot reproduces the UN-SDGs rankings satisfactorily. Any inconsistencies in Table 3 are justified by the fact that the CD HJ-Biplot explains approximately 40% of the variance of the initial dataset.

Table 3. Clustering membership for 149 countries worldwide (UN-SDGs)

	Country	Cl		Country	Cl		Country	Cl		Country	Cl
1	Sweden	1	39	Serbia	1	77	Jamaica	2	115	Pakistan	3
2	Denmark	1	40	Uruguay	2	78	Trinidad and Tobago	2	116	Swaziland	3
3	Norway	1	41	Romania	2	79	Iran	2	117	Myanmar	3
4	Finland	1	42	Chile	2	80	Botswana	2	118	Bangladesh	3
5	Switzerland	1	43	Argentina	2	81	Peru	2	119	Cambodia	3
6	Germany	1	44	Moldova	2	82	Bhutan	2	120	Kenya	3
7	Austria	1	45	Cyprus	2	83	Algeria	2	121	Angola	3
8	Netherlands	1	46	Ukraine	1	84	Mongolia	2	122	Rwanda	3
9	Iceland	1	47	Russia	2	85	Saudi Arabia	2	123	Uganda	3
10	United Kingdom	1	48	Turkey	2	86	Lebanon	2	124	Côte d'Ivoire	3
11	France	1	49	Qatar	2	87	Suriname	2	125	Ethiopia	3
12	Belgium	1	50	Armenia	2	88	Vietnam	2	126	Tanzania	3
13	Canada	1	51	Tunisia	2	89	Bolivia	2	127	Sudan	3
14	Ireland	1	52	Brazil	2	90	Nicaragua	2	128	Burundi	3
15	Czech Rep.	1	53	Costa Rica	2	91	Colombia	2	129	Togo	3
16	Luxembourg	1	54	Kazakhstan	2	92	Dominican Rep.	2	130	Benin	3
17	Slovenia	1	55	United Arab Emirates	1	93	Gabon	3	131	Malawi	3
18	Japan	1	56	Mexico	1	94	El Salvador	2	132	Mauritania	3
19	Singapore	1	57	Georgia	2	95	Philippines	2	133	Mozambique	3
20	Australia	2	58	North Macedonia	2	96	Cape Verde	2	134	Zambia	3
21	Estonia	1	59	Jordan	2	97	Sri Lanka	2	135	Mali	3
22	New Zealand	1	60	Montenegro	2	98	Indonesia	2	136	Gambia	3
23	Belarus	2	61	Thailand	2	99	South Africa	2	137	Yemen	3
24	Hungary	1	62	Venezuela	2	100	Kuwait	2	138	Sierra Leone	3
25	United States	2	63	Malaysia	2	101	Guyana	2	139	Afghanistan	3
26	Slovakia	1	64	Morocco	2	102	Honduras	2	140	Madagascar	3
27	South Korea	1	65	Azerbaijan	2	103	Nepal	3	141	Nigeria	3
28	Latvia	1	66	Egypt	2	104	Ghana	3	142	Guinea	3
29	Israel	1	67	Kyrgyzstan	2	105	Iraq	2	143	Burkina Faso	3
30	Spain	1	68	Albania	2	106	Guatemala	2	144	Haiti	3
31	Lithuania	1	69	Mauritius	2	107	Lao PDR	3	145	Chad	3
32	Malta	2	70	Panama	2	108	Namibia	2	146	Niger	3
33	Bulgaria	2	71	Ecuador	2	109	Zimbabwe	3	147	Congo D.R.	3
34	Portugal	2	72	Tajikistan	2	110	India	3	148	Liberia	3
35	Italy	1	73	Bosnia and Herzegovina	2	111	Congo Rep.	3	149	Central African Rep.	3
36	Croatia	2	74	Oman	2	112	Cameroon	3			
37	Greece	1	75	Paraguay	2	113	Lesotho	3			
38	Poland	2	76	China	2	114	Senegal	3			

Table 4. Contribution of variables to each axis (UN-SDGs)

	Positive	Negative
Factorial Axis 1	ZH4 (+9.027) [Prevalence of stunting (low height-for-age) in children under 5 years of age (%)], WB4 (+8.8) [Neonatal mortality rate (per 1000 live births)], WB9 (+8.442) [Traffic deaths rate (per 100,000 people)], ZH6 (+7.093) [Prevalence of wasting in children under 5 years of age (%)], PR1 (+7.014) [For all other countries: Tax revenue (% of GDP)], WB8 (+5.994) [Incidence of tuberculosis (per 100,000 people)], QE1 (+5.595) [Literacy rate of 15-24 year olds, both sexes (%)], SC2 (+3.987) [Annual mean concentration of particulate matter of less than 2.5 microns of diameter (PM2.5) (µg/m3) in urban areas],PJ3 (+3.438) [Homicides (per 100,000 people)]	EG4 (-11.261) [Employment-to-Population ratio (%)], WB6 (-10.914) [Daily smokers (% of population aged 15+)], NP2 (-10.564) [Poverty rate after taxes and transfers, poverty line 50% (% of population)], EG6 (-10.474) [Youth not in employment, education or training (NEET) (%)], RC2 (-10.432) [Non-recycled municipal solid waste (kg/person/year)], RI3 (-10.36) [Palma ratio], QE4 (-9.73) [Expected years of schooling (years)], QE2 (-9.616) [PISA score (0-600)], WB2 (-9.29) [Healthy life expectancy at birth (years)], PJ1 (-9.036) [Corruption Perception Index (0-100)], GE5 (-8.644) [Gender wage gap (% of male median wage)], II3 (-8.488) [Logistics Performance Index: Quality of trade and transport-related infrastructure], CE3 (-8.446) [CO2 emissions from fuel combustion and electricity output (MtCO2/TWh)]
Factorial Axis 2	WB10 (+9.877) [Mortality rate, under-5 (per 1,000 live births)], WB3 (+9.186) [Maternal mortality rate (per 100,000 live births)], WB1 (+8.798) [Adolescent fertility rate (births per 1,000 women ages 15-19)], NP1 (+8.789) [Poverty headcount ratio at $1.90 a day (2011 PPP) (% of population)], EG3 (+8.605) [Percentage of children 5–14 years old involved in child labor (%)], ZH5 (+7.479) [Prevalence of undernourishment (% of population)], GE1 (+7.478) [Estimated demand for contraception that is unmet (% of women married or in union, ages 15-49)], CA1 (+6.588) [Climate Change Vulnerability Monitor]	II2 (-10.433) [Proportion of the population using the internet (%)], CE2 (-9.889) [Access to non-solid fuels (% of population)], WS2 (-9.618) [Access to improved sanitation facilities (% of population)], RC3 (-9.34) [Municipal solid waste (kg/year/capita)], SC3 (-8.877) [Rooms per person], QE5 (-8.706) [Population aged 25-64 with tertiary education (%)], SC1 (-8.582) [Improved water source, piped (% of urban population with access)], II6 (-8.356) [Research and development researchers (per 1000 employed)], II4 (-8.335) [Mobile broadband subscriptions (per 100 inhabitants)], II1 (-8.313) [Quality of overall infrastructure], II7 (-8.082) [Research and development expenditure (% of GDP)].

3.2. Variational Autoencoder for assessing sustainability

The sustainability rankings of SAFE 2019 are shown in Appendix 5. Although VAE&GA is not a hierarchical technique, after training and checking, there is a 73% coincidence (120 out of 164 countries) in the grouping country memberships (Table 5) compared to the SAFE (Grigoroudis, E., Kouikoglou, V., Phillis, 2020) and ANFIS (Tan, Yongtao ; Shuai, Chenyang; Jiao, Liudan; Liyin, S., 2018) ranking models.

Hence, unsupervised techniques attempt to learn fundamental latent structures, relations, and patterns of given information without any assistance or supervision (Sarkar, D., Bali, R., & Sharma, T. (2018), and after defining the parameters and optimizing the Membership Functions, the process is very time efficient because it is based on the data training data rather than the expert knowledge as with the ANFIS method proposed by Tan, Yongtao ; Shuai, Chenyang; Jiao, Liudan; Liyin, S. (2018).

The grouping differences between SAFE and VAE&GA are shown in Table 9, where the largest differences belong to cluster 2, where countries of neighboring clusters are mixed by 20%, in comparison with cluster 1 (17%) and cluster 3 (17%) within each country respectively.

To evaluate the sustainability performance of countries, we divide it into 3 main clusters using K-means, as follows: cluster 1 (Developed Countries), cluster 2 (Intermediate), and cluster 3 (Developing Countries). And to complete the graphical analysis, we forced sustainability indicators to fall on the 2 axes: X and Y, and we have a good picture of sustainability indicators and country groups (Figure 9).

The upper countries were placed in the lower left quadrant of Figure 13 and form group 1 (Table 5), the most influential indicators on the negative X axis belonging to both the environmental and human dimensions and negative Y axis, all belonging to the human dimension (Table 7). The bottom countries were placed in the upper right quadrant of Figure 9 and form group 3 (Table 5). The most influential indicators are shown along the positive X axis belonging to both the environmental and human dimensions and positive Y axis, which also belong to both human and ecosystem dimensions (Table 7).

Table 5. Clustering membership for 164 countries worldwide (SAFE indicators)

	Country	Cl		Country	Cl		Country	Cl		Country	Cl
1	Denmark	1	42	Russia	2	83	Bosnia and Herz.	1	124	Rwanda	3
2	Sweden	1	43	Brunei	2	84	Zimbabwe	3	125	South Africa	3
3	Norway	1	44	Albania	1	85	Armenia	1	126	Cameroon	3
4	Switzerland	1	45	Cuba	1	86	Honduras	2	127	Mali	3
5	Austria	1	46	Peru	2	87	Seychelles	2	128	Swaziland	3
6	Finland	1	47	Brazil	2	88	Colombia	2	129	Belize	2
7	Slovenia	1	48	Morocco	2	89	El Salvador	2	130	Un. Arab Emirates	2
8	Netherlands	1	49	Mexico	2	90	Vietnam	3	131	Papua N.G.	3
9	Slovakia	1	50	Moldova	1	91	Botswana	2	132	Bahamas	2
10	United Kingdom	1	51	Venezuela	2	92	Nepal	3	133	Liberia	3
11	France	1	52	Thailand	2	93	Eq. Guinea	3	134	Ethiopia	3
12	Lithuania	1	53	Argentina	2	94	Lao PDR	2	135	Egypt	2
13	Iceland	1	54	Mongolia	2	95	Burkina Faso	3	136	Bahrain	2
14	Germany	1	55	Azerbaijan	2	96	Kiribati	2	137	Nigeria	3
15	Poland	1	56	Tunisia	2	97	Congo Rep.	3	138	Tanzania	3
16	Hungary	1	57	Serbia	1	98	Tajikistan	2	139	Djibouti	3
17	Ireland	1	58	Ghana	3	99	Jordan	2	140	Qatar	2
18	Czech Rep.	1	59	Paraguay	2	100	Algeria	2	141	Angola	3
19	Portugal	1	60	North Macedonia	1	101	Senegal	3	142	Mozambique	3
20	Latvia	1	61	Kyrgyzstan	1	102	Iran	2	143	Madagascar	3
21	Estonia	1	62	Malaysia	2	103	Saudi Arabia	2	144	Guinea	3
22	Spain	1	63	Namibia	3	104	Indonesia	2	145	Gambia	3
23	Croatia	1	64	Gabon	3	105	Togo	3	146	Oman	2
24	Australia	1	65	Israel	2	106	Kenya	3	147	Myanmar	3
25	Italy	1	66	Singapore	2	107	Turkmenistan	2	148	Burundi	3
26	Belgium	1	67	Dominican Rep	2	108	Maldives	2	149	Uganda	3
27	Malta	1	68	Ukraine	1	109	China	2	150	Bangladesh	2
28	Uruguay	2	69	Cape Verde.	2	110	Malawi	3	151	Guatemala	3
29	Luxembourg	1	70	Fiji	2	111	Trinidad and Tobago	2	152	Pakistan	3
30	New Zealand	1	71	South Korea	2	112	Uzbekistan	2	153	Chad	3
31	Canada	1	72	Ecuador	2	113	Côte d'Ivoire	3	154	Niger	3
32	Greece	1	73	Georgia	1	114	Lesotho	3	155	Congo D.R.	3
33	Cyprus	1	74	Panama	2	115	Benin	3	156	Iraq	3
34	Romania	1	75	Guyana	2	116	Sierra Leone	3	157	Guinea-Bissau	3
35	Japan	1	76	Nicaragua	2	117	Cambodia	3	158	Yemen	3
36	United States	1	77	Philippines	2	118	Jamaica	2	159	Central African Rep.	3
37	Bulgaria	1	78	Suriname	2	119	Zambia	3	160	Eritrea	3
38	Costa Rica	2	79	Kazakhstan	1	120	Kuwait	2	161	Sudan	3
39	Belarus	1	80	Bolivia	2	121	Libya	2	162	Mauritania	3
40	Chile	2	81	Mauritius	2	122	Lebanon	2	163	Haiti	3
41	Turkey	2	82	Sri Lanka	2	123	India	3	164	Afghanistan	3

Table 6. Clustering membership for 164 countries worldwide according to Rank SAFE and VAE&GA

Country	Rank	VAE	(-)	Country	Rank	VAE	(-)
Denmark	1	3	-2	Russia	42	38	4
Sweden	2	9	-7	Brunei	43	94	-51
Norway	3	12	-9	Albania	44	41	3
Switzerland	4	10	-6	Cuba	45	46	-1
Austria	5	11	-6	Peru	46	105	-59
Finland	6	19	-13	Brazil	47	109	-62
Slovenia	7	28	-21	Morocco	48	63	-15
Netherlands	8	1	7	Mexico	49	101	-52
Slovakia	9	30	-21	Moldova	50	40	10
United Kingdom	10	4	6	Venezuela	51	111	-60
France	11	25	-14	Thailand	52	76	-24
Lithuania	12	31	-19	Argentina	53	50	3
Iceland	13	16	-3	Mongolia	54	53	1
Germany	14	5	9	Azerbaijan	55	51	4
Poland	15	33	-18	Tunisia	56	65	-9
Hungary	16	35	-19	Serbia	57	42	15
Ireland	17	6	11	Ghana	58	122	-64
Czech Rep.	18	29	-11	Paraguay	59	107	-48
Portugal	19	24	-5	North Macedonia	60	43	17
Latvia	20	32	-12	Kyrgyzstan	61	52	9
Estonia	21	7	14	Malaysia	62	79	-17
Spain	22	23	-1	Namibia	63	118	-55
Croatia	23	34	-11	Gabon	64	113	-49
Australia	24	13	11	Israel	65	80	-15
Italy	25	26	-1	Singapore	66	77	-11
Belgium	26	2	24	Dominican Rep	67	99	-32
Malta	27	20	7	Ukraine	68	44	24
Uruguay	28	18	10	Cape Verde.	69	95	-26
Luxembourg	29	8	21	Fiji	70	92	-22
New Zealand	30	17	13	South Korea	71	72	-1
Canada	31	14	17	Ecuador	72	108	-36
Greece	32	27	5	Georgia	73	47	26
Cyprus	33	21	12	Panama	74	104	-30
Romania	34	37	-3	Guyana	75	86	-11
Japan	35	22	13	Nicaragua	76	112	-36
United States	36	15	21	Philippines	77	97	-20
Bulgaria	37	36	1	Suriname	78	88	-10
Costa Rica	38	84	-46	Kazakhstan	79	49	30
Belarus	39	39	0	Bolivia	80	110	-30
Chile	40	85	-45	Mauritius	81	90	-9
Turkey	41	62	-21	Sri Lanka	82	83	-1

Continuing Table 6. Clustering membership for 164 countries according to SAFE 2019 and VAE&GA

Country	Rank	VAE	(-)	Country	Rank	VAE	(-)
Bosnia and Herz.	83	45	38	Rwanda	124	163	-39
Zimbabwe	84	117	-33	South Africa	125	114	11
Armenia	85	48	37	Cameroon	126	144	-18
Honduras	86	106	-20	Mali	127	155	-28
Seychelles	87	78	9	Swaziland	128	120	8
Colombia	88	89	-1	Belize	129	87	42
El Salvador	89	103	-14	Un. Arab Emirates	130	70	60
Vietnam	90	74	16	Papua N.G.	131	130	1
Botswana	91	115	-24	Bahamas	132	82	50
Nepal	92	128	-36	Liberia	133	140	-7
Eq. Guinea	93	136	-43	Ethiopia	134	135	-1
Lao PDR	94	100	-6	Egypt	135	64	71
Burkina Faso	95	139	-44	Bahrain	136	68	68
Kiribati	96	93	3	Nigeria	137	141	-4
Congo Rep.	97	123	-26	Tanzania	138	132	6
Tajikistan	98	54	44	Djibouti	139	149	-10
Jordan	99	58	41	Qatar	140	71	69
Algeria	100	60	40	Angola	141	150	-9
Senegal	101	145	-44	Mozambique	142	125	17
Iran	102	61	41	Madagascar	143	131	12
Saudi Arabia	103	66	37	Guinea	144	142	2
Indonesia	104	98	6	Gambia	145	162	-17
Togo	105	129	-24	Oman	146	67	79
Kenya	106	116	-10	Myanmar	147	158	-11
Turkmenistan	107	56	51	Burundi	148	160	-12
Maldives	108	73	35	Uganda	149	134	15
China	109	75	34	Bangladesh	150	96	54
Malawi	110	119	-9	Guatemala	151	102	49
Trinidad and Tobago	111	81	30	Pakistan	152	154	-2
Uzbekistan	112	55	57	Chad	153	148	5
Côte d’Ivoire	113	138	-25	Niger	154	147	7
Lesotho	114	121	-7	Congo D.R.	155	152	3
Benin	115	137	-22	Iraq	156	127	29
Sierra Leone	116	133	-17	Guinea-Bissau	157	146	11
Cambodia	117	126	-9	Yemen	158	151	7
Jamaica	118	91	27	Central African Rep.	159	156	3
Zambia	119	124	-5	Eritrea	160	164	-4
Kuwait	120	69	51	Sudan	161	161	0
Libya	121	59	62	Mauritania	162	157	5
Lebanon	122	57	65	Haiti	163	143	20
India	123	153	-30	Afghanistan	164	159	5

Table 7. Contribution of variables to each axis (SAFE indicators 2019)

	Positive	Negative
Factorial Axis 1	Fertilizers, CO2_emissions NOx_emissions Water_stress	Fish_stock_status Mortality_PM Inflation Water_resources Foreign_direct_investment
Factorial Axis 2	Cardiovascular_incidence Hazardous_w Neoplastic_incidence Pesticides SO2_emissions Government_debt SLR_land_impact Forest_area (trend) Military_expenditure Terrestrial_prot_area Unemployment_gender_inequality	Malaria_incidence Physicians GNI Civil_ liberties Political_ rights Hospital_beds Access_sanitation Secondary_school_enrollement Infant_mortality Corruption Maternal_mortality

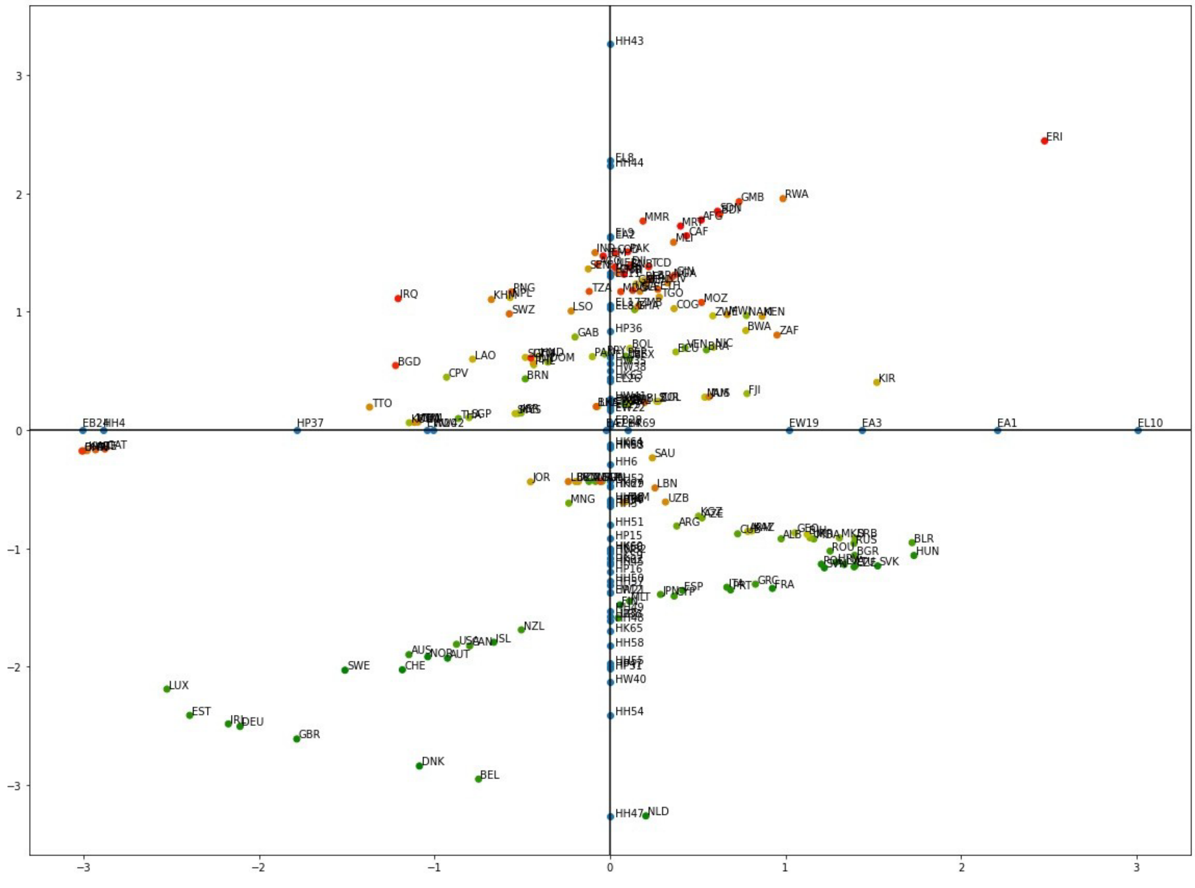

Figure 13. VAE&GA worldwide country sustainability performance SAFE 2019

CHAPTER 4. CONCLUSIONS, ORIGINAL CONTRIBUTION, RESEARCH ROADMAP, AND DISSEMINATION OF RESULTS

4.1. Conclusions

CD HJ-Biplots to portray graphically the sustainability position of a large number of countries are a useful complement to mathematical models of sustainability, just as graphs complement equations. Graphical information could be useful to planners it shows directly how countries are grouped according to the most related sustainability indicators. Thus, planners can prioritize social, environmental, and economic policies and make the most effective decisions.

As a general conclusion, a large number of countries remain in the areas of moderate or low sustainability. One could graphically observe the dynamic evolution of sustainability worldwide over time with a graphical approach used to draw relevant conclusions. In an era of climate change, species extinction, poverty, and environmental migration, such observations could aid political decision-making regarding the future of our planet.

Assessing sustainability is an extremely challenging task because the priorities of nations can change drastically, as evidenced by the impact of the COVID-19 pandemic. It is necessary to develop an integrated program including renewable energy, infrastructure, health care, education, and jobs to overcome the principal problems of inequities among countries. The key today is to redirect outlays now spent on fossil fuel-based technologies toward zero-carbon technologies instead (Sachs, 2019).

Fuzzy logic has proven to be an uncontested numerical method as it occurs with SAFE. An unsupervised learning method called Variational Autoencoder interplay Graphical Analysis (VEA&GA) has been proposed, to support sustainability performance with appropriate training data. The promising results show that this can be a sound alternative to assess sustainability, extrapolating its applications to other kinds of problems at different levels of analysis (continents, regions, cities, etc.) further corroborating the effectiveness of the unsupervised training methods.

4.2. Original contribution

This research complements current knowledge about sustainability assessment. This is due to a relatively small number of studies on the subject. In particular, there are no scientific studies framed around unsupervised learning techniques. The results are given herein allowed us to identify simultaneously country names and sustainability indexes in two dimensions.

The main personal contributions brought through the research underlying this work are the following:

i.) As the centerpiece of this research was assessing a country's sustainability performance using the CD-HJ-Biplot biplot, as a complement of hierarchical methods as SAFE, therefore, addressing them and by bringing light on their value constitutes an important contribution.

ii.) The unsupervised learning techniques of machine learning have been presented for the first time at an international level. In this regard, it emphasized the role of a variational autoencoders procedure.

4.3. Future research roadmap

The presentation of this study highlights that sustainability assessment is particularly associated with decision-making tasks. Given the great diversity of variables and the complexity of the tasks, due to their multicriteria variables, methods such as CD-HJ-Biplot and Variational Autoencoders are appropriate tools to help in this endeavor.

In a sense, CD HJ-Biplots verify statistically the findings of SAFE and UN-SDGs. However, one could go one step further and investigate relationships of indicators that could be excluded from these indices to reduce the dimensionality of the original models. Additionally, deviations of rankings between biplots and SAFE or UN-SDGs could serve as venues for possible improvements of these models. All these are subjects for future research.

The methodology used in this work could be very useful for research aimed at determining the importance of evaluating sustainability performance at different levels (cities, regions, among others). Practical and scientific importance would also be the fact that assessing sustainability can be generating sound actions to protect our natural resources for future generations.

4.4. Dissemination of results

4.4.1 Results produced within the frame of the Ph.D. thesis

A. Papers published in BDI journals

1. Aules, J; McLaren, B; & **Romero, F**. (2017). Contenido nutrimental del suelo y de la hojarasca del árbol pionero Cecropia en bosques maduros y secundarios de la zona húmeda tropical del Ecuador. Oecologia Australis, 21(2),182-190. https://doi.org/https://doi.org/10.4257/oeco.2017.2102.08

2. **Romero Cañizares, J.F**; Guacho Abarca, E. F; Caballero Naranjo, D. N., Vicente-Villardón, J. L, & Demey, J +. Caracterización de germoplasma de maíz local a través de marcadores SSR asistido por biplot logístico externo (BLE). (Poster) XXVI Simposio Internacional de Estadística 2016 Sincelejo, Sucre, Colombia, 8 al 12 de Agosto de 2016

B. Papers published in journals indexed by Clarivate Analytics (former ISI Web of Science)

1. **Cañizares, J.F.R**., Galindo, P.V., Phillis, Y., & Grigoroudis, E. (2020). Graphical sustainability analysis using disjoint biplots. *Operational Research*. https://doi.org/10.1007/s12351-020-00573-7. Journal classified **JCR** last year available (2018). FI: 1.485. Categories: Operations Research & Management Science (SCIE): 48/84 - Q3.Percentile: 43.45. **SJR** last year available (2018). SJR: 0.552. Categorías: Management of Technology and Innovation: 80/281 Q2. Strategy and Management: 139/442 -Q2. Management Science and Operations Research 73/193 -Q2

4.4.2 Results produced by participation in research teams external to the Ph.D. thesis scope

A. Papers published in BDI journals

1. Guambo, V; Arguello, C; Zurita, M & **Romero Cañizares, F**. (2016). El valor económico ambiental de los usuarios del servicio hidrológico de la Microcuenca del Río Cebadas, Provincia de Chimborazo. SATHIRI No 11, pp.206 219. ISSN 1390-6925. LATINDEX 21955. Julio – Diciembre 2016.

B. Papers presented at international conferences and symposiums

1. Duque Vaca, M., **Romero Cañizares, F** & Jiménez Builes, J. 2019. "Validating a Georeferenced Map Viewer Through Online and Manual Tests,". International Conference on Inclusive Technologies and Education (CONTIE), San Jose del Cabo, Mexico,2019, pp.91-916, doi:10.1109/CONTIE49246.2019.00026.

2. **Romero, F.,** Muñoz, E., Argüello, C., Zurita, M., Román, D., & González, A. (2018). Hacia un manejo adaptativo de la Reserva de Producción de Fauna Chimborazo y su zona de amortiguamiento. Sistematización de la aplicación de la metodología Manejo

Adaptativo de Riesgo y Vulnerabilidad en Sitios de Conservación (MARISCO). **Editorial:** Escuela Superior Politécnica de Chimborazo; GIZ. Programa ProCamBío II. Text. Quito, Ecuador. 56p. **Identifier:** 5394

BIBLIOGRAPHY

Alvarez, F. J. D., & Villardon, P. G. (2015). A Proposal for Spatio-Temporal Analysis of Traffic Matrices Using HJ-Biplot. In *2015 IEEE INTERNATIONAL WORKSHOP ON MEASUREMENTS AND NETWORKING (M&N)*.

Amor-Esteban, V., Galindo-Villardon, M. P., & Garcia-Sanchez, I. M. (2018). Industry mimetic isomorphism and sustainable development based on the X-STATIS and HJ-biplot methods. *ENVIRONMENTAL SCIENCE AND POLLUTION RESEARCH*, *25*(26), 26192–26208. https://doi.org/10.1007/s11356-018-2663-1

Amor-Esteban, V., Garcia-Sanchez, I. M., & Galindo-Villardon, M. P. (2018). Analysing the Effect of Legal System on Corporate Social Responsibility (CSR) at the Country Level, from a Multivariate Perspective. *SOCIAL INDICATORS RESEARCH*, *140*(1), 435–452. https://doi.org/10.1007/s11205-017-1782-2

Anita, Yadav, A., & Kumar, N. (2020). Artificial electric field algorithm for engineering optimization problems. *Expert Systems with Applications*, *149*. https://doi.org/10.1016/j.eswa.2020.113308

Avram, R., Olgin, J. E., & Tison, G. H. (2020). The Rise of Open-Sourced Machine Learning in Small and Imbalanced Datasets: Predicting In-Stent Restenosis. *CANADIAN JOURNAL OF CARDIOLOGY*, *36*(10), 1574–1576. https://doi.org/10.1016/j.cjca.2020.02.002

Bengio, Y. (2009). Learning deep architectures for AI. *Foundations and Trends in Machine Learning*, *2*(1), 1–27. https://doi.org/10.1561/2200000006

Bernal, E. F., del Rey, A. M., & Villardon, P. G. (2020). Analysis of Madrid Metro Network: From Structural to HJ-Biplot Perspective. *APPLIED SCIENCES-BASEL*, *10*(16). https://doi.org/10.3390/app10165689

Bolandnazar, E., Rohani, A., & Taki, M. (2020). Energy consumption forecasting in agriculture by artificial intelligence and mathematical models. *Energy Sources, Part A: Recovery, Utilization and Environmental Effects*, *42*(13), 1618–1632. https://doi.org/10.1080/15567036.2019.1604872

Cabrera, J. M. G., Martinez, M. R. F., Mateos, E. J. M., & Tavera, S. v. (2006). Study of the evolution of air pollution in Salamanca (Spain) along a five-year period (1994-1998) using HJ-Biplot simultaneous representation analysis. *ENVIRONMENTAL MODELLING & SOFTWARE*, *21*(1), 61–68. https://doi.org/10.1016/j.envsoft.2004.10.009

Cañizares, J. F. R., Galindo, P. V., Phillis, Y., & Grigoroudis, E. (2020). Graphical sustainability analysis using disjoint biplots. *Operational Research*. https://doi.org/10.1007/s12351-020-00573-7

Chorowski, J., Weiss, R. J., Bengio, S., & van den Oord, A. (2019). Unsupervised speech representation learning using WaveNet autoencoders. *IEEE/ACM Transactions on Audio Speech and Language Processing*, *27*(12), 2041–2053. https://doi.org/10.1109/TASLP.2019.2938863

Cubilla-Montilla, M., Nieto-Librero, A. B., Galindo-Villardon, M. P., & Torres-Cubilla, C. A. (2021). Sparse HJ Biplot: A New Methodology via Elastic Net. *MATHEMATICS*, *9*(11). https://doi.org/10.3390/math9111298

de Soete, G., & Carroll, J. D. (1994). K-means clustering in a low-dimensional Euclidean space. In *New approaches in classification and data analysis*.

de Soete, G., & Heiser, W. J. (1993). A latent class unfolding model for analyzing single stimulus preference ratings. *Psychometrika*, *58*(4), 545–565.

Deeplizard. (2017, November 21). *Machine Learning & Deep Learning Fundamentals*.

Diaz-Faes, A. A., Gonzalez-Albo, B., Galindo, M. P., & Bordons, M. (2013). HJ-Biplot as a tool for inspection of bibliometric data matrices. *REVISTA ESPANOLA DE DOCUMENTACION CIENTIFICA*, *36*(1). https://doi.org/10.3989/redc.2013.1.988
Dorado-Diaz, P. I., Sampedro-Gomez, J., Vicente-Palacios, V., & Sanchez, P. L. (2019). Applications of Artificial Intelligence in Cardiology. The Future is Already Here. *REVISTA ESPANOLA DE CARDIOLOGIA*, *72*(12), 1065–1075. https://doi.org/10.1016/j.rec.2019.05.014
Ferreira, V., Panagopoulos, T., Andrade, R., Guerrero, C., & Loures, L. (2015). Spatial variability of soil properties and soil erodibility in the Alqueva reservoir watershed. *SOLID EARTH*, *6*(2), 383–392. https://doi.org/10.5194/se-6-383-2015
Flach, P. (2012). *MACHINE LEARNING: The Art and Science of Algorithms that Make Sense of Data*. httphttp://2.180.2.83:801/opac/temp/11802.pdf
Fu, H., Lei, P., Tao, H., Zhao, L., & Yang, J. (2019). Improved semi-supervised autoencoder for deception detection. *PLoS ONE*, *14*(10). https://doi.org/10.1371/journal.pone.0223361
Fu, X., Wei, Y., Xu, F., Wang, T., Lu, Y., Li, J., & Huang, J. Z. (2019). Semi-supervised Aspect-level Sentiment Classification Model based on Variational Autoencoder. *Knowledge-Based Systems*, *171*, 81–92. https://doi.org/10.1016/j.knosys.2019.02.008
Gabriel, K. R. (1971). The biplot graphic display of matrices with application to principal component analysis. *Biometrika*, *58*(3), 453–467.
Galindo Villardón, P. (1986). An alternative for simultaneous representation: HJ-Biplot. *Questiió*, *10*(1), 13–23.
Gallego-Alvarez, I., Formigoni, H., & Antunes, M. T. P. (2014). CORPORATE SOCIAL RESPONSIBILITY PRACTICES AT BRAZILIAN FIRMS. *RAE-REVISTA DE ADMINISTRACAO DE EMPRESAS*, *54*(1), 12–27. https://doi.org/10.1590/S0034-759020140103
Gallego-Álvarez, I., Galindo-Villardón, M. P., & Rodríguez-Rosa, M. (2015). Analysis of the Sustainable Society Index Worldwide: A Study from the Biplot Perspective. *Social Indicators Research*, *120*(1), 29–65.
Garcia-Talegon, J., Vicente, M. A., Molina-Ballesteros, E., & Vicente-Tavera, S. (1999). Determination of the origin and evolution of building stones as a function of their chemical composition using the inertia criterion based on an HJ-biplot. *CHEMICAL GEOLOGY*, *153*(1–4), 37–51. https://doi.org/10.1016/S0009-2541(98)00151-X
Giddings, B., Hopwood, B., & O'Brien, G. (2002). Environment, economy and society: Fitting them together into sustainable development. *Sustainable Development*, *10*(4), 187-196.
Grigoroudis, E., Kouikoglou, V. S., & Phillis, Y. A. (2014). SAFE 2013: Sustainability of countries updated. *Ecological Indicators*, *38*, 61–66.
Grigoroudis, E., Kouikoglou, V. S., & Phillis, Y. A. (2021). SAFE 2019: Updates and new sustainability findings worldwide. *ECOLOGICAL INDICATORS*, *121*. https://doi.org/10.1016/j.ecolind.2020.107072
Hernandez, M., Espinosa, F., & Galindo, P. (2014). Tomato fruit quality as influenced by the interactions between agricultural techniques and harvesting period. *JOURNAL OF PLANT NUTRITION AND SOIL SCIENCE*, *177*(3), 443–448. https://doi.org/10.1002/jpln.201200642
Hou, B., Yang, J., Wang, P., & Yan, R. (2020). LSTM-Based Auto-Encoder Model for ECG Arrhythmias Classification. *IEEE Transactions on Instrumentation and Measurement*, *69*(4), 1232–1240. https://doi.org/10.1109/TIM.2019.2910342

Hizli, C., Karamatli, E., Cemgil, A. T., & Kirbiz, S. (2020). Joint Source Separation and Classification Using Variational Autoencoders. In *2020 28TH SIGNAL PROCESSING AND COMMUNICATIONS APPLICATIONS CONFERENCE (SIU)*.

Inza, I., Calvo, B., Armananzas, R., Bengoetxea, E., Larranaga, P., & Lozano, J. A. (2010). Machine Learning: An Indispensable Tool in Bioinformatics. *BIOINFORMATICS METHODS IN CLINICAL RESEARCH*, *593*, 25–48. https://doi.org/10.1007/978-1-60327-194-3_2

Kiers, H. A. L., Vicari, D., & Vichi, M. (2005). Simultaneous classification and multidimensional scaling with external information. *Psychometrika*, *70*(3), 433–460.

Litago, J. D. U., Rivas, N. M. C., & Gonzalez, A. G. (2017). MEDIA COVERAGE OF THE PROHIBITION OF BULLFIGHTING IN CATALUNA THROUGH A MULTIVARIATE ANALYSIS HJ-BIPLOT. *PRISMA SOCIAL*, *19*, 450–470.

Liu, G. G., Xie, L., & Chen, C. H. (2020). Unsupervised Text Feature Learning via Deep Variational Auto-encoder. *INFORMATION TECHNOLOGY AND CONTROL*, *49*(3), 421–437. https://doi.org/10.5755/j01.itc.49.3.25918

Macedo, E., & Freitas, A. (2015). The alternating least-squares algorithm for CDPCA. *Communications in Computer and Information Science*, 173–191.

Martinez-Ferrero, J., & Gallego-Alvarez, I. (2013). Application of the HJ Biplot Methodology to Variation Greenhouse Gas Emissions in International Companies. In M. A. FernandezIzquierdo, M. J. MunozTorres, & R. Leon (Eds.), *MODELING AND SIMULATION IN ENGINEERING, ECONOMICS, AND MANAGEMENT* (Vol. 145, pp. 10–22).

Neftci, E. O., & Averbeck, B. B. (2019). Reinforcement learning in artificial and biological systems. *Nature Machine Intelligence*. https://doi.org/10.1038/s42256-019-0025-4

Nieto-Librero, A. B., Sierra, C., Vicente-Galindo, M. P., Ruíz-Barzola, O., & Galindo-Villardón, M. P. (2017). Clustering Disjoint HJ-Biplot: A new tool for identifying pollution patterns in geochemical studies. *Chemosphere*. https://doi.org/10.1016/j.chemosphere.2017.02.125

Pambabay-Calero, J., Bauz-Olvera, S., Nieto-Librero, A., Sanchez-Garcia, A., & Galindo-Villardon, P. (2021). Hierarchical Modeling for Diagnostic Test Accuracy Using Multivariate Probability Distribution Functions. *MATHEMATICS*, *9*(11). https://doi.org/10.3390/math9111310

Phillis, Y. A., & Andriantiatsaholiniaina, L. A. (2001). Sustainability: an ill-defined concept and its assessment using fuzzy logic. *ECOLOGICAL ECONOMICS*, *37*(3), 435–456. https://doi.org/10.1016/S0921-8009(00)00290-1

Phillis, Y. A., Grigoroudis, E., & Kouikoglou, V. S. (2011). Sustainability ranking and improvement of countries. *Ecological Economics*, *70*(3), 542–553.

Phillis, Y. A., Kouikoglou, V. S., Andriantiatsaholiniaina, L. A., & Zhu, X. M. (2004). Environmental applications of fuzzy logic. In *2004 IEEE INTERNATIONAL CONFERENCE ON FUZZY SYSTEMS, VOLS 1-3, PROCEEDINGS* (pp. 341–346).

Ping, G., Chen, J. L., Pan, T. Y., & Pan, J. (2019). Degradation feature extraction using multi-source monitoring data via logarithmic normal distribution based variational auto-encoder. *COMPUTERS IN INDUSTRY*, *109*, 72–82. https://doi.org/10.1016/j.compind.2019.04.013

Qiuyu Zhu, R. Z. (2020). A Classification Supervised Auto-Encoder Based on Predefined Evenly-Distributed Class Centroids. *Computer Science*.

Rocca, J. (2019). Understanding Variational Autoencoders (VAEs). Building, step by step, the reasoning that leads to VAEs. *Towards Data Science*.

https://towardsdatascience.com/understanding-variational-autoencoders-vaes-f70510919f73

Rocci, R., Gattone, S. A., & Vichi, M. (2011). A New Dimension Reduction Method: Factor Discriminant K-means. *Journal of Classification*, *28*(2), 210–226.

Sachs, J. (2019). *Getting to a Carbon-Free Economy, the urgent is attainable, and at entirely affordable cost*. https://prospect.org/greennewdeal/getting-to-a-carbon-free-economy/

Sachs, J. (2020). *The world needs a prosperous and properly funded Europe*. https://www.ft.com/content/a32db296-5257-11ea-8841-482eed0038b1

Sachs, J., Schmidt-Traub, G., Kroll, C., Durand-Declare, D., Teksoz, K. (2016). SDG Index and Dashboards - Global Report. In *New York: Bertelsmann Stiftung and Sustainable Development Solutions Network (SDSN)*. https://www.sdgindex.org/reports/sdg-index-and-dashboards-2016/

San Martin, G., Droguett, E. L., Meruane, V., & Moura, M. D. (2019). Deep variational auto-encoders: A promising tool for dimensionality reduction and ball bearing elements fault diagnosis. *STRUCTURAL HEALTH MONITORING-AN INTERNATIONAL JOURNAL*, *18*(4), 1092–1128. https://doi.org/10.1177/1475921718788299

Sarkar, D., Bali, R., & Sharma, T. (2018). Practical Machine Learning with Python. In *Practical Machine Learning with Python*. https://doi.org/10.1007/978-1-4842-3207-1

Suarez, M. H., Perez, D. M., Rodriguez-Rodriguez, E. M., Romero, C. D., Borreguero, F. E., & Galindo-Villardon, P. (2016). The Compositional HJ-Biplot-A New Approach to Identifying the Links among Bioactive Compounds of Tomatoes. *INTERNATIONAL JOURNAL OF MOLECULAR SCIENCES*, *17*(11). https://doi.org/10.3390/ijms17111828

Sun, L., Li, B., Yuan, C., Zha, Z., & Hu, W. (2019). Multimodal semantic attention network for video captioning. *Proceedings - IEEE International Conference on Multimedia and Expo*, *2019-July*, 1300–1305. https://doi.org/10.1109/ICME.2019.00226

Tan, Y ; Shuai, C ;Jiao, L ;Shen, L. (2017). An adaptive neuro-fuzzy inference system (ANFIS) approach for measuring country sustainability performance. *Environmental Impact Assessment Review*, *65*, 29–40. https://doi.org/10.1016/j.eiar.2017.04.004

Tan, Yongtao ; Shuai, Chenyang; Jiao, Liudan; Liyin, S. (2018). Adaptive neuro-fuzzy inference system approach for urban sustainability assessment: A China case study. *Sustainable Development*. https://doi.org/10.1002/sd.1744

Tejedor-Flores, N., Vicente-Galindo, P., & Galindo-Villardon, P. (2017). Sustainability Multivariate Analysis of the Energy Consumption of Ecuador Using MuSIASEM and BIPLOT Approach. *SUSTAINABILITY*, *9*(6). https://doi.org/10.3390/su9060984

United Nations. (1992). Agenda 21: Programme of Action for Sustainable Development. In *United Nations Conference on Environment and Development (UNCED)*. https://sustainabledevelopment.un.org/content/documents/Agenda21.pdf.

Urruticoechea, A., & Vernazza, E. (2019). ENTERPRISE SUSTENTABILITY: ANALYSIS THROUGH BIPLOT METHODOLOGY. *CUADERNOS DEL CIMBAGE*, *21*(1), 87–115.

Valchev, N., Ivanova, M., Stoyanova, A., & Dospatliev, L. (2020). APPLICATION OF THE MATHEMATICAL MODEL HJ-BIPLOT TO IDENTIFYING THE LINKS AMONG BIOACTIVE COMPOUNDS OF THE TOMATO VARIETY PANEKRA. *SCIENTIFIC PAPERS-SERIES B-HORTICULTURE*, *64*(1), 490–497.

Vichi, M., & Kiers, H. A. L. (2001). Factorial k-means analysis for two-way data. *Computational Statistics and Data Analysis*, *37*(1), 49–64.

Vichi, M., & Saporta, G. (2009). Clustering and disjoint principal component analysis. *Computational Statistics and Data Analysis*, *53*(8), 3194–3208.

Vigneau, E., & Qannari, E. M. (2003). Clustering of Variables Around Latent Components. *Communications in Statistics Part B: Simulation and Computation*, *32*(4), 1131–1150.

Vines, S. K. (2000). Simple principal components. *Journal of the Royal Statistical Society. Series C: Applied Statistics*, *49*(4), 441–451.

Waas, T., Hugé, J., Verbruggen, A., & Wright, T. (2011). Sustainable development: A bird's eye view. *Sustainability*, *3*(10), 1637–1661.

Xavier, A., Freitas, M. D. C., Rosario, M. D., & Fragoso, R. (2018). Disaggregating statistical data at the field level: An entropy approach. *SPATIAL STATISTICS*, *23*, 91–108. https://doi.org/10.1016/j.spasta.2017.11.005

Xie, L., Liu, G. G., & Lian, H. F. (2019). Deep variational auto-encoder for text classification. In *2019 IEEE INTERNATIONAL CONFERENCE ON INDUSTRIAL CYBER PHYSICAL SYSTEMS (ICPS 2019)*.

Yan, Y., Conze, P. H., Decenciere, E., Lamard, M., Quellec, G., Cochener, B., & Coatrieux, G. (2019). Cascaded multi-scale convolutional encoder-decoders for breast mass segmentation in high-resolution mammograms. *Proceedings of the Annual International Conference of the IEEE Engineering in Medicine and Biology Society, EMBS*, 6738–6741. https://doi.org/10.1109/EMBC.2019.8857167

Yang, Y., Zheng, K., Wu, B., Yang, Y., & Wang, X. (2020). Network Intrusion Detection Based on Supervised Adversarial Variational Auto-Encoder with Regularization. *IEEE Access*, *8*, 42169–42184. https://doi.org/10.1109/ACCESS.2020.2977007

Yusiong, J. P. T., & Naval, P. C. (2019). AsiANet: Autoencoders in autoencoder for unsupervised monocular depth estimation. *Proceedings - 2019 IEEE Winter Conference on Applications of Computer Vision, WACV 2019*, 443–451. https://doi.org/10.1109/WACV.2019.00053

Zadeh, L. A. (1971). Similarity relations and fuzzy orderings. *Information Sciences*, *3*(2), 177–200.

Zhang, Z., Zhu, Q., Xie, G. Sen, Chen, Y., Li, Z., & Wang, S. (2020). Discriminative margin-sensitive autoencoder for collective multi-view disease analysis. *Neural Networks*, *123*, 94–107. https://doi.org/10.1016/j.neunet.2019.11.013

Zhu, J. Z., Shi, H. B., Song, B., Tao, Y., & Tan, S. (2020). Information concentrated variational auto-encoder for quality-related nonlinear process monitoring. *JOURNAL OF PROCESS CONTROL*, *94*, 12–25. https://doi.org/10.1016/j.jprocont.2020.08.002

Zhu, Q. yu, & Li, T. tian. (2020). Semi-supervised learning method based on predefined evenly-distributed class centroids. *Applied Intelligence*. https://doi.org/10.1007/s10489-020-01689-1

Zimmerer, D., Isensee, F., Petersen, J., Kohl, S., & Maier-Hein, K. (2019). Unsupervised Anomaly Localization Using Variational Auto-Encoders. In D. Shen, T. Liu, T. M. Peters, L. H. Staib, C. Essert, S. Zhou, P. T. Yap, & A. Khan (Eds.), *MEDICAL IMAGE COMPUTING AND COMPUTER ASSISTED INTERVENTION - MICCAI 2019, PT IV* (Vol. 11767, pp. 289–297). https://doi.org/10.1007/978-3-030-32251-9_32

Basic indicators References

- Esty DC, Levy M, Srebotnjak T, Sherbinin A (2005) 2005 Environmental Sustainability Index: Benchmarking National Environmental Stewardship, New Haven, CT, Yale Center for Environmental Law and Policy.
- FAO (Food and Agriculture Organization) Satistics data.
- IUCN (International Union for the Conservation of Nature) (1994) Guidelines for protected areas management categories, IUCN, Cambridge, UK and Gland, Switzerland.
- OECD (Organization of Economic Cooperation and Development) Statistics portal.
- OECD (2000) Education at a glance, OECD Publications, Paris.
- OECD (2004) Key environmental indicators 2004, OECD, Paris.
- Ordoubadi SMH (2005) World Development Indicators, The World Bank Development Data Center, Washington, DC.
- UNEP (United Nations Environmental Program), Geodata portal, electronic database.
- United Nations Statistics Division (2006) Population and vital statistics report, United Nations, New York, NY.
- UNDP (United Nations Development Program) (2003) Human Development Report 2003, Oxford University Press, New York.
- UNESCO (United Nations Educational, Scientific, and Cultural Organization), Institute for Statistics, Custom tables, electronic database.
- UNFCCC (United Nations Framework Convention on Climate Change), GHG emissions data.

- WHO (World Health Organization). Core health indicators, electronic database.
- World Bank (1995) Monitoring environmental progress: A report on work in progress, World Bank Environmentally Sustainable Development International Bank for Reconstruction and Development, Washington, DC.
- World Bank (2008) KI and KEI Indexes (KAM 2008), electronic database.
- Grigoroudis, E, Kouikoglou, VS, and Phillis, YA (2013). SAFE 2013: Sustainability of countries updated, Ecological Indicators 38, 61-66
- Kouikoglou VS, Phillis YA (2009). On the monotonicity of hierarchical sum-product fuzzy systems. Fuzzy Sets and Systems 160 (24), 3530–3538.
- Esty DC, Levy M, Srebotnjak T, Sherbinin A (2005) 2005 Environmental sustainability index: Benchmarking national environmental stewardship, Yale Center for Environmental Law & Policy, New Haven, CT.
- United Nations Statistics Division (2010) Composition of macro geographical (continental) regions, geographical sub-regions, and selected economic and other groupings.
- World Bank (2010) Country groups.

APPENDICES

Appendix 1. Basic indicators of sustainable development (SAFE model) (http://www.sustainability.tuc.gr/22.html)

Ecosystem

LAND Indicators

PR(LAND)

(1) Municipal waste generation (kg per capita per year)

Waste collected and treated by or for municipalities. It covers waste from households (including bulky waste), similar waste from commerce and trade, office buildings, institutions and small businesses, yard and garden waste, street sweepings, the contents of litter containers, and market cleaning waste. The definition excludes waste from municipal sewage networks and treatment, as well as municipal construction and demolition waste. Reducing waste generation improves land sustainability.

(2) Nuclear waste (tons of heavy metals per capita per year)

Nuclear waste is primarily due to spent fuel from nuclear power plants. It is assumed that nuclear waste influences land sustainability negatively due mainly to generation of heavy radioactive metals.

(3) Hazardous waste (tons of waste per capita per year)

Waste found in streams to be controlled according to the Basel Convention on the Control of Transboundary Movements of Hazardous Wastes and their Disposal. Reduction of hazardous waste improves land sustainability

(4) Population growth rate (percentage)

Average annual exponential rate of population change for given periods of years. Small or zero population growth rate is perceived as influencing positively land sustainability.

(5) Pesticide consumption (kg of pesticide consumption per hectare of arable land)

Pesticide use intensity refers to the amount of pesticide used per hectare of arable and permanent cropland. Excessive use of pesticides in agricultural activities has negative impacts on soil, water, humans and wildlife.

(6) Fertilizer consumption (kg of fertilizer per hectare of arable land)

Fertilizer consumption measures the quantity of plant nutrients used per unit of arable land in the form of nitrogenous, potash, and phosphate fertilizers (including ground rock phosphate). Excessive use of fertilizers from agricultural activities has a negative impact on soil and water, altering chemistry and levels of nutrients and leading to eutrophication of water bodies.

ST(LAND)

(7) Desertification of land (percent of dryland area)

Areas with a potential hazard of desertification. All major continents face problems of land degradation in dryland areas, commonly known as desertification. Dryland areas are ‘fragile’ in that they are extremely vulnerable to land degradation resulting from over-grazing and other forms of inappropriate land use.

(8) Forest area (percent of what existed in the year 2000)

Forest area is land under natural or planted stands of trees, whether productive or not. Forests maintain land sustainability.

RE(LAND)

(9) Forest change (annual rate of change

Forest area change is the net change in forests and includes expansion of forest plantations and losses and gains in the area of natural forests. A positive forest change improves land sustainability.

(10) Protected area (ratio to surface area)

An area of land and/or sea especially dedicated to the protection and maintenance of biological diversity, and of natural and associated cultural resources, and managed through legal or other effective means (IUCN 1994). Protected area ensures land sustainability.

(11-12) Recycling rates: glass[11], paper[12] (percent of apparent consumption)

Recycling rates are the ratios of the quantity collected for recycling to the apparent consumption. Reducing uncontrolled waste improves land sustainability.

WATER **Indicators**

PR(WATER)

(13) Total water withdrawals (percent of total renewable resources)

Total annual amount of water withdrawn per amount of renewable water resources. Excessive use of water reduces water sustainability.

ST(WATER)

(14) Organic water pollutant emissions

(BOD, biological oxygen demand in kg per capita per day)

Emissions of organic water pollutants are measured by biochemical oxygen demand, which is the amount of oxygen that bacteria in water will consume to break down waste. This is a standard water treatment test for the presence of organic pollutants.

(15) Phosphorous concentration (mg phosphorus per liter of water)

It is a measure of eutrophication, which affects the health of aquatic resources. High levels of phosphorus increase the chances of eutrophication.

(16) Metals concentration (micro-Siemens per centimeter)

It is a widely used bulk measure of metals concentration and salinity. Siemens is a unit of electric conductivity. High levels of conductivity correspond to high concentrations of metals.

RE(WATER)

(17) Public wastewater treatment plants (percent of population connected)

Connected means actually connected to a waste water treatment plant through a public sewage network. Non-public treatment plants, i.e., industrial waste water plants, or individual private treatment facilities such as septic tanks are not included. High connectivity improves water sustainability.

BIODIVERSITY Indicators

PR(BIOD)

(18-23) Threatened bird[18], mammal[19], plant[20], fish[21], amphibian[22], and reptile[23] species

(percentage)

Includes all species that are critically endangered, endangered, or vulnerable, but excludes introduced species, species whose status is insufficiently known, those known to be extinct, and those for which a status has not been assessed. IUCN has established detailed quantitative definitions for the above categories. Very briefly: Critically endangered is a species that faces an extremely high risk of extinction. A species in this category has experienced or will experience a population reduction of at least 80% within the next 10 years or the next 3 generations, whichever is longer and causes of extinction may not have ceased or may not be understood or may not be reversible.

Endangered species face a very high risk of extinction and the corresponding population reduction as above is at least 50%.

Finally, vulnerable species face a high risk of extinction and a corresponding population reduction of at least 30%.

ST(BIOD)

(7) **Desertification of land.**

(8) **Forest area.**

RE(BIOD)

(9) **Forest change.**

(10) **Protected area.**

AIR Indicators

PR(AIR)

(24) **Ozone depleting substances per capita**

(consumption in ozone depleting potential metric tons)

An ozone depleting substance is any substance containing chlorine or bromine, which destroy the stratospheric ozone layer that absorbs most of the biologically damaging ultraviolet radiation. Ozone depleting potential (ODP) refers to the amount of ozone depletion caused by a substance. ODP is defined as the ratio of the impact on stratospheric ozone of a substance to the impact of the same mass of CFC-11. CFC-11 has an ODP of 1.

(25) Greenhouse gas (GHG) emissions per capita (tons of CO_2 equivalent)

Emissions of total GHG (CO_2, CH_4, N_2O, hydrofluorocarbons (HFC's), perfluorocarbons (PFC's), and SF_6), excluding land-use change and forestry. To convert all emissions to CO_2 equivalent, the global warming potential (GWP) is used. GWP is an index used to translate the level of emissions of various gases into a common measure in order to compare the relative radiative forcing of different gases without directly calculating the changes in atmospheric concentrations. GWP is the ratio of the warming caused by a substance to the warming caused by the same mass of CO_2.

ST(AIR)

(26) Mortality from poor air quality

(number of deaths per 100,000 persons)

Diseases of the respiratory system generally cause irritation and reduced lung function, especially in more susceptible members of the population such as young children, the elderly and asthmatics.

(27-29) Atmospheric concentrations of NO_2[27], SO_2[28] and total suspended particulates[29] (µg/m^3 of air)

The values were originally collected at the city level. The number of cities with data provided by each country varies. Within each country the values have been normalized by city population for the year 1995, and then summed to give the total concentration for the given country. High concentrations decrease air sustainability.

RE(AIR)

(30) Renewable resources production (percent of total primary energy supply)

The higher the proportion of renewable energy sources is, the less a country relies on environmentally damaging sources such as fossil fuel and nuclear energy.

Human System

POLICY Indicators

PR(POLICY)

(31) Military spending (percent of GDP)

For members of the North Atlantic Treaty Organization (NATO) it is based on the NATO definition, which covers military-related expenditures of the defense ministry and other ministries. Civilian-type expenditures of defense ministries are excluded. Military assistance is included in the expenditure of the donor country. Purchases of military equipment on credit are recorded at the time the debt is incurred, not at the time of payment. Data for non-NATO countries generally cover expenditure of the ministry of defense; excluded are expenditures on public order and safety, which are classified separately.

(32) Refugees per capita

(ratio of refugees from a country to total population of that country)

Refugees are people who are recognized as refugees under the 1951 Convention Relating to the Status of Refugees or its 1967 Protocol, the 1969 Organization of African Unity Convention Governing the Specific Aspects of Refugee Problems in Africa, people recognized as refugees in accordance with the UNHCR (United Nations High Commissioner for Refugees) statute, people granted a refugee-like humanitarian status, and people provided with temporary protection.

(33) Poverty (percent of population below national poverty line)

National poverty rate is the percentage of population living below the national poverty line. The latter is usually estimated by finding the total cost of all the essential resources that an average human adult consumes in one year.

ST(POLICY)

(34) Political Rights

The Freedom House Annual Survey employs the Political Rights checklist to help determine the degree to which people can participate in the political process of their country. Each country is then rated on a seven-category scale, 1 representing the most free and 7 the least free.

(35) Civil Liberties

The Freedom House Annual Survey employs a Civil Liberties checklist to help monitor the progress and decline of human rights worldwide. As previously, each country is rated on a seven-category scale, 1 representing the most free and 7 the least free.

(36) Gini index

It measures the extent to which the distribution of income among individuals or households within an economy deviates from a perfectly equal distribution. A Gini index of zero would represent perfect equality and an index of 100 would imply perfect inequality—a single person or household accounting for all income or consumption.

(37) Corruption Perceptions Index

International Transparency, the coalition against corruption, gathers data for the last two years for all countries to compute the Corruption Perceptions Index (CPI). CPI (Transparency International 2007) ranges from 1 to 10 or from the most to the least corrupt countries and it expresses a degree of misuse of power by public officials and politicians for private gain such as bribes, favoritism, embezzlement of money, etc.

RE(POLICY)

(38) Environmental laws and enforcement

This index ranges: from zero to one and is obtained by a subjective assessment on the basis of various world reports and experts' knowledge. National environmental laws are included in the context of this indicator as well as international agreements such as the Convention on Biological Diversity, the Ramsar Convention on Wetlands of International Importance, the Convention on International Trade of Endangered Species (CITES), national environmental laws, etc.

(39) Tax revenue (percent of GDP)

Tax revenue refers to compulsory transfers (payments) to the central government for public purposes. Certain compulsory transfers such as fines, penalties, and most social security contributions are excluded. Refunds and corrections of erroneously collected tax revenue are treated as negative revenue.

WEALTH Indicators

(40) Implicit deflator (average annual percent growth rates)

Reflects changes in prices for all final demand categories, such as government consumption, capital formation, and international rate, as well as the main component, private final consumption. It is derived as the ratio of current to constant-price GDP. It is known as inflation indicator affecting the sustainability of a national economy.

(41) Imports (percent of GDP)

Shows the cost plus insurance and freight value in U.S. dollars of goods purchased from the rest of the world.

(42) Unemployment

Unemployment refers to the share of the labor force that is without work but available for and seeking employment. Definitions of labor force and unemployment differ by country.

(43) Unemployment gender gap

This variable shows the absolute difference between unemployment rate for female and male labor force.

ST(WEALTH)

(44) Central government debt (percent of GDP)

Debt is the entire stock of direct government fixed-term contractual obligations to others outstanding on a particular date. It includes domestic and foreign liabilities such as currency and money deposits, securities other than shares, and loans. It is the gross amount of government liabilities reduced by the amount of equity and financial derivatives held by the government. Because debt is a stock rather than a flow, it is measured as of a given date, usually the last day of the fiscal year.

(45) GNI per capita PPP (based on PPP, purchasing power parity)

PPP GNI is gross national income converted to international dollars using purchasing power parity rates. An international dollar has the same purchasing power over GNI as a U.S. dollar has in the United States. GNI is the total market value of all final goods and services produced within a country (also called gross domestic product or GDP), plus income received from other countries such as interest and dividends, minus similar payments made to other countries. PPP equalizes the purchasing power of different currencies for a given set of goods. Thus GNI PPP (U.S.$) is national income converted to international dollars using a conversion factor. International dollars correspond to the amount of a given basket of goods and services one could buy in the U.S. with a given sum of money. Data are in current international dollars. This indicator is commonly used to evaluate the status of wealth sustainability at the national level.

RE(WEALTH)

(46) Exports (percent of GDP)

Exports of goods and services represent the value of all goods and other market services provided to the rest of the world. Exports create wealth.

(47) Foreign direct investment, net inflows (percent of GDP)

Foreign direct investment is net inflows of investment to acquire a lasting management interest (10 percent or more of voting stock) in an enterprise operating in an economy other than that of the investor.

HEALTH Indicators

PR(HEALTH)

(48) Infant mortality rate

Number of infants who die before reaching one year of age, expressed per thousand live births in a given year.

(49) Maternal mortality rate

Annual number of deaths from pregnancy or childbirth related causes per 100,000 live births. A maternal death is defined by WHO as the death of a woman while pregnant or within 42 days of the termination of pregnancy from any cause related to or aggravated by the pregnancy, including abortion.

(50) HIV/AIDS prevalence (percent of population aged 15–49)

Prevalence of HIV refers to the percentage of people ages 15–49 who are infected with HIV.

(51) Tuberculosis prevalence (per 100,000 population)

It refers to people with all forms of TB, including TB in people with HIV infection.

(52) Malaria cases (per thousand people)

Standardized cases are derived from the total reported number of cases and an appreciation of the proportion of these cases that were laboratory-confirmed. Reported cases per country for the most recent year for which WHO/RBM (World Health Organization/Roll Back Malaria) received data. The standardized case reporting rate (per 1,000 per year) is calculated by dividing the standardized cases by the national population size estimated by the United Nations Population Division for the middle of the year under consideration.

ST(HEALTH)

(53) Life expectancy

Number of years a newborn infant would live if patterns of mortality prevailing at the time of its birth were to stay the same throughout its life.

(54-55) Infants immunized against severe diseases

Percent of one-year-old infants immunized against measles[54] and diphtheria-pertussis-tetanus (DPT)[55].

(56) Daily per capita calorie supply(percent of total requirements)

Data taken from the Food and Agriculture Organization (FAO) food balance sheets. The calories and protein actually consumed may be lower than the figure shown, depending on how much is lost during home storage, preparation, and cooking, and how much is fed to pets and domestic animals or discarded.

RE(HEALTH)

(57) Number of doctors (per thousand people)

The term doctors includes physicians that are defined as graduates of any facility or school of medicine who are working in the country in any medical field (practice, teaching, research).

(58) Hospital beds (per thousand people)

Hospital beds include inpatient beds available in public, private, general, and specialized hospitals and rehabilitation centers. In most cases beds for both acute and chronic care are included.

(59) Public health expenditure (percent of GDP

Consists of recurrent and capital spending from government budgets, external borrowings and grants, and social health insurance funds.

(60,61) Access to improved water sources[60] and to improved sanitation[61] (percent of population)

The percentage of population with access to the facilities that can provide them with safe water and sanitation. Access to the above is a fundamental need and a human right vital for the dignity and health of all people.

KNOWLEDGE Indicators

PR(KNOW)

(62-64) Ratio of students to teaching staff

(primary[62], secondary[63], and tertiary[64] education)

Teaching staff includes (OECD 2000) professional personnel involved in direct student instruction: classroom teachers, special education teachers, other teachers who work with students as a whole class, and chairpersons of departments; it does not include nonprofessional personnel who support teachers.

ST(KNOW)

(65, 66) Expected years of schooling; male[65] and female[66]

Average number of years of formal schooling that a child is expected to receive, including university education and years spent in repetition. It may also be interpreted as an indicator of the total educational resources, measured in school years, a child will require over the course of schooling.

(67, 68) Net school enrollment ratio; primary[67] and secondary[68]

Number of children of official school age, as defined by the education system, enrolled in primary or secondary school, expressed as percentage of the total number of children of that age.

(69) Literacy rate, adult total (percent of people with ages 15 and above)

Adult literacy rate is the percentage of people ages 15 and above who can, with understanding, read and write a short, simple statement on their everyday life.

(70) World Bank's Knowledge Economy Index (KEI)

KEI measures the degree to which a country uses knowledge efficiently to improve its economical development. It is an aggregate index that represents the overall level of development of a country or region towards the knowledge economy.

RE(KNOW)

(71) Public expenditure on R&D (percent of GDP)

Expenditures for research and development are current and capital expenditures (both public and private) on creative, systematic activities that increase the stock of knowledge. Included are fundamental and applied research and experimental development work leading to new devices, products, or processes.

(72) Public expenditure on education

ercentage of GNP accounted for by public spending on public education plus subsidies to private education at the primary, secondary, and tertiary levels. It may exclude spending by religious schools, which play a significant role in many developing countries. Data for some countries and for some years refer to spending by the ministry of education of the central government only, and thus exclude education expenditures by other central government ministries and departments, local authorities, and others.

(73) Personal computers (per thousand people)

Estimated numbers of self-contained computers used by a single person. Access to personal computers promotes knowledge development and educational sustainability.

(74) Internet users (per thousand people)

Number of computers directly connected to the worldwide network of interconnected computer systems, per 10,000 people. Access to the Internet facilitates knowledge acquisition.

(75) Information and communication technology expenditure (percent of GDP)

Information and communications technology expenditures include computer hardware (computers, storage devices, printers, and other peripherals); computer software (operating systems, programming tools, utilities, applications, and internal software development); computer services (information technology consulting, computer and network systems integration, web hosting, data processing services, and other services); communications services (voice and data communications services); and wired and wireless communications equipment.

Appendix 2. Python Coding

```
!pip install colour
!pip uninstall keras
!pip install keras==2.3

from   __future import absolute_import
from   __future import division
from __future__ import print_function

from keras.layers import Lambda, Input, Dense, LeakyReLU,
BatchNormalization
from keras.models import Model
from keras.datasets import mnist
from keras.losses import mse, binary_crossentropy
from keras.utils import plot_model
from keras import backend as K
import keras

import numpy as np
from colour import Color
import pandas as pd

import random

import matplotlib.pyplot as plt
import argparse
import os

"""# Common Functions"""

# reparameterization trick
# instead of sampling from Q(z|X), sample epsilon = N(0,I)
# z = z_mean + sqrt(var) * epsilon
def sampling(args):
    """Reparameterization trick by sampling from an isotropic unit
Gaussian.

    # Arguments
```

```
        args (tensor): mean and log of variance of Q(z|X)

    # Returns
        z (tensor): sampled latent vector
    """

    z_mean, z_log_var = args
    batch = K.shape(z_mean)[0]
    dim = K.int_shape(z_mean)[1]
    # by default, random_normal has mean = 0 and std = 1.0
    epsilon = K.random_normal(shape=(batch, dim))
    return z_mean + K.exp(0.5 * z_log_var) * epsilon

def plot_results(models,
                 data,
                 batch_size=128,
                 model_name="vae_mnist"):
    """Plots labels and MNIST digits as a function of the 2D latent
vector

    # Arguments
        models (tuple): encoder and decoder models
        data (tuple): test data and label
        batch_size (int): prediction batch size
        model_name (string): which model is using this function
    """

    encoder, decoder = models
    x_test, y_test = data
    os.makedirs(model_name, exist_ok=True)

    filename = os.path.join(model_name, "vae_mean.png")
    # display a 2D plot of the digit classes in the latent space
    z_mean, _, _ = encoder.predict(x_test,
                                   batch_size=batch_size)
    plt.figure(figsize=(12, 10))
    plt.scatter(z_mean[:, 0], z_mean[:, 1], c=y_test)
    plt.colorbar()
```

```
    plt.xlabel("z[0]")
    plt.ylabel("z[1]")
    plt.savefig(filename)
    plt.show()

    filename = os.path.join(model_name, "digits_over_latent.png")
    n = 10
    digit_size = 28

    digit_x = digit_size
    digit_y = digit_size

    figure = np.zeros((digit_x * n, digit_y * n))
    # linearly spaced coordinates corresponding to the 2D plot
    # of digit classes in the latent space
    grid_x = np.linspace(-4, 4, n)
    grid_y = np.linspace(-4, 4, n)[::-1]



    for  i,  yi  in  enumerate(grid_y):
        for j, xi in enumerate(grid_x):
            z_sample = np.array([[xi, yi]])
            x_decoded = decoder.predict(z_sample)
            digit = x_decoded[0].reshape(digit_x, digit_y)
            figure[i * digit_size: (i + 1) * digit_x,
                   j * digit_size: (j + 1) * digit_y] = digit

    plt.figure(figsize=(10, 10))
    start_range = digit_size // 2
    end_range = (n - 1) * digit_size + start_range + 1
    pixel_range = np.arange(start_range, end_range, digit_size)
    sample_range_x = np.round(grid_x, 1)
    sample_range_y = np.round(grid_y, 1)
    plt.xticks(pixel_range, sample_range_x)
    plt.yticks(pixel_range, sample_range_y)
    plt.xlabel("z[0]")
    plt.ylabel("z[1]")
```

```
    plt.imshow(figure, cmap='Greys_r')
    plt.savefig(filename)
    plt.show()

# Commented out IPython magic to ensure Python compatibility.
# %matplotlib inline
import matplotlib.pyplot as plt
from mpl_toolkits.mplot3d import Axes3D

def get_colors_array(n_colors):
    red = Color("green")
    colors = list(red.range_to(Color("red"),n_colors))
    hex_colors = [el.hex for el in colors]
    return hex_colors

def plot_results_3d(models,data):
    encoder, decoder = models
    x_test, y_test = data
    fig = plt.figure()
    ax = fig.add_subplot(111, projection='3d')

    z_mean, _, _ = encoder.predict(x_test)
    colors_grad = get_colors_array(len(y_test))

    ax.scatter(z_mean[:, 0], z_mean[:, 1], z_mean[:,
2],c=colors_grad)

def plot_results_2d(models,data):
    encoder, decoder = models
    x_t, y_t = data

    plt.figure(figsize=(12, 10))

    z_mean, _, _ = encoder.predict(x_t)
    colors_grad = get_colors_array(len(y_t))
    plt.scatter(z_mean[:, 0], z_mean[:, 1],c=colors_grad)
    return z_mean
```

```
def plot_results_2d_no_color(models, data):
    encoder, decoder = models
    x_t, y_t = data

    plt.figure(figsize=(12, 10))
    #fig = plt.figure()
    #ax = fig.add_subplot(111, projection='3d')

    z_mean, _, _ = encoder.predict(x_t)
    plt.scatter(z_mean[:, 0], z_mean[:, 1])
    return z_mean

import plotly.graph_objects as go

def plot_results_3d_plotly(models,data):
    encoder, decoder = models
    x_test, y_test = data

    z_mean, _, _ = encoder.predict(x_test)
    colors_grad = get_colors_array(len(y_test))

    fig = go.Figure(data=[go.Scatter3d(x=z_mean[:, 0], y=z_mean[:,
1], z=z_mean[:, 2],
                                   mode='markers')])
    fig.show()

class LossAndErrorPrintingCallback(keras.callbacks.Callback):
    epoch_to_display = 10

    def __init__(self, epoch=10):
        self.epoch_to_display = epoch

    def on_epoch_end(self, epoch, logs=None):
        if epoch%self.epoch_to_display==0:
            print('La perdida promedio para la epoch {} es {:7.2f} y
el MSE es {:7.4f}.'.format(epoch, logs['loss'], logs['val_loss']))
```

```
mcp_save = keras.callbacks.ModelCheckpoint('.mdl_wts.hdf5',
save_best_only=True, monitor='mse', mode='min')
reduce_lr_loss = keras.callbacks.ReduceLROnPlateau(monitor='mse',
factor=0.9, patience=1000, verbose=1)

"""# CLEAN DATA"""

from google.colab import drive
drive.mount('/content/gdrive')

df_ranks = pd.read_csv("/content/gdrive/My
Drive/AIDemos/FernandoSustentability/db/ranks.csv")
df_values = pd.read_csv("/content/gdrive/My
Drive/AIDemos/FernandoSustentability/db/data2.csv")
df_values_countries = df_values["Country"]
df_values_abrev = df_values["Country-Abrev"]
df_ranks_countries = df_ranks["Country"]
df_values = df_values.drop(["Country","Country-Abrev"], axis=1)

df_values = df_values.clip(0, 1)
df_values["Country"] = df_values_countries
df_values["Country-Abrev"] = df_values_abrev

merged = pd.merge(df_ranks,df_values,how='inner', on="Country")

print(len(df_values))
print(len(df_ranks))
print(len(df_values_countries))
print(len(merged))

df_values

df_ranks.head()

df = merged
df_country = df["Country"]
df_country_abv = df["Country-Abrev"]
```

```
df = df.drop(["Country", "Country-Abrev"], axis= 1)
df["Country"] = df_country_abv

df.head()

"""## Remove unused columns"""

labels = df["Country"]
useless_rows = ["Country"]
df = df.drop(useless_rows,axis=1)

df.head()

"""### Fix values"""

df["Rank"] = 1 - df["Rank"]/df["Rank"].max()
df_original = df.copy()

df.head()

cols = df.columns
cols = [c for c in cols if c != 'Rank']

dic_vals = {}

for c in cols:
  df[c] = df[c].pow(2)
  col_mean = df[c].mean()
  col_std = df[c].std()

  dic_vals[c] = {
      "mean": col_mean,
      "std": col_std
  }

  df[c] = (df[c] - col_mean) / col_std

df.head()
```

```
"""## Separate TRAIN and TEST data"""

msk = np.random.rand(len(df)) < 0.8
train = df[msk]
test = df[~msk]

print(len(df))
print(len(train))
print(len(test))

y_train = train["Rank"]
x_train = train.drop(["Rank"], axis=1)

y_test = train["Rank"]
x_test = train.drop(["Rank"], axis=1)

"""# CREATE VAE NETWORK"""

image_size = x_train.shape[1]
original_dim = x_train.shape[1]

# network parameters
input_shape = (original_dim, )
intermediate_dim = 128
batch_size = 80
latent_dim = 2
epochs = 4000

# VAE model = encoder + decoder
# build encoder model
inputs = Input(shape=input_shape, name='encoder_input')

x = Dense(intermediate_dim, activation='relu')(inputs)
x = LeakyReLU(alpha=0.2)(x)
x  =  BatchNormalization(axis=-1)(x)
x = Dense(512, activation='relu')(x)
x = BatchNormalization(axis=-1)(x)
```

```
x = Dense(512, activation='relu')(x)
x  =  BatchNormalization(axis=-1)(x)
x = Dense(256, activation='relu')(x)
x  =  BatchNormalization(axis=-1)(x)
x = Dense(256, activation='relu')(x)
x  =  BatchNormalization(axis=-1)(x)
x = Dense(128, activation='relu')(x)
x  =  BatchNormalization(axis=-1)(x)
x = Dense(128, activation='relu')(x)
x  =  BatchNormalization(axis=-1)(x)
x = Dense(64)(x)
x = LeakyReLU(alpha=0.2)(x)
x = BatchNormalization(axis=-1)(x)
x = Dense(32)(x)
x = LeakyReLU(alpha=0.2)(x)
x = BatchNormalization(axis=-1)(x)
x = Dense(10, activation='relu')(x)
x = Dense(3, activation='relu')(x)

z_mean = Dense(latent_dim, name='z_mean')(x)
z_log_var = Dense(latent_dim, name='z_log_var')(x)

# use reparameterization trick to push the sampling out as input
# note that "output_shape" isn't necessary with the TensorFlow
backend
z = Lambda(sampling, output_shape=(latent_dim,), name='z')([z_mean,
z_log_var])

# instantiate encoder model
encoder = Model(inputs, [z_mean, z_log_var, z], name='encoder')
encoder.summary()
plot_model(encoder, to_file='vae_mlp_encoder.png', show_shapes=True)

# build decoder model
latent_inputs = Input(shape=(latent_dim,), name='z_sampling')
x = Dense(intermediate_dim, activation='relu')(latent_inputs)
x = Dense(30, activation='relu')(x)
x = Dense(60, activation='relu')(x)
```

```
outputs = Dense(original_dim)(x)

# instantiate decoder model
decoder = Model(latent_inputs, outputs, name='decoder')
decoder.summary()
plot_model(decoder, to_file='vae_mlp_decoder.png', show_shapes=True)

# instantiate VAE model
outputs = decoder(encoder(inputs)[2])
vae = Model(inputs, outputs, name='vae_mlp')

models = (encoder, decoder)
#data = (x_test, y_test)
data = (x_test, [])

x_test.head()

reconstruction_loss = mse(inputs, outputs)
#reconstruction_loss = binary_crossentropy(inputs,outputs)

reconstruction_loss *= original_dim
kl_loss = 1 + z_log_var - K.square(z_mean) - K.exp(z_log_var)
kl_loss = K.sum(kl_loss, axis=-1)
kl_loss *= -0.5

vae_loss = K.mean(reconstruction_loss + kl_loss)
vae.add_loss(vae_loss)
vae.compile(optimizer='adam')
vae.summary()
plot_model(vae,
           to_file='vae_mlp.png',
           show_shapes=True)

vae.fit(x_train,
        epochs=epochs,
        batch_size=batch_size,
        verbose=0,
        callbacks=[LossAndErrorPrintingCallback(epoch=500)],
```

```
        validation_data=(x_test, None))
vae.save_weights('vae_mlp_sustentability_3.h5')

vae.load_weights("vae_mlp_sustentability_3.h5")

print(len(df))

y_val_data = df["Rank"]
#y_val_data = []
x_val_data = df.drop(["Rank"], axis=1)
#x_val_data = df.drop([], axis=1)

data = (x_val_data, y_val_data)

#plot_results_3d_plotly(models, data)
points = plot_results_2d(models, data)

x_val_data

original_data = df_original.drop(["Rank"], axis = 1)
#original_data = df_original
original_data.head()

transformed_data = {}

for col in original_data.columns:
  #transformed_data[col] = x_val_data[data]*points
  as_array = np.array(original_data[col])
  transformed_data[col] = {}
  transformed_data[col]['original_data'] = as_array
  transformed_data[col]['extended_data'] = points *  as_array[:,
np.newaxis]
  #print(as_array.shape)

vars_on_axis = []

for key in transformed_data.keys():
  x_axis = transformed_data[key]['extended_data'][:,0].sum()
```

```
  y_axis = transformed_data[key]['extended_data'][:,1].sum()

  print(x_axis, y_axis, key)
  #vars_on_axis.append([x_axis , y_axis])
  x_abs = np.absolute(x_axis)
  y_abs = np.absolute(y_axis)

  if x_abs > y_abs:
    vars_on_axis.append([x_axis , 0])
  else:
    vars_on_axis.append([0, y_axis])
  print(x_axis, y_axis, x_abs, y_abs)

xs = [p[0] for p in vars_on_axis]
ys = [p[1] for p in vars_on_axis]

print(xs[:10])
print(ys[:10])

plt.scatter(xs, ys)

plt.scatter(points[:,0], points[:,1])

max_x = np.max(np.absolute(points[:,0]))
max_y = np.max(np.absolute(points[:,1]))

print(max_x, max_y)

nx = points[:,0] * max_y / max_x
ny = points[:,1] #* max_x / max_y

plt.scatter(nx, ny)

mid_x = nx.mean()
mid_y = ny.mean()

print(mid_x, mid_y)
```

```
nx = nx - mid_x
ny = ny - mid_y

newPoints = np.column_stack((nx, ny))
plt.scatter(newPoints[:,0], newPoints[:,1])

for col in original_data.columns:
  as_array = np.array(original_data[col])
  transformed_data[col] = {}
  transformed_data[col]['original_data'] = as_array
  transformed_data[col]['extended_data'] = newPoints *  as_array[:,
np.newaxis]

vars_on_axis = []

for key in transformed_data.keys():
  x_axis = transformed_data[key]['extended_data'][:,0].mean()
  y_axis = transformed_data[key]['extended_data'][:,1].mean()

  print(x_axis, y_axis, key)
  #vars_on_axis.append([x_axis , y_axis])
  x_abs = np.absolute(x_axis)
  y_abs = np.absolute(y_axis)

  if x_abs > y_abs:
    vars_on_axis.append([x_axis , 0])
  else:
    vars_on_axis.append([0, y_axis])
  #print(x_axis, y_axis, x_abs, y_abs)

xs = np.array([p[0] for p in vars_on_axis])
ys = np.array([p[1] for p in vars_on_axis])

xs_mask = [0 if p[0] == 0 else 1 for p in vars_on_axis]
ys_mask = [0 if p[1] == 0 else 1 for p in vars_on_axis]

print(xs[:10])
print(xs_mask[:10])
```

```
print(ys[:10])
print(ys_mask[:10])

max_x = np.max(np.absolute(newPoints[:,0]))
max_y = np.max(np.absolute(newPoints[:,1]))

xs_t = 2.*(xs - np.min(xs))/np.ptp(xs)-1
ys_t = 2.*(ys - np.min(ys))/np.ptp(ys)-1

xs_t = xs_t * xs_mask
ys_t = ys_t * ys_mask

plt.figure(figsize=(18,12))

colors_grad = get_colors_array(len(y_val_data))
#plt.scatter(z_mean[:, 0], z_mean[:, 1],c=colors_grad)

plt.scatter(newPoints[:,0], newPoints[:,1], c=colors_grad)
#plt.scatter(newPoints[:,0], newPoints[:,1])
plt.scatter(xs_t*max_x*2, ys_t*max_y*2)
plt.show()

fig, ax = plt.subplots(figsize=(20,15))

var_names = original_data.columns


colors_grad = get_colors_array(len(y_val_data))
#plt.scatter(z_mean[:, 0], z_mean[:, 1],c=colors_grad)

ax.scatter(newPoints[:,0], newPoints[:,1], c=colors_grad)
#ax.scatter(newPoints[:,0], newPoints[:,1])
ax.scatter(xs_t*max_x, ys_t*max_y)

for i, txt in enumerate(xs_t):
  x_pos = xs_t[i]*max_x
  y_pos = ys_t[i]*max_y

  x_pos = x_pos+0.03 if x_pos == 0 else x_pos
```

```
  y_pos = y_pos+0.03 if y_pos == 0 else y_pos

  ax.annotate(var_names[i], (x_pos, y_pos))

for i, point in enumerate(newPoints):
  ax.annotate(f'{labels[i]}', (point[0]+0.01, point[1]+0.01))

plt.axhline(0, color='black')
plt.axvline(0, color='black')

#df_values_countries

plt.show()

from sklearn.cluster import KMeans

points_without_trans = plot_results_2d_no_color(models, data)

kmeans = KMeans(n_clusters=3, random_state=0).fit(points)

kmeans.labels_

kmeans.cluster_centers_

unique_groups = np.unique(kmeans.labels_)

unique_groups

groups = {}
for  g  in  unique_groups:
  m = kmeans.labels_ == g
  groups[g] = []
  for i, d in enumerate(labels):
    if m[i] == True:
      groups[g].append(d)

norms = np.linalg.norm(points, axis=1)
```

```
signs = [1 if s[1]>0 else -1 for s in points]

with_sign = signs * norms

results = pd.DataFrame({
    'names': labels,
    'distance': with_sign,
    'groups': kmeans.labels_
    })

results

sorted_output = results.sort_values(by=['distance'], ascending=True)

sorted_output

sorted_output.to_csv('countries.csv')

x_pos = xs_t*max_x
y_pos = ys_t*max_y

df_vars = pd.DataFrame(list(zip(var_names, x_pos, y_pos)),
               columns =['Name', 'X', 'Y'])

df_vars.to_csv('variables.csv')

x_pos = [p[0] for p in points]
y_pos = [p[1] for p in points]

df_countries_positions = pd.DataFrame(list(zip(labels, x_pos,
y_pos)),
               columns =['Country', 'X', 'Y'])

df_countries_positions.to_csv('countries_positions.csv')
```

Appendix 3: SAFE 2018 sustainability ranking of countries -Data for 1990-2016 (Grigoroudis et al., 2019)

	Country	SAFE		Country	SAFE		Country	SAFE
1	Denmark	0.8734	55	Mexico	0.6339	109	Senegal	0.5444
2	Norway	0.8686	56	Mongolia	0.6328	110	Un. Arab Emirates	0.5438
3	Sweden	0.8630	57	Argentina	0.6309	111	Jamaica	0.5387
4	Switzerland	0.8615	58	Morocco	0.6308	112	Eq. Guinea	0.5315
5	United Kingdom	0.8384	59	South Korea	0.6296	113	Kenya	0.5295
6	Austria	0.8296	60	Singapore	0.6278	114	Lesotho	0.5289
7	Netherlands	0.8259	61	Malaysia	0.6274	115	Benin	0.5217
8	Finland	0.8231	62	North Macedonia	0.6266	116	Egypt	0.5190
9	Slovenia	0.8192	63	Kyrgyzstan	0.6265	117	Bahrain	0.5187
10	Iceland	0.8141	64	Ghana	0.6259	118	Côte d'Ivoire	0.5147
11	France	0.8078	65	Paraguay	0.6259	119	South Africa	0.5104
12	Ireland	0.8032	66	Serbia	0.6250	120	Rwanda	0.5085
13	Germany	0.7975	67	Ecuador	0.6240	121	Oman	0.5041
14	Poland	0.7835	68	Cape Verde	0.6230	122	Malawi	0.5021
15	Czech Rep.	0.7834	69	Dominican Rep.	0.6226	123	Swaziland	0.5011
16	Slovakia	0.7790	70	Gabon	0.6224	124	Zambia	0.5007
17	Lithuania	0.7743	71	Guyana	0.6224	125	Cameroon	0.5006
18	Hungary	0.7731	72	Ukraine	0.6213	126	Cambodia	0.5002
19	Luxembourg	0.7681	73	Georgia	0.6204	127	Djibouti	0.4984
20	Portugal	0.7565	74	Suriname	0.6203	128	Sierra Leone	0.4918
21	Latvia	0.7546	75	Namibia	0.6184	129	Togo	0.4893
22	Australia	0.7525	76	Nicaragua	0.6164	130	India	0.4884
23	Spain	0.7518	77	Bolivia	0.6158	131	Libya	0.4852
24	Croatia	0.7517	78	Mauritius	0.6144	132	Papua N.G.	0.4803
25	Estonia	0.7517	79	Kazakhstan	0.6113	133	Burkina Faso	0.4711
26	Belgium	0.7496	80	Panama	0.6109	134	Guatemala	0.4709
27	Italy	0.7457	81	Philippines	0.6096	135	Bangladesh	0.4688
28	Uruguay	0.7451	82	Vietnam	0.6058	136	Tanzania	0.4610
29	New Zealand	0.7431	83	Sri Lanka	0.6026	137	Mali	0.4586
30	Cyprus	0.7355	84	Armenia	0.5949	138	Liberia	0.4543
31	Japan	0.7280	85	Trinidad and Tobago	0.5940	139	Gambia	0.4463
32	Malta	0.7270	86	Kuwait	0.5934	140	Myanmar	0.4457
33	Canada	0.7217	87	Bosnia and Herz.	0.5910	141	Ethiopia	0.4418
34	United States	0.7157	88	Honduras	0.5906	142	Nigeria	0.4364
35	Chile	0.7150	89	Colombia	0.5891	143	Madagascar	0.4343
36	Costa Rica	0.7150	90	Tajikistan	0.5828	144	Guinea	0.4289
37	Greece	0.7138	91	Zimbabwe	0.5818	145	Mozambique	0.4087
38	Bulgaria	0.7067	92	Lao PDR	0.5794	146	Burundi	0.4072
39	Romania	0.7000	93	Indonesia	0.5765	147	Uganda	0.4030
40	Belarus	0.6724	94	El Salvador	0.5762	148	Iraq	0.3924
41	Albania	0.6685	95	China	0.5750	149	Angola	0.3909
42	Israel	0.6630	96	Turkmenistan	0.5749	150	Niger	0.3881
43	Brunei	0.6585	97	Jordan	0.5748	151	Congo D.R.	0.3856
44	Russia	0.6542	98	Seychelles	0.5723	152	Chad	0.3817
45	Moldova	0.6459	99	Belize	0.5719	153	Guinea-Bissau	0.3783
46	Brazil	0.6456	100	Saudi Arabia	0.5660	154	Pakistan	0.3773
47	Thailand	0.6454	101	Qatar	0.5659	155	Central African Rep.	0.3767
48	Venezuela	0.6440	102	Uzbekistan	0.5659	156	Yemen	0.3766
49	Cuba	0.6439	103	Botswana	0.5635	157	Eritrea	0.3713
50	Turkey	0.6426	104	Nepal	0.5625	158	Haiti	0.3648
51	Peru	0.6418	105	Algeria	0.5588	159	Mauritania	0.3563
52	Fiji	0.6381	106	Congo Rep.	0.5507	160	Sudan	0.3500
53	Tunisia	0.6373	107	Lebanon	0.5506	161	Afghanistan	0.3267
54	Azerbaijan	0.6343	108	Iran	0.5464			

Appendix 4: UN-SDGs Index ranking of countries - Data for 2016 (Sachs, J., Schmidt-Traub, G., Kroll, C., Durand-Declare, D., Teksoz, K. (2016)

	Country	Score		Country	Score		Country	Score
1	Sweden	84.5	51	Tunisia	65.1	101	Guyana	52.4
2	Denmark	83.9	52	Brazil	64.4	102	Honduras	51.8
3	Norway	82.3	53	Costa Rica	64.2	103	Nepal	51.5
4	Finland	81.0	54	Kazakhstan	63.9	104	Ghana	51.4
5	Switzerland	80.9	55	Un. Arab Emirates	63.6	105	Iraq	50.9
6	Germany	80.5	56	Mexico	63.4	106	Guatemala	50.0
7	Austria	79.1	57	Georgia	63.3	107	Lao PDR	49.9
8	Netherlands	78.9	58	North Macedonia	62.8	108	Namibia	49.9
9	Iceland	78.4	59	Jordan	62.7	109	Zimbabwe	48.6
10	United Kingdom	78.1	60	Montenegro	62.5	110	India	48.4
11	France	77.9	61	Thailand	62.2	111	Congo Rep.	47.2
12	Belgium	77.4	62	Venezuela	61.8	112	Cameroon	46.3
13	Canada	76.8	63	Malaysia	61.7	113	Lesotho	45.9
14	Ireland	76.7	64	Morocco	61.6	114	Senegal	45.8
15	Czech Rep.	76.7	65	Azerbaijan	61.3	115	Pakistan	45.7
16	Luxembourg	76.7	66	Egypt	60.9	116	Swaziland	45.1
17	Slovenia	76.6	67	Kyrgyzstan	60.9	117	Myanmar	44.5
18	Japan	75.0	68	Albania	60.8	118	Bangladesh	44.4
19	Singapore	74.6	69	Mauritius	60.7	119	Cambodia	44.4
20	Australia	74.5	70	Panama	60.7	120	Kenya	44.0
21	Estonia	74.5	71	Ecuador	60.7	121	Angola	44.0
22	New Zealand	74.0	72	Tajikistan	60.2	122	Rwanda	44.0
23	Belarus	73.5	73	Bosnia and Herz.	59.9	123	Uganda	43.6
24	Hungary	73.4	74	Oman	59.9	124	Côte d'Ivoire	43.5
25	United States	72.7	75	Paraguay	59.3	125	Ethiopia	43.1
26	Slovakia	72.7	76	China	59.1	126	Tanzania	43.0
27	South Korea	72.7	77	Jamaica	59.1	127	Sudan	42.2
28	Latvia	72.5	78	Trinidad and Tobago	59.1	128	Burundi	42.0
29	Israel	72.3	79	Iran	58.5	129	Togo	40.9
30	Spain	72.2	80	Botswana	58.4	130	Benin	40.0
31	Lithuania	72.1	81	Peru	58.4	131	Malawi	39.8
32	Malta	72.0	82	Bhutan	58.2	132	Mauritania	39.6
33	Bulgaria	71.8	83	Algeria	58.1	133	Mozambique	39.5
34	Portugal	71.5	84	Mongolia	58.1	134	Zambia	38.4
35	Italy	70.9	85	Saudi Arabia	58.0	135	Mali	38.2
36	Croatia	70.7	86	Lebanon	58.0	136	Gambia	37.8
37	Greece	69.9	87	Suriname	58.0	137	Yemen	37.3
38	Poland	69.8	88	Vietnam	57.6	138	Sierra Leone	36.9
39	Serbia	68.3	89	Bolivia	57.5	139	Afghanistan	36.5
40	Uruguay	68.0	90	Nicaragua	57.4	140	Madagascar	36.2
41	Romania	67.5	91	Colombia	57.2	141	Nigeria	36.1
42	Chile	67.2	92	Dominican Rep.	57.1	142	Guinea	35.9
43	Argentina	66.8	93	Gabon	56.2	143	Burkina Faso	35.6
44	Moldova	66.6	94	El Salvador	55.6	144	Haiti	34.4
45	Cyprus	66.5	95	Philippines	55.5	145	Chad	31.8
46	Ukraine	66.4	96	Cape Verde	55.5	146	Niger	31.4
47	Russia	66.4	97	Sri Lanka	54.8	147	Congo D.R.	31.3
48	Turkey	66.1	98	Indonesia	54.4	148	Liberia	30.5
49	Qatar	65.8	99	South Africa	53.8	149	Central African Rep.	26.1
50	Armenia	65.4	100	Kuwait	52.5			

Appendix 5: SAFE 2019 sustainability ranking of countries -Data for 1990-2016 (Grigoroudis, Kouikoglou, & Phillis, 2021)

	Country	SAFE		Country	SAFE		Country	SAFE
1	Denmark	0.8691	56	Tunisia	0.6318	111	Trinidad and Tobago	0.5509
2	Sweden	0.8618	57	Serbia	0.6314	112	Uzbekistan	0.5493
3	Norway	0.8578	58	Ghana	0.6298	113	Côte d'Ivoire	0.5486
4	Switzerland	0.8387	59	Paraguay	0.6274	114	Lesotho	0.5472
5	Austria	0.8284	60	North Macedonia	0.6265	115	Benin	0.5395
6	Finland	0.8189	61	Kyrgyzstan	0.6264	116	Sierra Leone	0.534
7	Slovenia	0.8067	62	Malaysia	0.6262	117	Cambodia	0.5331
8	Netherlands	0.8044	63	Namibia	0.6254	118	Jamaica	0.5326
9	Slovakia	0.8043	64	Gabon	0.6252	119	Zambia	0.532
10	UK	0.8041	65	Israel	0.6245	120	Kuwait	0.5293
11	France	0.8039	66	Singapore	0.624	121	Libya	0.5285
12	Lithuania	0.8033	67	Dominican R	0.6229	122	Lebanon	0.5222
13	Iceland	0.797	68	Ukraine	0.6229	123	India	0.5216
14	Germany	0.7943	69	Cape Verde	0.6226	124	Rwanda	0.521
15	Poland	0.7927	70	Fiji	0.6226	125	South Africa	0.5208
16	Hungary	0.7903	71	South Korea	0.6223	126	Cameroon	0.5169
17	Ireland	0.7903	72	Ecuador	0.6219	127	Mali	0.5138
18	Czechia	0.7858	73	Georgia	0.6218	128	Swaziland	0.5092
19	Portugal	0.7597	74	Panama	0.6184	129	Belize	0.5086
20	Latvia	0.7583	75	Guyana	0.6162	130	U Arab Em	0.5002
21	Estonia	0.7567	76	Nicaragua	0.6158	131	Papua NG	0.4973
22	Spain	0.7552	77	Philippines	0.6125	132	Bahamas	0.4938
23	Croatia	0.7529	78	Suriname	0.6122	133	Liberia	0.4915
24	Australia	0.7517	79	Kazakhstan	0.6112	134	Ethiopia	0.4873
25	Italy	0.7516	80	Bolivia	0.6099	135	Egypt	0.4841
26	Belgium	0.7455	81	Mauritius	0.6099	136	Bahrain	0.4817
27	Malta	0.7446	82	Sri Lanka	0.6038	137	Nigeria	0.4814
28	Uruguay	0.7432	83	Bosnia and Herzegovina	0.5989	138	Tanzania	0.4795
29	Luxembourg	0.7424	84	Zimbabwe	0.5978	139	Djibouti	0.478
30	New Zealand	0.7385	85	Armenia	0.5957	140	Qatar	0.4689
31	Canada	0.7322	86	Honduras	0.5952	141	Angola	0.4563
32	Greece	0.7248	87	Seychelles	0.594	142	Mozambique	0.4552
33	Cyprus	0.721	88	Colombia	0.5918	143	Madagascar	0.4537
34	Romania	0.7194	89	El Salvador	0.5895	144	Guinea	0.4523
35	Japan	0.7175	90	Vietnam	0.5839	145	Gambia	0.452
36	USA	0.7129	91	Botswana	0.5818	146	Oman	0.4519
37	Bulgaria	0.7107	92	Nepal	0.5811	147	Myanmar	0.4484
38	Costa Rica	0.7054	93	Eq Guinea	0.5788	148	Burundi	0.4407
39	Belarus	0.6794	94	Lao PDR	0.5784	149	Uganda	0.4393
40	Chile	0.6757	95	Burkina Faso	0.578	150	Bangladesh	0.4365
41	Turkey	0.6609	96	Kiribati	0.5769	151	Guatemala	0.4295
42	Russia	0.6602	97	Congo R.	0.5764	152	Pakistan	0.4134
43	Brunei	0.6482	98	Tajikistan	0.5751	153	Chad	0.4126
44	Albania	0.6459	99	Jordan	0.5745	154	Niger	0.4048
45	Cuba	0.6428	100	Algeria	0.5706	155	Congo DR	0.4039
46	Peru	0.6396	101	Senegal	0.5704	156	Iraq	0.3957
47	Brazil	0.6388	102	Iran	0.5696	157	Guinea-Bissau	0.3934
48	Morocco	0.6374	103	Saudi Arabia	0.5692	158	Yemen	0.3862
49	Mexico	0.6366	104	Indonesia	0.5681	159	C African R	0.383
50	Moldova	0.6366	105	Togo	0.5659	160	Eritrea	0.3747
51	Venezuela	0.6363	106	Kenya	0.5646	161	Sudan	0.3664
52	Thailand	0.636	107	Turkmenistan	0.5598	162	Mauritania	0.3643
53	Argentina	0.6356	108	Maldives	0.5558	163	Haiti	0.364
54	Mongolia	0.6345	109	China	0.5532	164	Afghanistan	0.3621
55	Azerbaijan	0.633	110	Malawi	0.5527			